Pseudomonas sp. BIOFILM DYNAMICS – IMMUNEMODULATION AND ALVEOLAR EPITHELIAL INTERACTIONS

A THESIS PRESENTED BY

KEERTHI.S

TO

SREE CHITRA TIRUNAL INSTITUTE FOR MEDICAL SCIENCE AND TECHNOLOGY

Thiruvananthapuram

IN PARTIAL FULFILMENT OF REQUIREMENT FOR THE AWARD OF THE DEGREE OF

DOCTOR OF PHILOSOPHY

2020

DECLARATION BY THE STUDENT

I, Keerthi.S, hereby certify that I had personally carried out the work depicted in the thesis entitled **"*Pseudomonas* sp. Biofilm dynamics – Immunemodulation and Alveolar epithelial interactions"**. No part of the thesis has been submitted for the award of any other degree or diploma prior to this date.

Date: 16/06/2020

Keerthi.S

CERTIFICATE OF THE GUIDE

This is to certify that Ms. Keerthi.S, in the Division of Microbial Technology, BMT Wing of the institute has fulfilled the requirements prescribed for Ph.D degree of Sree Chitra Tirunal Institute for Medical Science and Technology, Thiruvananthapuram. The thesis entitled **"*Pseudomonas* sp. Biofilm dynamics – Immunemodulation and Alveolar epithelial interactions"** was carried under my direct supervision. No part of the thesis has been submitted for the award of any other degree or diploma prior to this date.

Date: 16/6/2020

Dr. A. Maya Nandkumar
Research supervisor
Scientist 'G' and Head
Division of Microbial Technology
SCTIMST, Thiruvananthapuram

The thesis entitles

***Pseudomonas* sp. Biofilm Dynamics – Immunemodulation and Alveolar Epithelial Interactions**

Submitted by

Keerthi.S

For the degree of

DOCTOR OF PHILOSOPHY

of

SREE CHITRA TIRUNAL INSTITUTE FOR MEDICAL SCIENCES AND TECHNOLOGY

Thiruvananthapuram

is evaluated and approved by

30/9/2022

Dr. A. Maya Nandkumar

(Guide)

Dr. A. MAYA NANDKUMAR
Scientist & Head
Department of Microbial Technology
Bio Medical Technology Wing
Sree Chitra Tirunal Institute for
Medical Sciences and Technology
Poojappura P.O., Thiruvananthapuram
Kerala - 695 012.

Pradyot Prakash

(Examiner)

Sr Pradyot Prakash MD. PhD.MAMS
Professor & Head
Department of Microbiology
Institute of Medical Sciences
Banaras Hindu University
Varanasi, India.

ACKNOWLEDGEMENT

The work presented in the thesis would not have been possible without close association with many people. I take this opportunity to extend my heartfelt gratitude to all those who has made this possible.

First and foremost, I would like to extend my sincere and heartfelt gratitude and respect to my Ph.D supervisor Dr. A Maya Nandkumar. I thank her for the constant motivation, support and encouragement throughout the course of my study. Her advice has helped me to remain focused on my work. Over these years with her, I realized that research is not just lab work, but analyzing and revisiting the data over and over to know the results. She always encouraged me to be an independent researcher.

I would like to thank all my doctoral advisory committee members – Dr. Sabu Thomas (Rajiv Gandhi Center for Biotechnology), Dr. G. Srinivas (Dept. of Biochemistry, SCTIMST) and Dr. P.V. Mohanan (Div. of Toxicology) for their constant support and critical reviews.

I am thankful to the Director SCTIMST and Head BMT wing for providing the facilities provided to us. I am grateful to the registrar Dr. Santhosh Kumar B and all the staff of academic division for their support during the period.

I am thankful to Dr. Kavita Raja (Dept. of Microbiology, SCTIMST). The clinical isolates used in the study was a kind gift from the department.

I express my sincere gratitude to Dr. Anoopkumar T, Mr. Vishnu Raj and Mr. Amal Wilson Varghese and other members of the division of molecular medicine for helping me with worm killing assays.

Very special thanks to Dr. Bejoy Vijayan, for the help, support and guidance as a senior. Thank you for helping me with the statistical analysis of my data.

I would like to thank my friend and partner Ms Amalu Navas for all the time spent together on standardizations, discussions and many more.

My labmates, Mr Pradeep Kumar SS, Ms Sreeja, Ms. Ashtami and Dr Chitra Pandey for their friendship and love.

I would like to thank Department of Science and Technology (DST) for the DST INSPIRE fellowship.

And to my parents, husband and daughter, for their love, support and encouragement. This thesis is a result of your sacrifice and prayers.

Keerthi.S

CONTENTS

LIST OF FIGURES

LIST OF TABLES

LIST OF ABBREVIATIONS

2D	Two – dimensional
AHL	Acyl Homoserine Lactone
AIDS	Acquired Immune Deficiency Syndrome
ALI	Air – Liquid Interface
AO	Acridine Orange
ATCC	American Type Culture Collection
AZM	Azithromycin
CDC	Centre for Disease Control and Prevention
CF	Cystic Fibrosis
COPD	Chronic Obstructive Pulmonary Disease
CV	Crystal Violet
Cy.Di.GMP	Cyclic di guanosyl monophosphate
DC	Dendritic cells
DCFDA	Dichloro – fluorescein diacetate
DMSO	Dimethyl Sulfoxide
ECIS	Electrical Cell Substrate Impedance Sensing
eDNA	Extracellular DNA
EDTA	Ethylene – Diamine – tri acetate
ELISA	Enzyme Linked Immunosorbant Assay
EPS	Exopolysaccharides
ETT	Endotracheal tube
FBS	Fetal Bovine Serum
IFN	Interferons
IL	Interleukin
LPS	Lipopolysaccharides
MCP	Monocyte Chemo attractant Protein
MIC	Minimal Inhibitory Concentration
NGM	Nematode Growth Medium

NIH	National Institute of Health
NLR	Nod – Like – Receptors
OD	Optical Density
PA	*Pseudomonas aeroginosa*
PAMPs	Pathogen Associated Molecular Patterns
PBS	Phosphate Buffered Saline
PCN	Pyocyanin
PI	Propidium Iodide
PRRs	Pathogen Recognition Receptors
QS	Quorum sensing
ROS	Reactive Oxygen Species
SCID	Severe combined Immunodeficiency
SEM	Scanning Electron Microsope
TLR	Toll – Like Receptors
TNF	Tumor Necrosis Factor
VAP	Ventilator Associated Pneumonia

SYNOPSIS

Pseudomonas is an opportunistic pathogen and a leading cause of a variety of infections like ventilator-associated pneumonia (VAP), cystic fibrosis, non-cystic fibrosis bronchiectasis, burn infections, endocarditis, meningitis, septicemia etc. With a relatively large genome size of >5Mbps, metabolic versatility, high degree of adaptability, multiple drug resistance and many virulence factors, pathogenesis is inbuilt. Chronic *Pseudomonas* infections are caused by biofilms which are defined as three dimensional aggregates of bacteria in self-produced exopolysaccharide matrix containing polysaccharides, proteins and DNA. The National Institute of Health (NIH) suggests that 80% of bacterial infections are biofilm-related. Studies have reported the presence of *Pseudomonas* in the alveoli of ventilated patients. However, the mechanism of *Pseudomonas* biofilm-induced lung injury remains elusive. Therapeutic options are becoming increasingly limited warranting a detailed understanding of the host-pathogen interactions and the mechanisms of persistence of infections. The objectives defined against this background were:

1. To understand the dynamics of biofilm formation by *Pseudomonas* isolates
2. To establish a suitable *in-vitro* system to study the interaction of *Pseudomonas* biofilms with the epithelium
3. Role of epithelium and monocytes in particular in *Pseudomonas* sp. biofilm infection.

For this study, the *Pseudomonas* strains used were *Pseudomonas aeroginosa* ATCC 27853, clinical isolates S373, S402, S125, S253, S135, S268, S45, S277, S18 isolated from cases of bronchiectasis maintained in the Department of Microbiology, Sree Chitra Tirunal Institute for Medical Sciences and Technology, Trivandrum. The biochemical profile and antibiotic sensitivity pattern were established using classical microbiological methods. All the clinical isolates were found to be resistant to Ceftazidime.

Chapter one of the thesis deals with the study of the dynamics of biofilm formation. Crystal violet assay was used to quantify biofilm formation at 24, 48, and 72hrs. It was observed that clinical isolates showed increased biofilm formation in comparison to the ATCC isolate at 48hrs and subsequently, biofilm formation

decreased. *Pseudomonas* being a ubiquitous microorganism with the ability to colonise a wide variety of environments, the effect of temperature and pH was analysed. Temperature plays a significant role in bacterial multiplication, metabolism, and propagation. Ambient temperature (25 ± 3ºC), and 37ºC supported biofilm formation in all the isolates. pH is one of the factors that change rapidly *in-vitro* and would influence many of the bacterial activities and our studies showed that physiological pH of 7.4 supported maximum biofilm formation by the isolates. Iron is a critical nutrient in bacterial metabolism, being the redox metal found in regulatory proteins, enzymes etc, and central to respiration, metabolism, and DNA repair. Our experiments showed that iron concentration of 50mM maximised biofilm formation by all *Pseudomonas* isolates. Ceftazidime (cephalosporin), Gentamicin (Aminoglycoside), and Norfloxacin (fluoroquinolone) are the common antibiotics used to treat *Pseudomonas* infections. The role of varying concentrations of these antibiotics in biofilm formation in all the strains of *Pseudomonas* was analysed. It was observed that sub-inhibitory concentrations of all the antibiotics used in the study augmented biofilm formation by all strains. eDNA an integral part of the biofilm, helps in maintaining biofilm architecture and plays an important role in antibiotic resistance. On analysing the influence of antibiotics on eDNA release from *Pseudomonas* biofilms it was observed that Ceftazidime, a cell wall synthesis inhibitor did not influence eDNA release from the biofilms at sub-inhibitory concentrations, even when the sub-inhibitory concentration of Ceftazidime augmented biofilm formation. On the other hand, an aminoglycoside- gentamicin, and fluoroquinolone- Norfloxacin sub-inhibitory concentrations increased eDNA release from the biofilm.

Pathogenicity is defined as the ability to cause diseases in a host. The pathogenicity of the *Pseudomonas* isolates was assessed by *C. elegans* killing assay. The study revealed that clinical isolates increased the death of *C. elegans* when compared to ATCC isolates. Three, out of the 9 clinical isolates S373, S253 and S45 exhibited increased killing of *C. elegans* and hence were used for further studies. Bacterial virulence factors are molecules that facilitate host-pathogen interactions including immune responses. *Pseudomonas* employs a repertoire of virulence factors to evade, colonize and persist within a host. Some of the major virulence factors are

pyocyanin, rhamnolipids, and alkaline proteases. The secreted virulence factors such as pyocyanin, rhamnolipids, and alkaline proteases were assayed in the culture supernatant through biochemical methods. Clinical strains S373, S402, S125, S253, S135, S268, S45, S277, and S18 showed increased expression of all the three virulence factors when compared with the ATCC 27853 strain.

The establishment of a suitable *in-vitro* system to study host- pathogen interactions is essential to understand the mechanisms of persistence of *Pseudomonas* infection in alveolar epithelium. A549, a Type 2 pneumocyte was used as a representative of the alveolar epithelium and THP1 was the monocyte system used. Two different culture systems were evaluated – a submerged/2D culture system and an Air Liquid interface system (ALI). A multiplicity of infection of 100:1 (A549: bacteria) was found suitable for infection and in order to simulate biofilms *Pseudomonas* biofilm on endotracheal tubes were used. The systems were microscopically evaluated every 2hr for changes in morphology and viability. The viability was assessed by live- dead staining of the epithelial cells. It was observed that A549 cells at Air –Liquid interface infected with endotracheal tube containing *Pseudomonas* biofilms could represent the *in-vivo* conditions of ventilator associated pneumonia. To study interactions of planktonic *Pseudomonas* with the epithelium A549 at ALI was infected with PBS suspension of *Pseudomonas*.

Chapter three deals with the third objective of deciphering role of epithelium, monocytes and co-culture (epithelium - monocyte) to a challenge by *Pseudomonas* biofilms. Epithelial layer forms the first line of defense to any challenge or stimuli. Alveoli of the lung are lined by the Type 1 pneumocytes, which form the gas exchange surface and the type 2 pneumocytes which act as the alveolar stem cells and as secretory cells synthesizing surfactant proteins A,B,C and D and other inflammatory molecules like MCP,IL-1β, IL-6, IL-8 etc. Response of alveolar type II pneumocytes and the role of monocyte as the second line of defence on challenge with *Pseudomonas* biofilms was studied at microscopic and molecular levels. Primary response of cells to an infection is generation of reactive oxygen species (ROS) which has both an inflammatory and signalling role. A reduction in ROS generation was observed in the cells infected with *Pseudomonas* biofilms vis~ a~ vis the planktonic cells. This could

be due to the ability of *Pseudomonas* to produce superoxide dismutase or the ability of biofilm matrix to scavenge the ROS molecules. Phagocytosis an innate immune mechanism for clearing pathogens was studied by Gentamicin protection assay and observing bacterial internalisation by THP 1 cells. The results revealed that biofilm bacteria resisted internalisation and phagocytosis by monocytes.

Electrical cell substrate impedance sensing (ECIS) is an emerging technology which helps in studying bacterial interactions with epithelial cells in real time by measuring the changes in impedance, a direct measure of the monolayer integrity. The study revealed that changes in barrier integrity of the cells was initiated by the bacteria as early as 2hr post infection while, changes in cellular morphology occurred only by 15hr post infection. The role of azithromycin in barrier protection was assessed during infection using ECIS. It was noticed that A549 monolayers treated with azithromycin resisted infection with ATCC strain and infection by clinical isolates was delayed up to 7hr to 8hr. Acridine orange staining of A549 and THP1cells infected with planktonic *Pseudomonas* strains of ATCC and clinical isolates S373, S253 and S45showed loss of membrane integrity and cellular contents pointing towards necrotic cell death. Upregulation of mRNA expression of proinflammatory cytokines IL8, TNFα and IL6 and increase in TNFα and IL8 protein expression by ELISA was also observed. On the other hand, when these cells were exposed to biofilms, Hoechst staining revealed DNA fragmentation with an in intact nuclear membrane - an intriguing observation. A549, THP1 cells and cells in co-culture exposed to biofilms showed cellular swelling and rupture. At the same time, TNFα gene and protein expression was found to be up regulated. Thus, biofilm treated cells showed classic features of both apoptosis and necrosis. All these observations suggested involvement of pyroptotic cell death in biofilm infected A549, THP1 cells and in co-cultures.

For better understanding the mechanism of infection the expression of caspases 1, 3, and IL-1β was analysed. A549, THP1 and the co-cultures, exposed to biofilms of *Pseudomonas* showed a twofold increase in Caspase 1and upregulation of IL1β. Caspase 3 was expressed only at basal levels. These data strongly suggest the involvement of pyroptotic mechanism of cell death in biofilm infected cells.

In conclusion the study establishes the mechanisms of virulence of *Pseudomonas* biofilms, its persistence through immune modulations both at the epithelial and monocyte level. The co-culture model developed of A549 and THP-1 cells at air-liquid interphase was shown as a suitable *in vitro* system to study biofilm interactions with alveolar epithelium and study of mechanisms of immune modulation. Pyroptosis as a possible mechanism of immune modulation leading to biofilm persistence was demonstrated which could lead to chronic inflammation in the host as it causes host tissue damage and prevents removal of biofilms.

1. INTRODUCTION

Pseudomonas is an opportunistic pathogen capable of infecting a wide range of host and tissues like respiratory, damaged or burned skin, or injured cornea (Moradali et al., 2017). CDC (2014) report suggests that over 50,000 healthcare-associated *P. aeruginosa (PA)* infections occur every year in the US and more than 13% of these are multi-drug resistant. In 2017, *Pseudomonas* was listed as the 2nd most common agent causing Ventilator-Associated Pneumonia (VAP). CDC also reports that more than 400 deaths occur every year due to such infections. The International Nosocomial Infection Control Consortium had identified *Pseudomonas* as a global threat in healthcare facilities (2016). *Pseudomonas* accounts for 60 % - 80% of lung infections in cystic fibrosis (CF) patients and increases CF-related morbidity and mortality (Acosta et al., 2020).

The success of *P. aeruginosa* in colonizing diverse environments can be attributed to their ability to synthesize a large number of virulence factors like flagella, alginate, type IV pili, lipopolysaccharides, phospholipases, pyocyanin, pyoverdine, and secreted virulence factors including toxins, exotoxins A, alkaline proteases, elastase and hemolysins (Jurado-Martín et al., 2021). *P. aeruginosa* infections have become a matter of serious concern due to the increased resistance of the bacterium to most of the existing antimicrobial agent (Pang et al., 2019).

Pseudomonas naturally grows in association with surfaces leading to the formation of biofilms. Biofilms can be defined as a structured consortium of bacteria enclosed in a self–producing polymeric matrix (Karygianni et al., 2020). The development and differentiation of microorganisms in biofilms can be broadly compared with a multi-cellular biological differentiation system (Penesyan et al., 2021). Cellular differentiation and division of labor are hallmark features observed during the biofilm mode, which otherwise are classically non – differentiating (Gestel et al., 2015). Various stages of multi-cellular organization like, confined dissolution of biofilm exopolysaccharide matrix followed by the dispersal of bacteria from the microcolony and programmed cell death within the microcolony provide them with a survival advantage over their planktonic counterparts (Yin et al., 2019).

One of the most important and intriguing facts about biofilm is their decreased susceptibility to antimicrobial compounds. Biofilm bacteria require more than 1000

times the concentration of antibiotic that is required to kill planktonic bacteria (D. Sharma et al., 2019). This could be due to either tolerance or resistance to the particular antibiotic. Tolerance allows the bacterial cells to survive but they neither grow nor are killed aided by biofilm formation, while antibiotic resistance is acquired over time (C. W. Hall & Mah, 2017). The exopolysaccharide matrix of the biofilm plays a crucial role in protecting the biofilm bacteria from antibiotics (Karygianni et al., 2020).

Exponentially growing cells which form the external layer of the biofilm are readily killed by conventional antibiotics (Olivares et al., 2020). The drug efflux pumps of *Pseudomonas* (Type II, Type III secretary system) are actively involved in removing the antibiotic from growing cells (Alav et al., 2018; Soto, 2013). The inner layers of the biofilm comprise stationary phase or dormant phase bacterial micro colonies, which help in survival, as antibiotics act only on metabolically active cells (Lebeaux et al., 2014; Wood et al., 2013). Oxygen limitation facilitates an anaerobic condition deep inside the biofilm limiting metabolic activity. The bacteria in a biofilm are in close proximity facilitating horizontal plasmid /gene transfer (Schieber & Chandel, 2014). The pH, partial pressure of CO_2 and O_2 within the micro-environment of biofilm further limits action of antimicrobials (Lebeaux et al., 2014; Muhammad et al., 2020).

Pseudomonas is capable of causing direct tissue infections and device related infections (Gellatly & Hancock, 2013). Biofilms of *Pseudomonas* has been implicated in direct tissue infections like otitis media, chronic wounds and chronic osteomyelitis (Bjarnsholt et al., 2013). They are known to colonize device surfaces like contact lenses, central venous catheters, mechanical heart valves, peritoneal dialysis catheters, prosthetic joints, pacemakers, urinary catheters (Jamal et al., 2018). Biofilm infections are often chronic and resistant to antibiotic therapy and host immune defences (D. Sharma et al., 2019).

The effective surveillance by the immune system protects the host from pathogens. Extensive research over the past few decades has revealed the complex host pathogen interactions. This has improved our understating of signal transduction pathways, cellular signalling, mechanism of cell death and various immune evasion

strategies adopted by bacteria. This knowledge has been instrumental in designing pathogen – targeted therapies safe for use in hosts (Welch, 2015). But most of the host pathogen interactions studied holds true for planktonic bacterial infections i.e acute infections. Immune responses to biofilms are less well characterized. Mechanism of persistence of biofilms within the host, despite the active involvement of both the arms of immune system, is intriguing (González et al., 2018).

Epithelium is the first line of defense in an organ or tissue of an organism. The response elicited by the epithelium dictates the cascade of immune response that follows (Günther & Seyfert, 2018). This study was aimed at understanding the interactions the trigonal interactions between the pathogen the host cell and the device surface specifically the alveolar epithelium and monocytes with biofilms of *Pseudomonas* developed on endotracheal tubes (Fig.1).

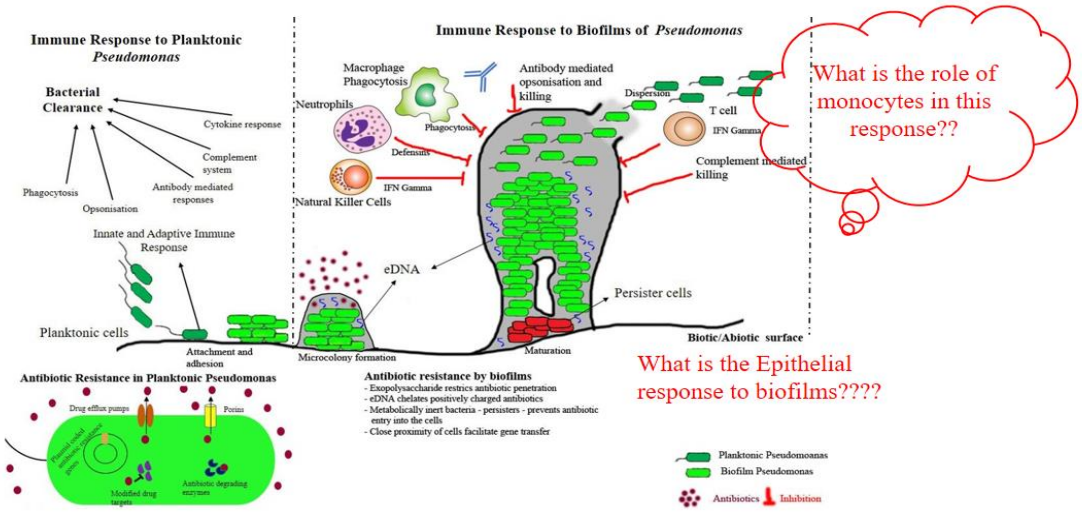

Fig.1: Pictorial representation questions asked in the mechanism of *Pseudomonas* persistence in the host. Planktonic *Pseudomonas* is eliminated from the host with the help of innate and adaptive immune responses. On the other hand, simultaneous involvement of both the arm of the immune system fails to remove biofilms of *Pseudomonas*. Planktonic *Pseudomonas* shows intrinsic resistance to antibiotics through mechanisms depicted in the figure. Biofilm formation further reduces the susceptibility of the bacteria to antibiotics. They deploy multiple mechanisms to resist antibiotics and the host immune defences resulting in recalcitrant/ persistent infections.

1.2. Objectives of the study:

Based on the above the study had three objectives –

1. Understand the dynamics of biofilm formation by *Pseudomonas aeroginosa* ATCC 27853 strain and clinical isolates of *Pseudomonas.*
2. Design and develop suitable *in-vitro* system to study the interactions of *Pseudomonas* biofilms with alveolar epithelium.
3. To study the role of alveolar epithelium and monocytes in immune response to *Pseudomonas* biofilm infections and mechanism of pathogenesis of *Pseudomonas* biofilm.

2. REVIEW OF LITERATURE

2.1. *Pseudomonas* BIOFILMS

Pseudomonas naturally grows in association with surfaces leading to the formation of biofilms (Rasamiravaka et al., 2015). Biofilms can be defined as a structured consortium of bacteria enclosed in a self – producing polymeric matrix (Karygianni et al., 2020). The development and differentiation of microorganisms in biofilms can be broadly compared with multi-cellular biological differentiation system (Penesyan et al., 2021). Cellular differentiation and division of labour are hallmarks of features observed during the biofilm mode, which otherwise are classically non – differentiating. Various stages of multicellular organization like, confined dissolution of biofilm exopolysaccharide matrix followed by the dispersal of bacteria from the microcolony and programmed cell death within the microcolony provides them with a survival advantage over their planktonic counterparts (Penesyan et al., 2021). Biofilm formation imparts a lot of benefits to the bacterium (table 1). In addition to the resistance to changing environmental conditions biofilm production helps them with a number of properties of communal existence like division of metabolic burden, gene transfer and altruistic behaviour and therefore survival (Kostakioti et al., 2013).

Confocal Laser Scanning Microscopy (CSLM) of the hydrated biofilms has revealed the three dimensional architecture of a biofilm (Reichhardt & Parsek, 2019). More than 85% of the biofilm is occupied by the exopolymeric matrix and approximately 15% of the volume by microbial cells (microcolonies) (Donlan & Costerton, 2002; Kokare et al., 2009). The exopolysaccharide matrix backbone is composed of 1, 3- or 1,4 - β linked hexose residues (Limoli et al., 2015). Between the microcolonies are water channels which basically function as a rudimentary circulatory system, supplying nutrients, oxygen and removing waste products (Yeor-Davidi et al., 2020). Heavily hydrated nature of biofilms prevents their dehydration (Donlan & Costerton, 2002).

Interestingly microbial cells at different zones of the biofilms vary considerably in their gene expression patterns. The maturation of the microcolony is accompanied by increase in volume, therefore the bacteria deep within the biofilm has minimal access to the nutrients and usually become metabolically inert. On the other

hand the cells at the periphery gain access to nutrients and oxygen and continuously multiply providing metabolic diversity (Kostakioti et al., 2013).

Pel, Psl and alginate are the major constituents of the EPS matrix, which helps adhesion, aggregation and in when combined with eDNA decides the architecture of the biofilm. Psl plays a major role in the early stages of biofilm formation. Arranged helically on the cell surface, Psl molecules help type IV pili mediated cell migration, cell adhesion and biofilm formation. Zegans and his group revealed that Psl protects the biofilms from a variety of antibacterial agents and a broad range of antibiotics during the early stages of development (Moradali et al., 2017; Zegans et al., 2012).

Pel polysaccharide, is involved in maintaining cell – cell interaction in the biofilms. Pel and Psl are the predominant structural polysaccharide in biofilms of non – mucoid isolates of *Pseudomonas.* It is found abundantly in the stalk of the biofilm and complexes with eDNA, providing structural stability to the biofilm. Colvin et al., found that the absence of Pel, increased the susceptibility of *Pseudomonas* biofilms to aminoglycoside antibiotics (Ciofu & Tolker-Nielsen, 2019). Alginate, the third major polysaccharide of the EPS, was found to be overproduced in the mucoid phenotypes from Cystic Fibrosis patients. Alginate was found to be important for biofilm maturation, structural stability and persistence of biofilms. Composition of alginate greatly influence viscoelasticity, volume, cell numbers, structure, cell – cell interaction, adhesion, and aggregation in the biofilms of *Pseudomonas* (Orgad et al., 2011)

2.1.1. Factors affecting biofilm formation

Various environmental factors effect *Pseudomonas* biofilm formation. Some of the common environmental cues that influence biofilm formation are i) temperature, ii) pH, iii) iron concentration, iv) glucose concentration and v) presence of antibiotics. Kannan and Gautam reported that a temperature of 37ºC and pH of 7.4 facilitated increased biofilm formation in *Pseudomonas* MTCC 2297 strain. Their study suggested that, under the above mentioned conditions there was increase in biofilm mass, exopolysaccharide production and the formed biofilms strongly adhered to the substrate (Kannan & Gautam, 2015). pH is an important factor that influence

biofilm formation. Jones et al studied the influence of pH on chronic wound healing process. The pH of intact skin ranges from 4.0 to 6.0. Pathogenic colonization of wounds resulted in an increase in pH upto 10 (Jones et al., 2015).

	PLANKTONIC CELLS	BIOFILMS
PHYSIOLOGICAL PROPERTIES	• Free swimming often in aqueous environment • Metabolic products continuously removed • Physical chemical and biological stress • Source of infection • Express virulence factors.	• Slow growth • Higher tolerance to antibiotics H_2O_2, phagocytosis. • Stress conditions – lower metabolic activity • Develop stress responses. • Unique gene expression patterns • Source of infection • Express virulence factors.
STRUCTURAL PROPERTIES	• Flagella used for movement	• Attached to substrate • Dormant, smaller cells, no active cell division. • Flagella absent. • Cell adhesion molecules like fimbriae expressed

Table 1: Structural and Physiological differences between planktonic and biofilm bacteria

Iron is an important element involved in the physiological processes in both prokaryotes and eukaryotes. Acquisition of iron is mediated by two siderophores – pyochelin and pyoverdine. Iron is important for the expression of virulence factors by the bacterium (Cornelis & Dingemans, 2013). Multiple studies have reported that iron deprivation leads to reduction in twitching motility and biofilm formation by *Pseudomonas* biofilms (Banin et al., 2005; Cai et al., 2010). Moreau-Marquis et al, suggest that an increase in extracellular iron concentrations increased biofilm formation by *Pseudomonas* biofilms (Moreau-Marquis et al., 2009; Oglesby-Sherrouse et al., 2014). Glucose is an important source of carbon. She et al., (2019), showed that clinical isolates varied in their sensitivity to glucose, but the presence of glucose increased biofilm formation (She et al., 2019). Huynh et al., observed that

glucose deprivation induced dispersion of biofilms of *Pseudomonas in-vitro* (Huynh et al., 2012).

Pseudomonas is intrinsically resistant to a wide range of antibiotics (Pachori et al., 2019). Multiple mechanisms act synergistically in *Pseudomonas* to resist a wide range of antibiotics. Down regulation of OPrD, up regulation of drug efflux pumps, β-lactamases and extended spectrum β-lactamases help *Pseudomonas* develop resistance to several of classes of antibiotics used (Pachori et al., 2019). *Pseudomonas* is naturally resistant to certain antibiotics. The characteristics like cellular structures and its composition protects the bacterium from antibiotics and toxic molecules. Modification of drug targets, presence drug efflux pumps and antibiotic degrading enzymes are some of the common methods of antibiotic resistance in *Pseudomonas.* The bacteria limit the penetration of hydrophilic drug molecules by expressing semi-permeable porin channels that selectively allow nutrient inflow. This method of adaptation is used by the bacteria to resist carbapenems and cephalosporins (broad spectrum antibiotics). These isolates were deficient in OprD porin, which facilitates influx of carbapenems (Pachori et al., 2019).

Genome/ plasmid encoded drug efflux pumps significantly increase antibiotic resistance in *Pseudomonas*. The efflux pumps have broad substrate specificity and therefore expel various classes of antibiotics (D. Sharma et al., 2019). MexAB-OprM, MexXY/OprM(OprA), MexCD-OprJ, and MexEF-OprN are the major types of drug efflux pumps expressed by *Pseudomonas*. Drug efflux pumps are also involved in the development of chronic infections. This is accomplished by expelling the quinolone signals of the PQS (quorum sensing system), which reduces its intracellular concentration and thereby reducing the expression of virulence factors resulting in chronicity of infection (Blanco et al., 2016).

Resistance can also develop by mutation in genes or by horizontal gene transfer. In this case resistant phenotypes are selected by antibiotic therapy and results in irreversible resistant phenotypes. Such antibiotic resistance mechanisms are adopted by clinical and environmental isolates to acquire resistance to a broad range of antibiotics. Mutation that results in overproduction of antibiotic resistance molecules

has helped *Pseudomonas* combat β- lactams. Henrichfreise et al, showed that 73% of the clinical isolates resistant to 3rd and 4th generation cephalosporins over express AmpC which degrades the antibiotics (Chavan et al., 2017; Henrichfreise et al., 2007). Loss of function mutation leading to the over production of drug efflux pumps is an effective strategy adopted by *Pseudomonas* against carbapenems. Fluoroquinolones are resisted by *Pseudomonas* by mutating the DNA gyrase enzyme or topoisomerase IV or overexpression of drug efflux pumps (Hooper & Jacoby, 2016).

Multi drug resistant clinical isolates of *Pseudomonas* have been reported to possess plasmids coding for antibiotic resistance. These plasmids coding for beta lactamases, carbapenemases, aminoglycoside modifying enzymes and 16SrRNA methylases have been identified in multidrug resistant clinical isolates. Plasmid mediated colistin resistance in *Pseudomonas* was reported by El-Baky et al (Abd El-Baky et al., 2020). Pan multi-drug resistant *Pseudomonas* is a cause of major concern worldwide (Horcajada et al., n.d.).

2.1.2. Biofilm Formation and antibiotic resistance

One of the most important and intriguing facts about biofilm is their decreased susceptibility to antimicrobial compounds. Biofilm bacteria require more than 1000 times the concentration of antibiotic that is required to kill planktonic bacteria (D. Sharma et al., 2019). This could be due to either tolerance or resistance to the antibiotic. Tolerance allows the bacterial cells to survive but they neither grow nor are killed aided by biofilm formation, while antibiotic resistance is acquired over time (C. W. Hall & Mah, 2017). The exopolysaccharide matrix of the biofilm plays a crucial role in protecting the biofilm bacteria from antibiotics. Significant reduction in antibiotic penetration through the EPS has been reported by Sharma, Misba and Khan (D. Sharma et al., 2019). Anionic groups present in the EPS matrix along with extracellular DNA (eDNA) is found to be involved in the sequestration of positively charged aminoglycoside antibiotics, thus preventing the diffusion of the antibiotic into the interior of the biofilm (Wilton et al., 2015). Also, the ion chelating properties of eDNA and the exopolysaccharide help biofilm in protection against tobramycin and heavy metals like Zn, Cu and Pb. The presence of layers or regions of metabolic

diversity within the biofilm provides an excellent mechanism for antibiotic resistance. Exponentially growing cells which form the external layer of the biofilm are readily killed by conventional antibiotics. The drug efflux pumps of *Pseudomonas* (Type II, Type III secretary system) are actively involved in removing the antibiotic from growing cells (Amaral et al., 2014). The inner layers of the biofilm comprise stationary phase or dormant phase bacterial micro colonies, which help in survival, as antibiotics act only on metabolically active cells (Lempp et al., 2020; D. Sharma et al., 2019). Oxygen limitation facilitates an anaerobic condition deep inside the biofilm limiting metabolic activity. The bacteria in a biofilm are in close proximity facilitating horizontal plasmid /gene transfer (Stalder & Top, 2016). The micro-environment within biofilm such as, pH, partial pressure of CO_2 and O_2 further limits action of antimicrobials (Lebeaux et al., 2014).

Alternatively, it has been proposed that resistant *P. aeruginosa* variants may be selected during antibiotic therapy itself. Antibiotic resistant phenotypic variants of *P. aeruginosa*, with enhanced biofilm forming ability was isolated *in-vitro* and from CF lungs by Drenkard and Ausubel (Drenkard & Ausubel, 2002). It was identified that regulatory protein PvrR was responsible for the conversion from antibiotic sensitive and resistant forms. A locus *ndvB* was identified by Mah et al, which helped in the synthesis of periplasmic glucan that physically interacts with tobramicin thereby sequestering the antibiotic (Mah, 2012; Tseng et al., 2013). At the same time glucan is also capable of inducing ethanol oxidation genes in growing cells within biofilms. Taken together it is evident that multiple biofilm –specific mechanisms are activated simultaneously and synergistically to resist antibiotic action. A sub – population within the biofilm called as persister cells exhibit very high degree of resistance to antibiotics and other environmental stress (Barrett et al., 2019). These persister cells survive despite extensive antibiotic therapy and under favorable conditions regrow and cause relapsing chronic infections (Fisher et al., 2017). Sub-inhibitory concentrations of antibiotics have shown to augment biofilm formation by *Pseudomonas* in-vitro. During an antibiotic treatment, bacteria are exposed to sub-MIC concentration during the beginning and end of the regimen or between doses (Tezel et al., 2016; Yousefpour et al., 2021). Also, cell deep inside the biofilm are constantly exposed to sub-MIC

concentration of antibiotics due to the limited permeability of exopolysaccharide matrix (Lebeaux et al., 2014). It was observed that concentration below the MIC increased biofilm formation (Olivares et al., 2020).

It was observed by Gellatly and Hancock, that the isolates obtained from chronic infections had significant phenotypic differences from those isolated from acute infections (Gellatly & Hancock, 2013). Virulence factors were abundantly expressed by isolates from acute infection whereas it was down regulated in isolates from chronic infection *(eg. Flagella, pili, type iii secretion system)* (Gellatly & Hancock, 2013).

2.1.3. eDNA and its role in biofilms of *Pseudomonas*

eDNA is one of the most important components of the biofilm's matrix. Sharma and Singh, revealed that addition of DNaseI into a mature *Pseudomonas* biofilms dissolved the biofilms and presence of DNaseI in the medium inhibited biofilm formation by *Pseudomonas* (K. Sharma & Pagedar Singh, 2018). eDNA was also found to play vital roles in adhesion of bacteria on the substrate (Campoccia et al., 2019; Regina et al., 2014). The eDNA forms loop like structures on the surface of bacterial cells helping them to adhere in surfaces (Das et al., 2010, 2016) Atomic force microscopy (AFM) and water contact angle studies suggest that the presence of eDNA on the surface of bacteria significantly influence their surface hydrophobicity and hence surface adhesion (Das et al., 2010). The exogeneous addition of DNA into bacterial cultures induced bacterial aggregation and biofilm formation (Campoccia et al., 2021a). Multiple studies have shown that eDNA contributes to horizontal gene transfer within biofilms. The close proximity of cells within biofilms facilitates horizontal gene transfer (Campoccia et al., 2021a). It was observed that within a biofilm a sub-population of cells undergo autolysis and leads to the release of DNA. This in turn leads to acquisition of beneficial adaptation like antibiotic resistance and pathogenicity (Ibáñez de Aldecoa et al., 2017). The anionic nature of eDNA facilitates the binding of cations and cationic antimicrobial peptides. It is responsible for the chelation of divalent cations like – Mg^{2+}, Ca^{2+}, Mn^{2+} and Zn^{2+} (Lewenza, 2013). The lack of Mg^{2+} ions activated the *prm* operon in *Pseudomonas*, leading to changes in

lipopolysaccharides. These changes result in the masking of bacterial outer membrane, which is negatively charged. *Pseudomonas* is known to use this adaptive mechanism to resist antimicrobial peptides and aminoglycoside antibiotics which again is positively charged (Gellatly & Hancock, 2013).

2.1.4. *Pseudomonas* BIOFILMS IN CHRONIC INFECTIONS

Chronic infections exhibit a very slow progression compared to acute infections and are recalcitrant to antibiotic therapy. Chronicity or persistent bacterial infection is due to biofilm formation. This leads to adaptive immune response dominated by mononuclear leucocytes and IgG antibodies resulting in chronic inflammation (P. Ø. Jensen et al., 2010). Biofilm formation facilitates chronic infection and reduces the efficiency of antibiotic therapy (D. Sharma et al., 2019).Table 2 lists the major infections caused by *P. aeruginosa* biofilms.

It has been estimated both by, Centre for Disease Control and Prevention (CDC) and National Institute of Health (NIH) that biofilms are responsible for 65% to 80% of all infections (Jamal et al., 2018). Over the last two and half decades there has been an extensive study on medical device related biofilm infections. Major device related infections from which *Pseudomonas* has been isolated include Catheter Associated Urinary Tract Infection, valvular endocarditis, kerato-conjunctivitis, Ventillator Associated Pneumonia, Central Line Associated Bloodstream Infections, surgical/transplant infections etc (Table 2).

The insertion of artificial devices into humans in a variety of clinical contexts has become common place in modern medicine. Common medical devices include endotracheal tubes (ETTs), urinary catheters, vascular catheters, peritoneal catheters, orthopedic implants, prosthetic joints, and prosthetic cardiac valves. These abiotic devices can quickly become coated with a conditioning film of host proteins that can then support bacterial attachment, which can occur as early as 1 day after insertion (Khatoon et al., 2018). Biofilm bacteria can subsequently undergo dispersal, allowing the planktonic forms of the bacteria to potentially cause disseminated infection (Guilhen et al., 2017). Although antibiotics can be effective against the planktonic forms of the bacteria, device removal is often the only effective way to completely

eliminate the source of infection (Fung et al., 2010; Hughes & Webber, 2017). After tracheal intubation, a bacterial biofilm rapidly forms on polyvinyl-chloride ETTs and represents a significant source of bacterial inoculation into the lungs. Intubated patients on mechanical ventilation are at a high risk for bacterial colonization leading to the development of VAP, a major health threat that carries an attributable 60-day mortality of 1.5% among critically ill patients (D. Wu et al., 2019). In the majority of cases of VAP, the same organism isolated from the ETT biofilm matches the causative organism identified on respiratory cultures. Furthermore, the production of the QS-dependent virulence factor, rhamnolipids, by colonizing *P. aeruginosa* isolates was found to be associated with the development of VAP (Jurado-Martín et al., 2021; Köhler et al., 2010).

2.1.5. STAGES OF BIOFILM FORMATION:

Transition to biofilm mode of growth is governed by multitude of regulatory pathways. Changes in gene expression and finally mediating structural and functional rearrangements in the community (Liu et al., 2020). Biofilm formation involves the four stages viz. (i) Attachment (ii)Adhesion (iii)Maturation and(iv)Dispersion as depicted in Fig.1 (Muhammad et al., 2020).

2.1.5.1.ATTACHMENT

Bacterial attachment is regulated by physical forces acting at nano distances like Vander Vaals forces (Ramezanian et al., 2018). In PA variety of bacterial structures like type IV pili, LPS and adhesions, regulated by various environmental cues. Motility – sessility switch is regulated by a key second messenger molecule – Cyclic – di guanosyl monophosphate (Cy-Di-GMP).Cellular levels of Cy-Di-GMP, regulates the life style of *Pseudomonas,* like an increase in C-di-GMP concentration increases adhesion of PA to surfaces and inhibits motility (Ha & O'Toole, 2015; Valentini & Filloux, 2016).

40 different proteins involved in synthesis and degradation of Cy-di-GMP regulate its levels in the cell in response to signals. Cy-di-GMP regulates multiple pathways in biofilm formation. It is involved in the polymerization of alginate, down regulation of

flagella biosynthesis and Pel and Psl synthesis. Wsp, a chemosensory system in *Pseudomonas* is involved in the regulation of biosynthesis of Cy-di-GMP. Surface attachment results in signalling cascade activating Wsp R, a Cy-di-GMP synthesizing molecule (Valentini & Filloux, 2016).

Infection	Major risk factors
Soft tissue	Open wounds, burns, surgical wounds
UTI	Use of urinary catheters
Bacteremia	Immunocompromised (AIDS, SCID)
Diabetic foot	Diabetes, impaired microvascular circulation.
Respiratory	*COPD, #CF, +VAP
Otitis externa	Tissue injury, water blockage in the ear canal
Keratitis	Contact lens, contaminated contact lens storage solution
Otitis media folliculitis	Improperly cleaned hot tubs

Table 2: Common *Pseudomonas* infections and major risk factors involved. (*Chronic Obstructive Pulmonary Disease, # Cystic Fibrosis, + Ventilator Associated Pneumonia)

2.1.5.2.MATURATION

The initial attachment is followed by bacterial multiplication, overproduction of EPS matrix and formation of water channels. This helps the development of physiological gradients (nutrient, oxygen etc..) facilitating formation of physiologically and biochemically diverse phenotypes of PA within the biofilm. Maturation phase is regulated by quorum sensing signals of PA (Singh et al., 2021).

2.1.5.3.DISPERSION

Sloughing, erosion and seed dispersal are the three modes of dispersal in PA biofilms facilitating bacterial colonization at newer sites (Kaplan, 2010). Shear stress induces sloughing off, of a large portion of biofilm and erosion happens when smaller portions are dispersed. Seed dispersal is characterised by the release of planktonic cells from the centre of the biofilm mass and is an active process. The size of the microcolony is the critical factor that decides the dispersion of biofilm. Spatial differentiation i.e., differential localisation of motile and non – motile bacteria, plays very important role in this phase, inducing dissolution of EPS matrix and release of

planktonic bacteria (Kaplan, 2010; Muhammad et al., 2020). Several environmental cues like the presence of chemicals, nutrients, oxygen, pH, Nitric Oxide (NO) is also known to regulate dispersion in PA biofilms. Nutrient like glucose in the medium reduced C-di-GMP levels, inducing the expression of flagella followed by dispersion of biofilms. Hypoxia also induces degradation of C-di-GMP thereby inducing dispersion. NO increases phosphodiesterase activity, which reduces C-di-GMP levels resulting in dispersion (Kaplan, 2010; K. Lee & Yoon, 2017; Muhammad et al., 2020).

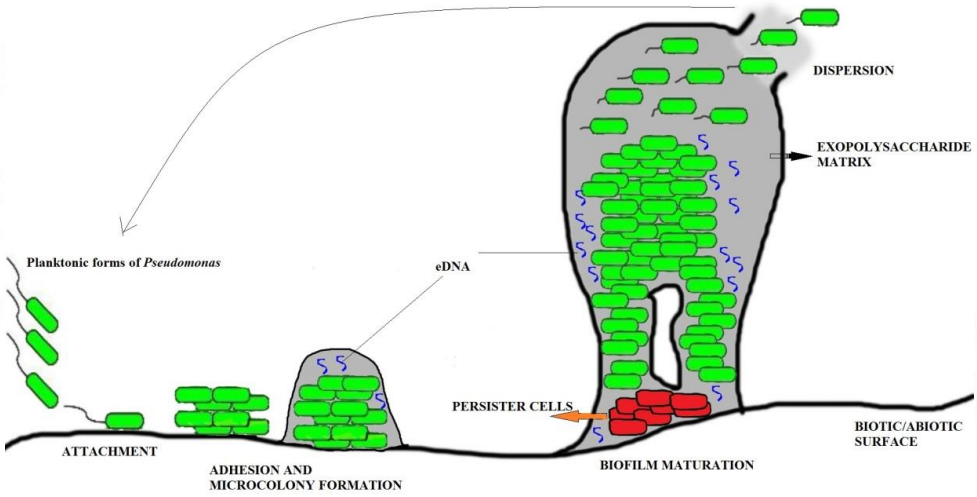

Fig 2: Pictorial representation of steps involved in biofilm formation by *Pseudomonas*. Initial attachment to the surface is mediated by weak forces of interactions, followed by adhesion on the surface using special appendages like pili fimbriae. The bacteria multiply and form microcolonies. The microcolonies increase in size and volume upon reaching a critical volume disperse planktonic bacteria into the surrounding medium and the cycle continues. Persister cells are observed in mature biofilm which are dormant cells.

2.1.6. QUORUM SENSING (QS)

QS mechanism shared by many bacteria allows for a coordinated adaptation in bacterial populations to environmental changes (Abisado et al., n.d.; Zhao et al., 2020). This is mediated by small, membrane-diffusible molecules called autoinducers. These molecules are constitutively produced by each bacterium and act as cofactors of specific transcriptional regulators when they reach critical threshold concentrations. The coordinated expression of genes and virulence factors, mediated through the QS system, helps in survival and colonization in the host. The QS is directly involved in the regulation of approximately 10% genes in the genome and 20% of the expressed

proteome (Gellatly & Hancock, 2013).The QS consists of two major players – 1st regulator proteins (LasR, RhlR and PqsR), which are activated by the autoinducers and act as transcriptional activators of genes and the 2nd autoinducer synthases (LasI, RhlI and PqsABCDH). *Pseudomonas aeroginosa* produces three autoinducers (Fig 2). Two of these autoinducers are acyl homoserine lactones (AHLs): 3-oxo-dodecanoyl homoserine lactone (3-oxo-C12 HSL) is produced by the LasI AHL synthase and acts on the *LasR* transcriptional activator and butyryl homoserine lactone (C4 HSL) produced by the RhlI AHL synthase, which acts on the *RhlR* transcriptional activator. The third autoinducer is a 2-heptyl-3-hydroxy-4-quinolone designated the *Pseudomonas* quinolone signal, which is synthesized by a complex multistep process involving two operons, *pqsABCDE* and *phnAB*, and three genes located outside these operons, *pqsR, pqsH, and pqsL*.LasR and RhlR dominates during the early stages of cell growth, which is then taken over by the PQS system. Cell survival, biofilm formation, and virulence are controlled by these systems and strains deficient in any one of these systems demonstrate reduced pathogenicity (Kostylev et al., 2019).QS Deficient mutants (Δ*lasR:*Δ*rhlR* and Δ*lasI:*Δ*rhlI*) showed weak biofilm formation which was susceptible to antibiotic treatment. At the same time, Bjarnsholt et al showed that the presence of at least one of the QS system i.e. Rhl system resulted in mucoid phenotypes (by over production of alginate and rhamnolipids) producing chronic infections (Bjarnsholt et al., 2010; Okkotsu et al., 2014). Rhamnolipids are key molecule involved in the formation of water channels facilitating availability of water and nutrients (Rikalovic et al., 2017). Pyocyanin, one of the major virulence factors of *Pseudomonas*, which is involved in eDNA release is also under the control of the QS system (Das et al., 2016). It can be noted that, most of the secreted products augment growth and survival of bacteria, at the same time had deleterious effect on the host tissue. Secretome analysis of the pulmonary exacerbation of infected patients shows the overexpression of QS controlled virulence factors like elastase, Protease, Pyocyanin, exotoxins, rhamnolipids and Hydrogen Cyanide (Moradali et al., 2017).

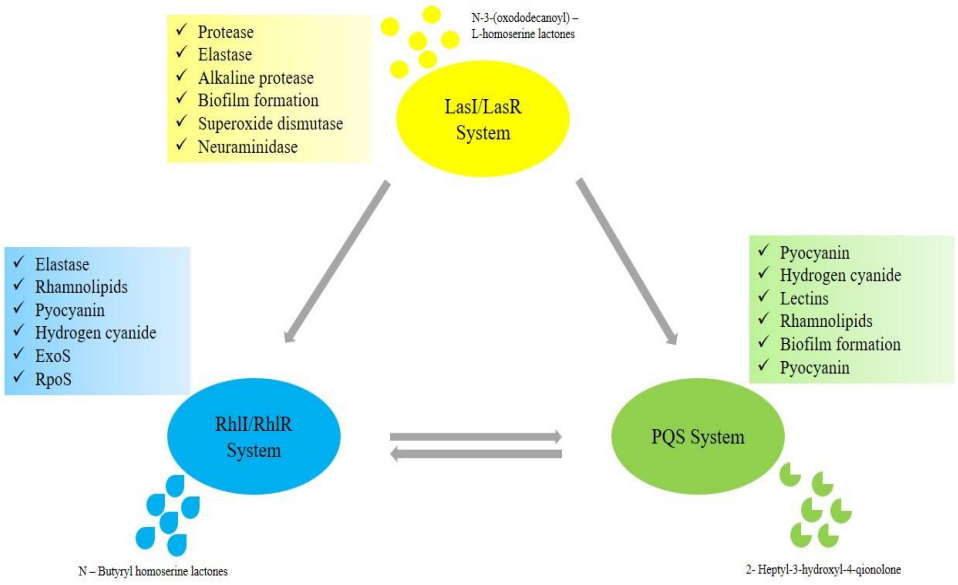

Fig.3: Schematic representation of the quorum sensing systems of *Pseudomonas* and the virulence factors controlled by QS. Biofilm formation and the expression of all the major virulence factors are under the control of the QS system. It helps coordinated gene expression in the bacterial population.

2.1.7. Virulence factors in *Pseudomonas*

Virulence factors are molecules that help bacteria survive and evade host immune response during the early stages of infection (Moradali et al., 2017). Although these factors are responsible for growth and survival of bacteria, they cause extensive toxicity to the cells. Production of virulence factors is energy dependent process and QS controlled (García-Contreras, 2016; Jurado-Martín et al., 2021). Pulmonary secretions and bronchial exacerbations from CF patients showed the presence of virulence factors like proteases, phenazines (pyocyanin), exotoxin A, rhamnolipids and hydrogen cyanide (J. Lee & Zhang, 2015; Moradali et al., 2017). The factors are known to impair barrier integrity, inhibit protein synthesis in the host and induce cell death (J. Lee & Zhang, 2015).

Pyocyanin (PCN) is one of the best studied virulence factors of *Pseudomonas*. Pyocyanin was detected in sputum samples, ear secretions, wounds and urine samples of patients with chronic *Pseudomonas* infections (S. Hall et al., 2016; Žukovskaja et al., 2017). Cytotoxicity by PCN is mediated by the production of oxidative stress in the cells, due to its ability to increase the superoxide radical levels (Priyaja et al., 2016).

Das and Manefield, observed that strains that overproduced PCN, showed increased cytotoxicity and eDNA release (Das & Manefield, 2012) . PCN in turn intercalates with the release eDNA and enhance biofilm formation. PCN plays multiple roles in pathogenesis of *Pseudomonas*. Rada et al, showed an increase in pro inflammatory cytokine gene expression in airway epithelial cells upon exposure to PCN (Rada et al., 2011).

Rhamnolipids are bio-surfactants containing rhamnose sugar linked to β – hydroxylated fatty acid chains (Chong & Li, 2017). Presence of rhamnolipids increases cell surface hydrophobicity enabling bacterial surface adhesion (Hamzah et al., 2020; Nickzad & Déziel, 2014). The production of rhamnolipids is under the regulation of the QS system (Reis et al., 2011). Rhamnolipids induced faster cell death in the eukaryote *Dictyostelium discoideum*. Rhamnolipids were found to induce actin remodelling in macrophages, reducing its ability to phagocytose (Thakur et al., 2021). Zulianello and colleagues, revealed that rhamnolipids promote early infiltration of primary airway epithelial cells. Addition of rhamnolipids altered the paracellular permeability and transepithelial resistance by disrupting the tight junctions (Zulianello et al., 2006). This facilitated an increase in tissue invasion by *Pseudomonas*.

Pseudomonas is known to secrete a number of proteases and is under the regulation of QS system (X.-H. Li & Lee, 2019). Although the extact role of protease is unclear, it was proposed that they help in nutrient scavenging. Elastase and alkaline protease are the two most studied proteases of *Pseudomonas*. Elastase is capable of degrading ealstin and collagen in tissues (Kon et al., 1999). Both elastase and protease play detrimental roles during the pathogenesis. Proteases increase the epithelial permeability of the lung by the disruption of the tight junctions. They are capable of inhibiting fibroblast growth and degradation of components of the host immune response like the complement proteins, surfactant proteins, cytokines and immunoglobulins (Kon et al., 1999).

2.2. *In-vitro* systems to study *Pseudomonas* biofilm interactions

Understanding the multifaceted host pathogen interaction is important in developing host targeted treatment strategies. This can be accomplished by the use of an *in-vitro* model system that could simulate the *in-vivo* conditions (Crabbé et al., 2014). The physiologically relevant factors like apical – basal polarity, junctional complexes, mucus, multi-cellularity, and extracellular matrix proteins, have to be considered while designing an *in-vitro* system (Crabbé et al., 2014).

In-vitro cell and tissue culture models are being extensively used to study both host and pathogen responses during an infection. More physiologically relevant models are necessary because cell and tissue culture models often lack multicellular complexity and `lack properties of parental tissue (Barron et al., 2021; Bermudez-Brito et al., 2013). The availability of animal models has been instrumental in understanding disease progression and pathogenesis, but fails to mimic human physiology (King, 2012; Zhao & Bhattacharyya, 2018). Most often, answers to fundamental questions are addressed by the use of *in-vitro* models and confirmed using animal models.

2.2.1. Two Dimensional cultures:

2D cultures often consist of a single type of cell grown on non-permeable surface. Cells used for understanding the lung infections of *Pseudomonas* are A549 (Type II pneumocyte), 16HBE (human bronchial epithelial cells) and CFBE (human cystic fibrosis bronchial epithelial cells). Primary cells from healthy volunteers, lung biopsies, nasal polyps etc are also used to develop 2D cultures (Choi et al., 2020; Ordovas-Montanes et al., 2018). They are cost effective, can be easily maintained and manipulated in laboratory set up. 2D systems consist of homogeneous cell population and results obtained are highly reproducible. The major disadvantage of using 2D system is that the cells lack polarity and fail to express apical basolateral markers. They fail as an infection model as cells detach easily upon infection (Youk et al., 2020).

2.2.2. Two-Dimensional Air – Liquid Interface culture

This model system uses cell monolayers formed on semi - permeable Transwell membranes. Airway epithelial cells are lifted to air – liquid interface by removing the media from the apical side of the transwell inserts (Müller et al., 2013). Media is supplemented from the basal compartments of the inserts. Primary airway epithelial cells grown at an air liquid interface were shown to be successful in mimicking in-vivo conditions and expresses polarity and tight junctions. Few limitations associated with the use of ALI system is that they are expensive and time consuming and have limited high throughput capabilities (Upadhyay & Palmberg, 2018). The amenability of this system to the inclusion of multiple cell types and biomechanical forces a makes them an ideal candidate to study host pathogen interaction in-vitro (Strässle et al., 2021).

2.2.3. Electrical cell substrate impedance sensing (ECIS) to study bacterial pathogenesis

Electrical cell substrate impedance sensing (ECIS) is a label free, non – invasive, impedance-based method to study cell responses to stimuli. Changes in morphology, locomotion and changes in cytoskeleton of the cells have been studied using ECIS. A small alternating current (AC) is applied across an electrode in the ECIS arrays, and the resultant potential is measured. When cells attach and spread over the electrodes, the plasma membranes act as insulators i.e., prevent the flow of current (https:/www.biophysics.com). The increase in the number of cells spread on the electrodes increases the impedance and the results are plotted as impedance against time.

Altering the AC frequencies reveal characteristic features of cellular responses. At lower frequency (<2000Hz), the current flows through focal adhesion points and intercellular junctions and reveals the integrity of cellular junctions (Fig 4). At higher frequencies (>40000Hz), the direction of current flow is directly through the insulating membranes of cell and reveals electrode coverage or number of cells attached on electrodes (https:/www.biophysics.com). The first evidence of impedance based changes in cell response was provided by Giaever and Keese (Giaever & Keese, 1991).

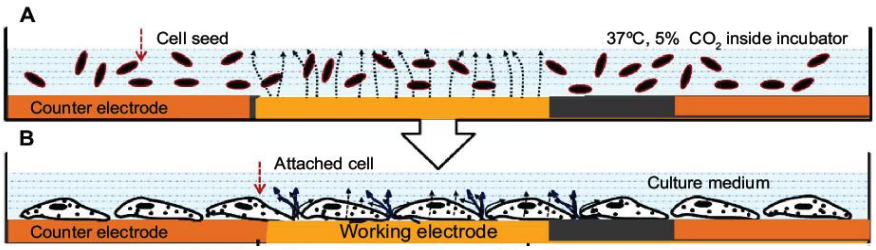

Fig.4: Seeding of cells on ECIS electrode arrays. A. The cells were seeded on the electrodes. B. As the cells attach and spread on the working electrode and counter electrode, impedance is increased. Image Source – https:/www.biophysics.com

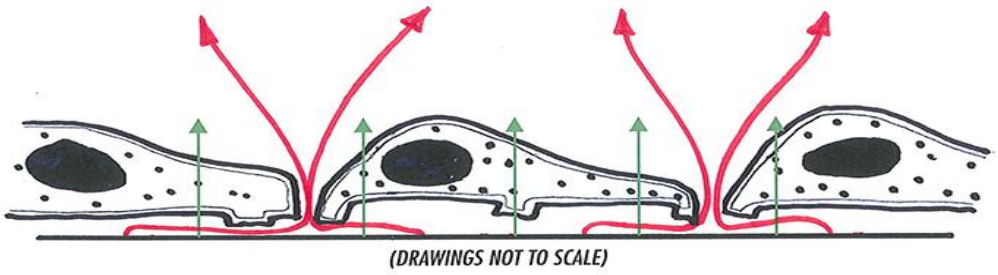

@ Frequency < 2000Hz

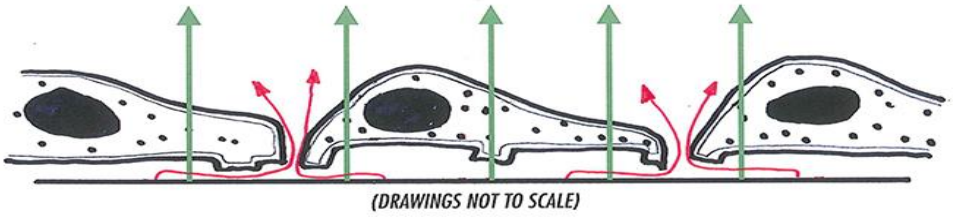

@ Frequency < 40000Hz

Fig.5: Effect of frequencies on flow of current across the cells. At lower frequencies the path followed by the current is between the focal adhesion points and inter cellular junctions and at higher frequencies the current flows directly through the insulating membrane of the cells. Image Source – https:/www.biophysics.com

Every cell type has a specific growth and adhesion curve which is controlled by seeding densities (Fig 4). The characteristics are analysed as by changes in capacitance and resistance. As the cells start attaching and spreading on the surface of the cells, there is a reduction in capacitance and increase in resistance (Fig 5). Any changes in junctional integrity, morphology or detachment of cells will result in decrease in impedance measured.

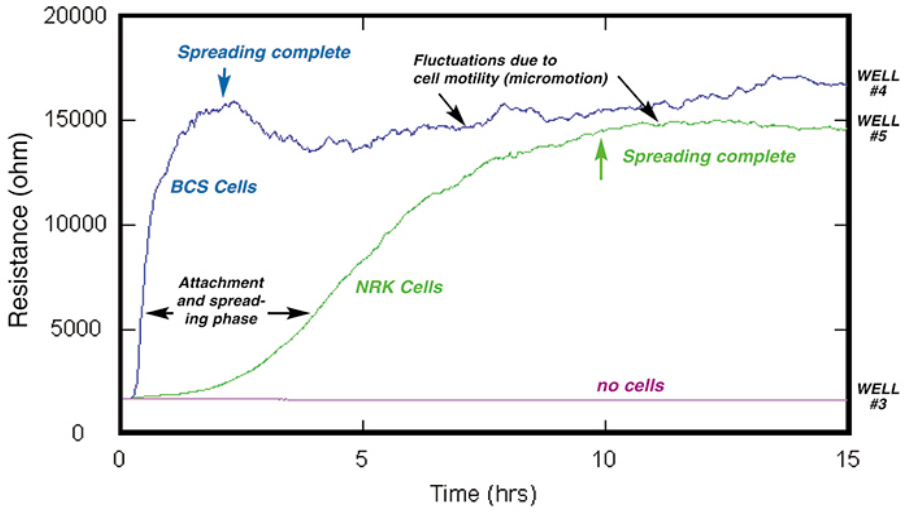

Fig.6: The attachment and growth rate of different cells are different. As the cells spread an increase in impedance was observed and once the electrode coverage is complete i.e., at confluence the impedance attains plateau. Any manipulations at this stage can reveal effect of these manipulations on the junctional integrity and morphology. Image Source – https:/www.biophysics.com

ECIS is being used to study multiple aspects of cancer metastasis, toxicology, wound healing and other related fields. Increasing studies suggest the use of ECIS in studying the pathogenesis of lytic viral infections (Pennington & Walle, 2017). The study revealed the feasibility of using ECIS to study the effect of multiplicity of infection of lytic viral infections. Not many studies have revealed the use of ECIS in studying bacterial pathogenesis.

2.3. Immune response to biofilms of *Pseudomonas.*

When Iilya Metchnikoff and Paul Ehrlich got the Nobel Prize in 1908 Immunology was introduced as an academic discipline and gained prominence. The effective surveillance by the immune system protects the host from infection by invading pathogens. Numerous studies have explored the diverse nature of immune response to pathogens on invading microorganisms (Chaplin, 2010). But most of the studied mechanisms of immune responses were true for infection by planktonic organisms (acute). The knowledge of the immune responses to biofilm infections (chronic) is limited (P. Ø. Jensen et al., 2010). Recent research in this field has discovered the involvement of both the arms of immune system in response to biofilm infections. Both innate and adaptive immune system plays key role in the process. It

can be noticed that the simultaneous involvement of both the arms of the immune system still is not capable of eliminating the biofilm but instead cause host tissue damage providing a favourable niche for the microorganism (P. Ø. Jensen et al., 2010; J. Leid, 2009).

2.3.1. INNATE IMMUNE RESPONSE TO BIOFILMS

The innate immune response provides non-specific protection to host from invading pathogens. It was observed that exposing disrupted components of *Pseudomonas* biofilms to neutrophils and macrophages induced responses like respiratory burst, accumulation, penetration, phagocytosis and killing of biofilm bacteria (Moser et al., 2021). Van Gennip et al, provided experimental evidence of the presence of activated neutrophil and its accumulation around the biofilm in mouse lung (VAN GENNIP et al., 2009). In response to *Pseudomonas* biofilm infection in the lung, activated neutrophils were also observed in the airways (Maurice et al., 2018; Rada, 2017). The accumulation of neutrophils around the *S. aureus* biofilm induced hypoxia, which further activates neutrophils (Hajdamowicz et al., 2019). The activation of neutrophils occurs by direct contact with bacteria, by lipopolysaccharide-immune complexes or by alginate also neutrophils may be primed by bacterial endotoxins and by soluble components of the innate immune response such as tumor necrosis factor-α (TNF-α), platelet-activating factor, leukotriene B4, and interleukin-8 (IL-8). The presence of activated and accumulated neutrophils has also been demonstrated in chronic wound infections (P. Ø. Jensen et al., 2010). Jensen et al., found that oxidative burst in response to biofilms were 25% lesser than in response to planktonic *Pseudomonas* (E. T. Jensen et al., 1990; Maurice et al., 2018). Neutrophils exposed to mature *Pseudomonas* biofilms were found to reduce motility and apparently undergo necrotic cell death (Maurice et al., 2018). The EPS rich in rhamnolipids induced neutrophil death and impaired chemotaxis. Mucoid strains of *Pseudomonas* are found to resist the neutrophil extracellular traps (made of DNA and granule proteins). Instead eDNA and actin from neutrophils are assimilated into the biofilm matrix evade host immune responses and antimicrobials (Maurice et al., 2018). The ability of the innate immune system to recognize these pathogens are due to the

presence of PRRs (pathogen recognition receptors) which detects various conserved sequences of the pathogen called PAMPs (Pathogen Associated Molecular Patterns) (Mogensen, 2009). Various PRRs and their associated PAMPs are listed in Table 2. PRR specific for biofilm infections has not yet been identified. Macrophages are involved in active phagocytosis and clearance of bacteria from the host. Mittal et al., suggest that biofilms of *Pseudomonas* induce stronger pro-inflammatory cytokine response than its planktonic counterparts (Mittal et al., 2009). In fact, exposure of *Pseudomonas* biofilms to macrophage secretome was found to accelerate expression of virulence factors and biofilm formation (Mittal et al., 2006). Dendritic cells are the major antigen presenting cells of the innate immune system. Studies in mouse model of chronic *Pseudomonas* biofilm infection reveals the presence of activated dendritic cells in the lung on day 2 and in the local lymph nodes by day 7. The initial responses showed an increase in pro inflammatory cytokines IL 6 and IL12, which was followed by an anti-inflammatory response (IL10) suggesting that DCs down regulates prolonged inflammatory responses (González et al., 2018).

The role of complement system in immune responses is remarkable. But their role in biofilm infection is far from being established (Moser et al., 2021). A few studies report the presence of activated complement in the sputum of CF patient with chronic *Pseudomonas* infection. However, it was not determined whether this activation was due to biofilm or by planktonic bacteria. Studies reported that the alkaline phosphatase and elastase released by *Pseudomonas* is capable of degrading the complement proteins (Gellatly & Hancock, 2013). Davies et al., demonstrated that *Pseudomonas* isolated from chronic infection avoided binding to complement receptors, avoiding complement activation (Moser et al., 2021). The presence of very high levels of alginate in the extrapolymeric matrix has been attributed to the ability of *Pseudomonas* to evade complement proteins. O-acetylation, O-glycosylation and Psl polysaccharide components help protect the biofilms from complement mediated opsonisation. *Pseudomonas* is also known to inhibit lectin mediated complement activation pathway (Moser et al., 2021).

Pathogen recognition and subsequent activation of innate immune response is mediated by a group of PRRs called the Toll Like Receptors (TLRs) (Table 3).

Different TLRs, their cellular location and their corresponding PAMPs have been listed in table 3. Since TLRs are the major group of PRRs involved in pathogen recognition, it has been suspected to play crucial role in biofilm related infections (E. T. Jensen et al., 1990; P. Ø. Jensen et al., 2010). It was discovered by Koller et al., that TLR5 is the only MyD88 dependent TLR, upregulated in chronically infected Cystic Fibrosis patients (Moser et al., 2021). Another group of PRRs namely Nod Like receptors (NLRs) have been identified to play vital role in innate immune responses. The study revealed that Nod1 could detect *Pseudomonas* peptidoglycan and subsequent activation of Nf-κB leading to cytokine secretion and bacterial killing (Caruso et al., 2014). Further, bacterial killing and cytokine secretion was found to be significantly altered when Nod1 deficient cells were infected with *Pseudomonas*. All these suggest a possible vital role for NLRs in immune response to biofilms, which needs to be thoroughly investigated. TLR 5 mediated enhanced phagocytosis was the major mechanism of killing in flagella intact planktonic bacteria.

Other potent activators of TLR responses could be the bacterial DNA and alginate in the extracellular polymer matrix (Moser et al., 2021). Bacterial DNA activates the neutrophils via the TLR 9 dependent pathway. It has been proposed that alginate might induce the production of cytokines by monocytes that can have immune modulatory activity. It is also possible that the specific components of the polysaccharide namely Psl and Pel could generate biofilm specific responses (Rybtke et al., 2020). It was identified by Jensen and group that the rhamnolipids produced by *Pseudomonas* were powerful in eliminating the neutrophils and acted as a neutrophil shield (P. Ø. Jensen et al., 2010). The study also elucidated an increase in rhamnolipid expression by biofilms when exposed to neutrophils (VAN GENNIP et al., 2009).

Dossel and group, in their study on beta-defensins in innate immune response to PA biofilms, reported that the rhamnolipid component of the biofilms significantly inhibited beta defensins in keratinocytes (Dössel et al., 2012).

Receptor (location)	Target (source)	Effect of recognition
Complement (blood stream, tissue fluids)	Microbial cell wall components	Complement activation, opsonization, lysis
Mannose binding lectins	Mannose containing bacterial carbohydrates	Complement activation opsonization
C reactive protein	Phosphatidyl choline, pneumococcal polysaccharide	Complement activation opsonization
Lipopolysaccharide receptor	Bacterial lipopolysaccharide	Delivery to cell membrane
Toll like receptors	Microbial components not found in host	Induce innate response
NOD family of receptors	Bacterial cell wall components	Induce innate response
Scavenger receptors	Many receptors	Induce phagocytosis and endocytosis

Table 3: Receptors of the innate immune system, their ligands, and consequences of ligand receptor binding

They also demonstrated the inhibitory activity of flagellin on IL-1β a potent activator of beta defensins, indirectly supporting biofilm formation. The high alginate content with O – acetylation in the extra polymeric matrix of biofilm was effective in inhibiting the soluble components of innate immune response like the complement system (Ørning et al., 2016).

2.3.2. ADAPTIVE IMMUNE REPONSE

Adaptive immune response had developed as a specific immune response to an antigenic challenge. Memory cells of adaptive responses also have characteristic that enables the system to eliminate the pathogen easily and quickly during a second infection having same antigen (Marshall et al., 2018). Adaptive immune response comes into action together with or after a brief interval following the activation of innate immunity. Adaptive immune response is similar for both planktonic and biofilms components (Marshall et al., 2018).

Adaptive immune response/ Acquired immunity identified specific molecules of pathogens and maintain memory of the same, for a more effective response on

repeated exposure. It is obvious that the innate immune response has a significant role in deciding the type of adaptive response. Biofilm formation results in persistent infections that can repel antibodies, phagocytosis and other components of the host response (P. Ø. Jensen et al., 2010). Deleterious effects occur when activated immune products and immune cells attack the surrounding tissue. Instead a compromised immune response results is caused by degradation of surface molecules on the immune cells by the host cell released factors (Hänsch, 2012). The presence of neutralizing antibodies against elastase, lipopolysaccharide and flagella has been reported in *Pseudomonas* infections in CF patients (P. Ø. Jensen et al., 2010).Development of biofilms in CF lungs was found to disturb the balance in Th1/Th2 responses. Chronic infections were hallmarked by the presence of IL-4 in abundance, which is a Th2 cytokine. IFNγ was the most abundant cytokine in non – chronic infections. This clearly suggests a paradigm shift from Th1 to Th2 responses in chronic biofilm infections (González et al., 2018; Yamada & Kielian, 2019). Moser et al, showed that C3H/HeN mice (predominant Th1 response), produced large quantities of IFNγ and were more effective in clearing *Pseudomonas* infection than BALB/c mice, in which IL4 was found in abundance and predominantly exhibited Th2 responses. CF patients were also detected with high levels of IL 10 (anti – inflammatory), B cells and IgA antibodies confirming Th2 responses (Moser et al., 1997; MOSER et al., 2002).

One of the major cell subsets that activate the adaptive immune response are the dendritic cells (DC). It was observed by Moser et al that in cystic fibrosis patients DC2 response that activates the Th2 response was observed (Moser et al., 2005).Adaptive immunity is also characterized by the production of large amounts of neutralizing antibodies and also help in antibody mediated complement activation. Analysis of antibodies in chronic infection revealed the presence of antibodies with low antigen affinity resulting from failure of affinity maturation (T cell activated B cell produce antibodies with high affinity). However, Moser et al, provide evidence for the presence of protective antibody responses to *Pseudomonas* biofilms (Moser et al., 2021).

3. MATERIALS AND METHODS

3.1. Phase I – To understand the dynamics of biofilm formation by *Pseudomonas* isolates

3.1.1. Bacterial Isolates and Characterization:

Pseudomonas aeroginosa ATCC 27853 isolate was obtained from American Type Culture Collection. ATCC 27853 was obtained from blood culture of a septicaemia patient. The clinical isolates S373, S402, S125, S253, S135, S268, S45, S277 and S18 was obtained from the culture repository at Dept. of Microbiology, Sree Chitra Tirunal Institute for Medical Science and Technology (SCTIMST), Thiruvananthapuram- 11. The isolates were obtained from bronchiectasis patients.

The isolates were cryopreserved in Soyabean Casein Digest medium (TSB) containing 15% glycerol as cryoprotectant. The cultures were revived in TSB and maintained in Soyabean Casein Digest Agar (TSA) slants and stored at 4ºC for a month. Once revived, the isolate was sub-cultured only till 5 passages to prevent genetic variation.

Bacterial characterization was performed by classic microbiological methods and the result are depicted in Table 4.

3.1.2. Antibiotic sensitivity by Agar Diffusion method

Antibiotic sensitivity of the isolates was assessed by Agar diffusion method. Overnight culture adjusted to a Mac Farland standard 0.5 was swabbed to obtain lawn cultures on Muller Hinton Agar plates. Antibiotic discs (Amikacin, Ceftazidime, Ciprofloxacin, Gentamicin and Norfloxacin - HiMedia laboratoires) were placed appropriately on the MHA spread with the culture and incubated overnight at 37ºC. Zone of inhibition was measured and compared with the HiMedia Antibiotic sensitivity chart to understand sensitivity to the particular antibiotic.

3.1.3. Biofilm Quantification - Crystal Violet assay

The ability of *Pseudomonas* isolates to develop biofilms were assessed by Crystal Violet assay (CV assay) as described by O.Toole, with slight modification, in 96well microtitre plates (O'Toole, 2011). In Brief, 100µl overnight culture of *Pseudomonas*, adjusted to an OD_{600nm} of 1.0, was added to 100µl of TSB in 96 well format. The setup

was then incubated at 37ºC. Following incubation, the media was removed from the wells. The loosely adhered bacteria were washed off with Phosphate buffered saline (PBS) thrice and stained using 200µl of 0.1% crystal violet and incubated for 15min. the unbound stain was washed using PBS thrice. The bound crystal violet was eluted using 95% ethanol. Absorbance at 600nm was measured using Synergy H1 multimode reader (Merritt et al., 2005; Xi & Wu, 2010). For all the biofilm experiments ATCC 27853 was the positive control used.

Test	**ATCC 27853**	**S373**	**S402**	**S125**	**S253**	**S135**	**S268**	**S45**	**S277**	**S18**
Gram's reaction	-ve	-ve	-ve	-ve	-ve	-ve	-ve	-ve	-ve	-ve
Shape	Rods	Rods	Rods	Rods	Rods	Rods	Rods	Rods	Rods	Rods
Motility	Motile	Motile	Motile	Motile	Motile	Motile	Motile	Motile	Motile	Motile
Indole	-ve	-ve	-ve	-ve	-ve	-ve	-ve	-ve	-ve	-ve
Methyl red	-ve	-ve	-ve	-ve	-ve	-ve	-ve	-ve	-ve	-ve
Voges proskauer	-ve	-ve	-ve	-ve	-ve	-ve	-ve	-ve	-ve	-ve
Citrate	+ve	+ve	+ve	+ve	+ve	+ve	+ve	+ve	+ve	+ve
TSI	AK/AK	AK/AK	AK/AK	AK/AK	AK/AK	AK/AK	AK/AK	AK/AK	AK/AK	AK/AK
Oxidase	+ve	+ve	+ve	+ve	+ve	+ve	+ve	+ve	+ve	+ve
Catalase	+ve	+ve	+ve	+ve	+ve	+ve	+ve	+ve	+ve	+ve
Nitrate reduction	+ve	+ve	+ve	+ve	+ve	+ve	+ve	+ve	+ve	+ve
Urease	-ve	-ve	-ve	-ve	-ve	-ve	-ve	-ve	-ve	-ve

Table 4: Biochemical characterization of ATCC 27853 strain and clinical isolates of *Pseudomonas.* AK/AK – Alkaline butt and Alkaline slant

3.1.4. Effect of pH on biofilm formation:

pH is known to significantly influence biofilm formation. Jones et al, studied chronic wound healing and suggested that bacterial colonization in wounds resulted in alteration of pH (4 – 10) (Jones et al., 2015). Therefore, the influence of pH in biofilm formation by *Pseudomonas* was evaluated. The effect of pH on biofilm formation was assessed by using TSB at different pH (4.0, 7.4 and 10.00). Biofilm formation at varying pH was analysed at 48hr of incubation by CV Assay methods described previously.

3.1.5. Effect of Temperature on biofilm formation:

Temperature plays important role in biofilm formation by *Pseudomonas.* The effect of temperature was analysed by quantifying biofilms formed at different temperatures at ambient temperature (27 ± 2°C), physiological temperature 37ºC and fever temperature on 39ºC. The biofilms were quantified using CV assay as described previously.

3.1.6. Effect of glucose in biofilm formation:

Glucose is an important carbon source and is known to influence biofilm formation. Effect of glucose was analysed by quantifying biofilms formed in minimal media supplemented with varying concentrations of glucose (0µg/ml, 10µg/ml, 20µg/ml, 40µg/ml, 60µg/ml, 80µg/ml and 100µg/ml). The biofilms formed were quantified by CV assay as described in section 3.2.9.

3.1.7. Effect of Iron on biofilm formation:

Kang et al, suggested that iron is an important cofactor necessary for biofilm formation (Kang & Kirienko, 2018). *Pseudomonas* is capable of siderophoric and non-siderophoric acquisition of iron. Effect of iron on biofilm formation was assessed by quantifying biofilms formed at different concentration of Iron (0mM, 10mM, 50mM and 100mM). CV assay was performed at 48hr of incubation, by the method described in the section 3.1.3.

3.1.8. Effect of antibiotics on biofilm formation:

Antibiotics are the first line of treatment of bacterial infections (Paterson et al., 2016). It was observed that the Minimal inhibitory concentrations of antibiotics needed to kill

biofilms are 100 - 1000 times more than that for planktonic counterparts (Penesyan et al., 2021; D. Sharma et al., 2019). Hence we assessed that effect of varying concentration of Cephalosporin (Ceftazidime MIC - 30µg/ml), Aminoglycoside (gentamicin MIC 10µg/ml) and Fluoroquinolone (Norfloxacin MIC 10µg/ml), was assessed by developing biofilms at varying concentration of these antibiotics (Crandon et al., 2012). CV was used to quantitate biofilms.

eDNA is an integral part of the biofilm. It plays important roles in the development of biofilms and maintenance of the 3D architecture of biofilms. eDNA is known to chelate positively charged antibiotics and prevents its entry into the biofilm. We evaluate the effect of antibiotics on eDNA release by *Pseudomonas* biofilms (Devaraj et al., 2019).

3.1.9. eDNA extraction:

eDNA isolation from biofilms was carried out by the method described by Kaplan et al (Kaplan et al., 2012). In brief, *Pseudomonas* was cultured in 6 well microtitre plates for 48hr. following incubation the media from the wells were carefully removed, and 1ml TE buffer was added to each well (10mMTris, 1mMEDTA (pH 8)). Using a cell scrapper, the biofilms were scrapped from the wells and transferred into a 1.5ml centrifuge tube. The tubes were centrifuged for 25sec at 13000rpm. The supernatant was discarded. The pellet was resuspended in 200µl TE buffer and centrifuges again at 13000rpm for 25sec. 30µl of the supernatant want electrophoresed through 1% agarose gels and visualised by Ethidium Bromide staining.

3.1.10. Effect of antibiotics on eDNA release in biofilms

To assess the effect of antibiotics on eDNA release, *Pseudomonas* was cultured in 6 well microtitre plates in 4ml TSB containing different concentrations of antibiotics Cephalosporin (Ceftazidime MIC - 30µg/ml), Aminoglycoside (gentamicin MIC 10µg/ml) and Fluoroquinolone (Norfloxacin MIC 10µg/ml).The concentrations used were Ceftazidime 7.5µg/ml, 15µg/ml, 30µg/ml and 45 µg/ml, Gentamicin 2.5µg/ml, 5µg/ml, 10µg/ml and 15µg/ml. and Norfloxacin 2.5µg/ml, 5µg/ml, 10µg/ml and 15µg/ml. eDNA from the antibiotic treated biofilms were isolated and viewed by the method described in section 3.2.10.

3.1.11. Estimation of secreted virulence factors:

3.1.11.1. Estimation of Pyocyanin

Pyocyanin was estimated from culture supernatant acidified solution by method described by Essar et al (Essar et al., 1990). Overnight culture of *Pseudomonas* was adjusted to OD_{600nm} of 1.0 and inoculated into TSB. Following 48hr of incubation, 1ml of culture supernatant was added with 450µl of chloroform and 150µl 0.2 M HCl, vortexed and centrifuged at 10,000g for 2min at 4ºC. The absorbance of the pink colored upper aqueous layer was measured at 520nm. The standard reference strain ATCC 27853 was used as the positive control.

3.1.11.2. Estimation of Rhamnolipids:

Rhamnolipids were quantified by method described by Rasamiravaka (Rasamiravaka et al., 2016). The culture supernatant was adjusted to a pH of 2.3 using 1N HCl. To 500µl of this supernatant 500µl of ethyl acetate was added, vortexed for 20sec and centrifuged at 10,000rpm for 10min. This extraction was done thrice, and the supernatants were pooled, centrifuged at 10,000rpm for 10min and air dried to remove ethyl acetate. 1ml of chloroform containing 100µl of methylene blue was added, mixed, and incubated at ambient temperature (25ºC to 28ºC) for 15min. To this 500µl of 0.2M HCl was added, and vortexed. This mixture was centrifuged at 10000rpm for 10min, and absorbance of the aqueous phase was measured at 630nm using Synergy H1 plate reader. ATCC 27853 was used as the positive control.

3.1.11.3. Estimation of proteases:

Protease was assessed in culture supernatants of biofilms by the method described by El-Mowafy et al. (El-Mowafy et al., 2014). In brief, the cell free supernatant (500µl) was added to 1ml of 1.25% w/v skimmed milk solution and incubated at 37ºC for 30min. Resultant turbidity was measured at 600nm using synergy H1 plate reader. ATCC 27853 was the standard reference strain and was used as the positive control.

3.1.12. *C. elegans* killing assay

C. elegans killing is one of the model systems used to understand bacterial virulence. This system allows for the understanding of virulence and host responses. Therefore the virulence of *Pseudomonas* isolates was assessed by *C. elegans* killing assay as described by Tan et al (Tan et al., 1999). Briefly, overnight culture was spread plate on Nematode Growth Medium (NGM) and incubated overnight. 30 – 40 L4 stage

nematodes were added on to each plate and incubated at 25ºC. Dead nematodes were counted at 24hr and 48hr post infection. The nematodes that do not respond to touch was considered dead. The nematodes that got stuck at the wall of the plate were excluded from the study. The negative control used in the study was *E. coli* OP50. For statistical analysis all the experiments were done in triplicates.

3.2. Phase II. Development of a suitable *in-vitro* system

3.2.1. Cell lines and culture conditions

Human Lung adenocarcinoma cell line A549 was used as a representative of Type II alveolar epithelial cells. The cell line was obtained from American Type Culture Collection (ATCC) and used at passage numbers P23 to P 26. The cells were cultured in Nutrient Hams F12K medium supplemented with 10% Fetal Bovine Serum (FBS), Gentamicin (10µg/ml) and Amphotericin B (2.5µg/ml) and incubated at 37ºC with 5% CO_2. Upon 90% confluence, the cells were trypsinised and sub-cultured in the ratio 1:6. The cells were cryopreserved (-80ºC) in complete media supplemented with 5% Dimethyl sulphoxide (v/v) (DMSO). Long term preservation was done in Liquid Nitrogen vapor phase.

Monocyte cell line THP1 of human origin, isolated from a case of acute monocytic leukemia was obtained from ATCC. They are phagocytic to latex beads and sensitized erythrocytes and do not express surface or cytoplasmic immnoglobulins. The cells were maintained in RPMI-1640 medium supplemented with 10% FBS, gentamicin (10µg/ml) and amphotericin B (2.5µg/ml) and incubated at 37ºC with 5% CO_2. Upon 90% confluence, the cells were split in the ratio 1:6. The cells were cryopreserved (-80ºC) in complete media supplemented with 5% DMSO (v/v). Long term preservation was done in liquid nitrogen vapor phase.

Both the cell lines were checked at regular intervals for *Mycoplasma* contamination using TaKaRa PCR Mycoplasma Detection Kit (cat.no.6601, TaKaRa, Japan)

3.2.2. Development of submerged cultures

Submerged cultures were developed using A549 cells to study the interaction between alveolar epithelial cells and biofilms. 10^5 (in 500µl medium) A549 cells were

seeded per well in 24 well plates (Thermoscientific, Germany) and incubated at 37ºC and 5%CO_2 (Diabaté et al., 2021). Upon confluence (24hr – 36hr after seeding), the medium was changed to F12K without antibiotics supplemented with 25mM 4-(2-hydroxyethyl) – 1- piperazineethanesulfonic acid (HEPES).

3.2.3. Infection of submerged cultures

The feasibility of using submerged cultures to study interaction of *Pseudomonas* biofilms with A549 cells was assessed. Overnight culture of *Pseudomonas* was adjusted to an OD_{600nm} of 1.0. The *Pseudomonas* culture was diluted to get a multiplicity of infection of 100:1(bacteria: host cells) and A549 cells were infected (the MOI of 100:1 was verified multiple times by viable count method – part of standardisation). The cells were incubated at 37ºC. The cells were evaluated for morphological changes on Leica Phase Contrast Microscope over a period of 8hr.

3.2.4. Development of Air Liquid Interface culture:

To better simulate the *in-vivo* conditions, air liquid interface cultures were developed. A549 monolayers were developed on 24 well Costar™ Transwell transparent permeable supports with pore size 0.4µm. Upon confluence the media from the apical side of the membrane was removed. The media in the basal chamber was changed to F12K without antibiotics and with 25mM HEPES 2hr prior to infection experiments (J. Wu et al., 2017).

3.2.5. *Pseudomonas* infection of A549 at Air – Liquid interface

Biofilm on live A549 cells were developed as described by Woodworth et al, (Woodworth et al., 2008). In short, confluent monolayers of A549 was infected using *Pseudomonas* overnight culture adjusted to an OD_{600nm} 1.0. A MOI of 100:1 (bacteria: host cells) was used for infection. *Pseudomonas* diluted in Luria Bertani broth and Phosphate Buffered saline was used for infection to establish an appropriate medium for infection (Woodworth et al., 2008).

3.2.6. Development of *Pseudomonas* biofilms on endotracheal tube.

Rusch® Endotracheal tubes (ETT) size Internal Diameter 6.5mm, Outer Diameter 8.7mm and cuff 20.5mm made of polyvinyl chloride (PVC) were used as a substrate to develop biofilms of *Pseudomonas*. *Pseudomonas* biofilms were developed on ETT according to the method described by Pericolini et al, with slight modification (Pericolini et al., 2018). Briefly, ETT was cut into small pieces roughly

of the same size and sterilized by ethylene oxide sterilization at 37ºC. Overnight culture adjusted to OD_{600nm} of 1.0 was used to inoculate 25ml TSB containing pieces of ETT in a conical flask (250ml). It was incubated at 37ºC for 48hr.

3.2.6.1.Evaluation of biofilm formed on ETT

The biofilms formed on the surface of ETT was evaluated by staining with crystal violet and Acridine orange. Following 48hr of biofilm formation ETT pieces were washed thrice with PBS and stained using 1% crystal violet for better imaging and imaged using Leica microscope.

Crystal violet stains both bacteria and the surrounding exopolymeric matrix (Amador et al., 2021). To visualize *Pseudomonas* within the biofilm, the biofilms formed on ETT pieces were stained using acridine orange. ETT pieces also were stained using Acridine orange (0.1% solution) to evaluate the biofilms formed on its surface and imaged using Leica microscope (100X) (Harrison et al., 2006).

3.2.7. Infection of A549 cells at Air-Liquid Interface using biofilms on ETT pieces

A549 monolayers were developed at an air – liquid interface on Costar™ transwell transparent permeable supports with pore size 0.4µm. Following confluence, the media from the apical side was removed, and the media in the basal compartment was changed to F12K without antibiotics and supplemented with 25mM HEPES. The ETT with biofilm was washed thrice with PBS to remove loosely adhered *Pseudomonas and* introduced from the apical side of the membrane and incubated at 37ºC. A549 cells were evaluated for changes in morphology.

3.2.8. Assessment of cell viability by Live Dead staining:

The viability of A549 cells following infection was assessed by Live /Dead® Viability/Cytotoxicity test kit (Molecular Probes) as per kit instructions. In short, A549 cells post infection was washed gently with PBS thrice. Depending upon the surface area, 50 - 100µl of the staining solution (0.5µl of Calcein AM and 2µl of Ethidium bromide in 1ml PBS) was added. Incubated for 30min and imaged under Ziess Axiovision. Live cells appear green and dead cells appear red.

3.2.9. Scanning Electron Microscopy

The biofilms developed on Costar™ Transwell Membranes were evaluated by SEM. The membranes post 8hr infection was fixed using 2.5% gluteraldehyde for

30min at room temperature. The samples were dehydrated using increasing concentration of ethanol and subjected to critical point drying and gold plated. This was then visualised on SEM, JEOL JSM-6400F (JEOL, USA).

3.3.Phase III –

3.3.1. Electrical Cell Substrate Impedance Sensing (ECIS) to Assess changes in barrier integrity during *Pseudomonas* infection.

3.3.2. Impedance measurement with ECIS

The changes in barrier integrity during *Pseudomonas* infection was analysed by ECIS. ECIS is non-invasive, label free, impedance-based method to study the behaviour of cells to a stimulus. Impedance was measured by the method described by Szuleck et al, with a few modifications (Szulcek et al., 2014). Prior to the experiment the array holder was warmed to 37ºC in the incubator. Before seeding the cells, the 400µl of complete cell culture media was added into the 8Well electrodes. The arrays placed on the array holder such that the gold-plated electrode pads are aligned with the spring-loaded pogo pins and the screw was tightened. The connectivity and impedance of each well was checked. Electrode were stabilised and cell free impedance was measured for 1hr at multiple frequencies (MFT).

After 1hr the impedance measurement was paused, and arrays were removed. The media in the wells were replaced with fresh F12K medium. A549 cells were seeded at a density of 10^4 cells per electrode. The electrodes were placed on the array holder, the connectivity to each well was checked an impedance measurement was continued. As the cells adhere and spread on the electrode the impedance increases. Once the complete electrode coverage is attained, the impedance measured attains plateau.

3.3.3. Infection of A549 cells on the Electrodes

Impedance measurements were carried out till confluence by the method described in Section 3.3.1.2. Following confluence, the impedance measurement was paused. Medium in the wells were replaced by F12K without antibiotics. *Pseudomonas* overnight culture adjusted to an OD_{600nm} of 1.0 was added into appropriate wells at a multiplicity of infection of 50:1 (bacteria: host) and the impedance measurement was resumed. MOI of 50:1 was found to be optimal after ECIS experiments with varying

MOI (part of standardization). Following 24hr of infection the experiment was terminated, and the results acquired. The graph was represented as impedance vs time.

3.3.4. Effect of Azithromycin on *Pseudomonas* infection of alveolar epithelium

Azithromycin is a macrolide antibiotic used for treatment of wide range of bacterial infections of the lower respiratory tract. Its MIC ranges from 0.06 mg to 256 mg/liter. Here a concentration of 40ug/mL was used based on Hallderson et al., (Halldorsson et al., 2010). The effect of azithromycin treatment on *Pseudomonas* infection of alveolar epithelial cells was assessed by ECIS. The impedance was measured by the method described in section 3.3.1.1 and 3.3.1.2 with few changes. The F12K medium containing Gentamicin was replaced by F12K with 40µg/ml Azithromycin. Azithromycin pre-treatment was given for 72hrs. Upon confluence, the media was replaced by media without antibiotics and impedance measurement was resumed. All experiments were performed in triplicates for statistical analysis.

3.3.5. Quantification of reactive oxygen species generation

Reactive oxygen species generation cells were measured by Dichlorofluorescein diacetate (DCFDA) method. A549 cells were grown to confluence in 96 well cell culture plates. Upon confluence the monolayers were treated with 25µM DCFDA in PBS for 30min. The monolayers were then exposed to planktonic forms of *Pseudomonas* and ETT with biofilms of *Pseudomonas* isolates. The ROS was quantified by measuring the fluorescence intensities at 485nm/535nm (D. Wu & Yotnda, 2011).

ROS production in monocytes was assessed by DCFHDA method. Briefly THP1 cells were pretreated with 10µM concentration of DCFDA in PBS for 30min. The cells were then exposed to planktonic and biofilms forms of *Pseudomonas*. The ROS was quantified by measuring the fluorescence intensities at 485nm/535nm.

The fluorescence intensity from the cell free culture medium (negative control) was subtracted from the rest of the experimental groups. The fluorescence intensity obtained in positive control (50µM H_2O_2) was considered as 100%. The percentage DCFDA fluorescence intensity when compared with the positive control was plotted against time.

3.3.6. Assessment of bacterial internalization by gentamicin protection assay

Bacterial internalization was assessed by gentamicin protection assay. THP1 cells were exposed to planktonic and biofilms of *Pseudomonas*. The exposed monocytes were washed thrice with PBS and treated with 100µg/ml concentration of gentamicin for 20 min at 37ºC. The THP1 cells were then lysed by 0.1% Triton X 100. Lysates were serially diluted and plated on soyabean casein digest agar and incubated at 37ºC overnight and CFUs were counted. CFU/ml over a period of 8hr was plotted.

3.3.7. Assessment of cell death by acridine orange / propidium iodide staining

Post infection events leading to cell death in A549 cells and THP1 cells were assessed by acridine orange and propidium iodine staining. The cells post infection (4hr and 8hr) with planktonic, or biofilm of *Pseudomonas* was stained using staining solution (1µl of AO (5mg/ml) and 1µl of PI (5mg/ml) in 1ml PBS) and incubated at room temperature for 10min. The cells were then washed thrice with PBS and imaged using Ziess axio vision fluorescent microscope within 30min of staining (Kntayya et al., 2018).

3.3.8. Assessment of nuclear changes

Nuclear changes in A549 cells and THP1 cells exposed to planktonic and biofilm forms of *Pseudomonas* were assessed by staining with Hoechst 33342 (Invitrogen) staining. Infected cells were washed thrice with PBS and stained using 1:2000 diluted solution of Hoechst (10mg/ml). incubated for 5 – 10min in dark, washed thrice with PBS and imaged using Ziess Axio vision fluorescence microscope.

3.3.9. RNA extraction:

Total RNA was extracted from the experimental groups using Trizol™ (Invitrogen). 0.3ml – 0.4ml of trizol was added per 10^7 cells and mixed thoroughly to ensure complete lysis of the cells. The mixture was incubated for 5min at room temperature. 100µl of chloroform was added to the lysate and incubated for 2-3min and centrifuged at 12000*g for 15min at 4ºC for phase separation. The upper aqueous phase containing RNA was transferred to fresh tubes. Following this RNA was

precipitated using 250µl of isopropanol and centrifuged at 12000*g for 10min at 4ºC. A gel like RNA pellet was obtained at the bottom of the tube. The supernatant was discarded, and the pellet was resuspended in 500µl of 75% ethanol. The sample was then vortexed and centrifuged at 7500*g for 5min at 4ºC. Supernatant was discarded and the pellet was air-dried for 5 – 10min. The final pellet was then resuspended in 20 - 40µl of RNase free water and the purity was assessed by obtaining the ratio of absorbance at 260nm/280nm. A ratio of 1.8 to 2 was considered pure and the samples were used for cDNA synthesis. Less pure samples were re-extracted using trizol.

3.3.10. cDNA synthesis

Reverse transcription was carried out using reverse transcription core kit (Origin diagnostics). The reaction was set up as indicated in table.

Reagents	**Volume**
RNA	1- 2 µl**
5X RT Reaction Buffer (Includes, 10mM dNTPs)	2 µl
8mM DTT	0.5 µl
RTase	0.5 µl
RNase free water	Made up to 20 µl

Table 5: Reagents used in cDNA synthesis and the volumes used. ** the volume of RNA used is dependent on RNA concentration.

The reagents were mixed, and the reaction conditions were set in the thermal cycler with initial incubation at 50°C for 60 minutes and the final inactivation of the reaction mixture with incubation at 95°C for 5 minutes.

3.3.11. Real time polymerase chain reaction

RT PCR was carried out using Takyon™ qPCR for syber® assays. The kit components and the volumes used are mentioned in table

Reagent	**Volume used**	**Final concentration**
Takyon master mix (2X)	10µl	1X
Forward primer	2µl	50-300nM
Reverse primer	2µl	50-300nM
cDNA template	2µl	-

Water	Made upto 20µl	-

Table 6: Reagents and volumes used for RTPCR syber green assay. Equal volumes of cDNA template was used for the assay.

qTower^3/G real time PCR system was used for RTPCR assays. The reaction conditions are mentioned in table

Process	**Temperature (ºC)**	**Time**
Takyon activation	95ºC	3min
Denaturation	95ºC	3sec
Annealing /extension	50 – 60 ºC***	20- 30 sec
Go to step 2 and repeat 39 cycles		
Melt curve analysis from 50ºC - 95ºC		

Table 7: Reactions conditions used for RT PCR. *** annealing temperature was decided based on the melting temperature (Tm) of primers

3.3.12. Quantification of cytokine by Enzyme-Linked Immunosorbent Assay (ELISA)

The cytokine protein expression was quantified using ELISA. For this, prior to infection, the cell culture media was replaced by, serum-free medium without antibiotics. 2hr and 6hr post-infection media was removed and centrifuged at 1000g for 20min. The supernatant was used for protein estimation by Bradfords method. Equal amount of protein (80-100µg) was used for ELISA. The ELISA Kits of TNFα, IL8 and IL1β was purchased from Origin Diagnostics. ELISA was performed as per the kit protocol.

3.3.13. Caspase 1 Assay

Caspase 1 activity in biofilm infected A549, THP1 and their cocultures were assayed (6hr post infection) using Caspase -Glo® 1 – inflammasome assay kit (Promega, WI, USA). The reagents were reconstituted, and assay was performed according to the kit protocol. Prior to testing the reagents were equilibrated to room temperature. Cell-culture media without cells were used as blank and uninfected cells was the negative control used.

To half of the wells containing (100µl of blank, negative controls and infected group), 100µl Caspase -Glo® 1 reagent was added. To the other half Caspase -Glo® 1 YVAD-CHO (inhibitor of caspase1) was added. The plate was sealed, and the contents were mixed using a plate shaker at 400rpm for 30sec. The plate was incubated at room

temperature for at least 1hr for the luminescence to stabilise. The luminescence is read at 60min, 90min and 120min. The background luminescence was subtracted from the control and experimental groups and luminescence intensities were plotted.

3.3.14. Statistical Analysis

All experiments were carried out thrice in triplicates and mean and SD values have been plotted. The statistical analysis used was Two Way ANOVA and Grouped T test. GraphPad Prism 6 was the statistical analysis tool used.

4. RESULTS

The results consist of three phases: Phase 1 deals with the Dynamics of biofilm formation by *Pseudomonas* isolates. Phase II deals with the development of an *in-vitro* test system to study cell–material - microbial interactions, in particular the interaction of *Pseudomonas* biofilm on the endotracheal tubes with the host cell and immune modulations. Part III deals with understanding the molecular mechanism involved in these interactions, which leads to pathogenicity. Here the interaction of biofilms of different isolates of *Pseudomonas* with host cells, i.e., alveolar epithelial cells and immune cells, were studied.

4.1. Phase I: Dynamics of biofilm formation by *Pseudomonas* isolates

The influence of environmental factors like time temperature, pH, Iron concentration, glucose, and antibiotics on biofilm formation by the *Pseudomonas* isolates was analyzed. Crystal violet assay was used to quantify the biofilms

4.1.1. Antibiotic sensitivity patterns

		Zone size (mm)				
	Antibiotic	AMIKACIN (18-26)	CETAZIDIME (22-29)	CIPROFLOXACIN (25-33)	GENTAMICIN (16-21)	NORFLOXACIN (22-29)
Pseudomonas isolates	ATCC 27853	22	22	30	18	23
	S373	**15**	**0**	**0**	**0**	**0**
	S402	**17**	**18**	26	18	23
	S125	18	**16**	26	20	25
	S253	18	**19**	**22**	12	**13**
	S135	20	**14**	30	20	24
	S268	20	**10**	27	20	23
	S45	**17**	**12**	28	20	23
	S277	18	**20**	28	18	22
	S18	18	**19**	26	20	22

Table 8. Antibiotic sensitivity patterns of *Pseudomonas* ATCC 27853 and isolates. The zone of inhibition was measured and tabulated. The values depicted in red show resistance to the antibiotic. It can be observed that the reference strain ATCC 27853 was sensitive to all the antibiotics tested and the clinical isolate S373 was resistant to the antibiotics tested. All the clinical isolates used in the study were resistant to ceftazidime.

The antibiotic sensitivity patterns of *Pseudomonas* clinical isolates were evaluated using Kirby Bauer agar diffusion method. The zone of inhibition was measured in millimeters. Table 8 shows the antibiotic sensitivity patterns of ATCC 27853 and clinical isolates. It was observed that the ATCC 27853 isolate was sensitive to all the antibiotics tested. All *Pseudomonas* clinical isolates showed resistance to Ceftazidime, a cephalosporin antibiotic. All clinical isolates except S373 and S253 showed sensitivity to ciprofloxacin and norfloxacin (fluoroquinolone antibiotics). All the clinical isolates except S373 showed sensitivity to gentamicin (aminoglycoside).

4.1.2. Biofilm formation by isolates of *Pseudomonas* at varying time points.

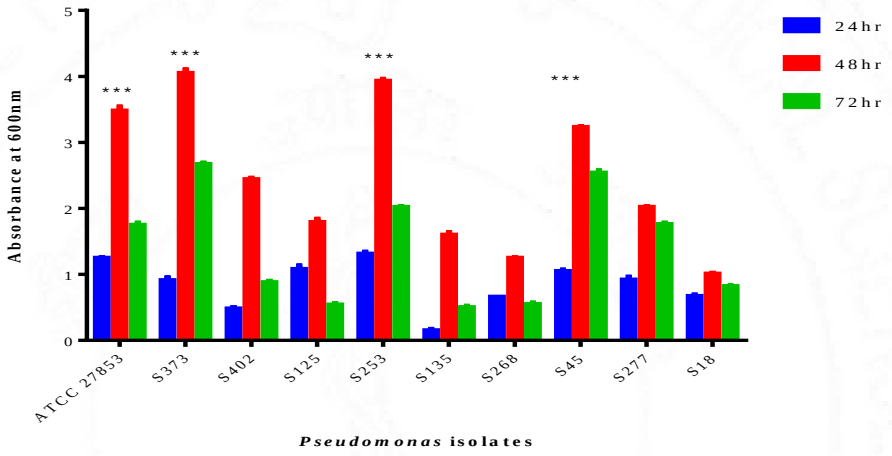

Fig.7: Biofilm quantification by crystal violet assay. Crystal violet assay was used to quantify biofilm formation by ATCC 27853 and clinical isolates over a period of 24hr, 48hr, and 72hr. n=3 or more and statistical analysis was done by Student's t-test ***p<0.001

Biofilm formation by ATCC 27853 and clinical isolates of *Pseudomonas* was evaluated by crystal violet assay. Fig.7. shows biofilm formation by isolates of *Pseudomonas* over a period of 72hr. ATCC 27853 was the standard reference strain used. It was observed that both ATCC 27853 and all clinical isolates produced biofilm maximally by 48 hours and then enter a phase of maturation, leading to a decrease in biofilm formed at 72hr. (Fig.7). Fig7 also establishes that the isolates differ in their ability to develop biofilms. S373, S253, and S45 isolates (indicated by *** p-value <0.001) showed increased biofilm formation and were comparable to ATCC 27853. Other clinical isolates showed reduced biofilm formation when compared to ATCC 27853.

4.1.3. Effect of pH on biofilm formation

Fig 8 shows the effect of pH on biofilm formation by *Pseudomonas* isolates. A physiological pH of 7.4 was found to support maximal biofilm formation, although the amount of biofilm formed was strain specific. Both ATCC 27853 and clinical isolates synthesized maximum biofilm at pH 7.4. Interestingly, an acidic pH of 4.0 also supported biofilm formation by both ATCC and clinical isolates of *Pseudomonas*, while an alkaline pH did not favor biofilm formation by all the isolates.

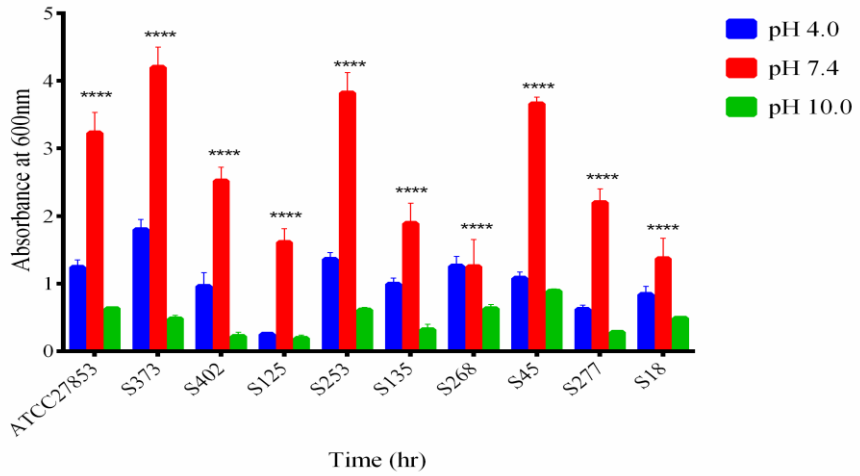

Fig 8: Effect of pH on biofilm formation. The ability of *Pseudomonas* ATCC 27853 and clinical isolates to develop biofilms at pH of 4.0, 7.4 and 10 was evaluated by crystal violet assay. Both ATCC 27853 and clinical isolates showed increased biofilm formation at the physiological pH (7.4). n=3 or more and statistical analysis was done by Students T test, ****p<0.0001

4.1.4. Effect of temperature on biofilm formation

Temperature is one of the important factors that influence biofilm formation. Fig (9) shows the effect of temperature on biofilm formation by *Pseudomonas* isolates. The physiological temperature of 37ºC promoted biofilm formation in all the isolates. A significant increase in biofilm formation was observed at 37ºC (***p<0.001) compared with the other temperatures.

All the isolates showed increased biofilm formation at 37ºC. Room temperature/ Ambient temperature (27 ± 2 °C) was also conducive to the synthesis of biofilm by all the isolates, while pyrogenic conditions did not favor biofilm formation

in ATCC 27853, S373, S45, and S277 isolates (Fig 9). A higher temperature (fever temperature - 39ºC) significantly reduced biofilm formation by *Pseudomonas* isolates, an indication of one of the effective defense mechanisms in the host on a challenge with biofilms as happens in medical device-related infections where biofilms form on implanted devices leading to biofilm formation and resultant inflammatory response.

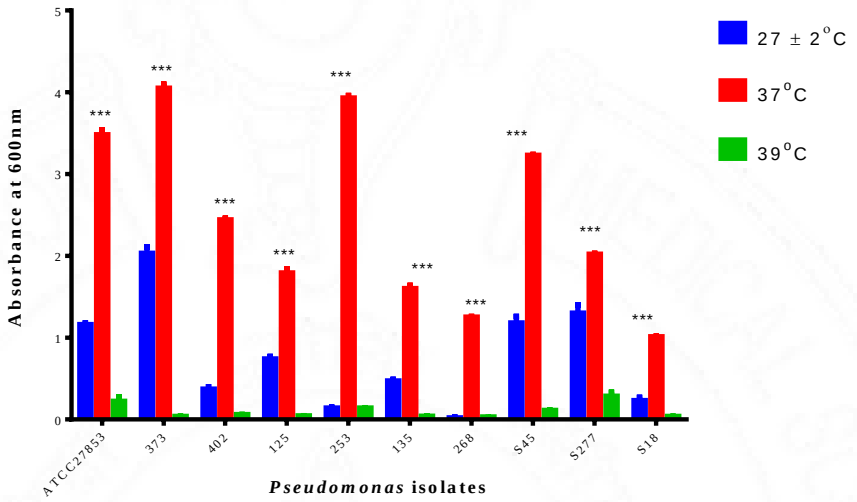

Fig.9: Effect of temperature on biofilm formation. The influence of temperature on biofilm formation by *Pseudomonas* ATCC 27853 and clinical isolates, were assessed by crystal violet assay. It was observed that a physiological temperature of 37°C increased biofilm formation in all the isolates. n =3 or more and statistical analysis was done by Student's t-test *** p<0. 001

4.1.5. Effect of Fe^{3+} on biofilm formation

Fe^{3+} is an essential cofactor for many biochemical processes of the living systems. *Pseudomonas* adopts Siderophoric and non-siderophoric methods for the acquisition of ferric irons. Minimal media (Davis minimal medium without glucose) did not support biofilm formation (fig.10).

Various concentrations of $FeCl_3$ (10mM, 50mM, and 100mM) were tested for their ability to support biofilm formation (Fig 10). A very significant increase in biofilm formation was observed at 50mM concentration of Fe^{3+}, with 50mM being the optimal concentration while lower and higher Fe^{3+} concentrations reduced biofilm formation.

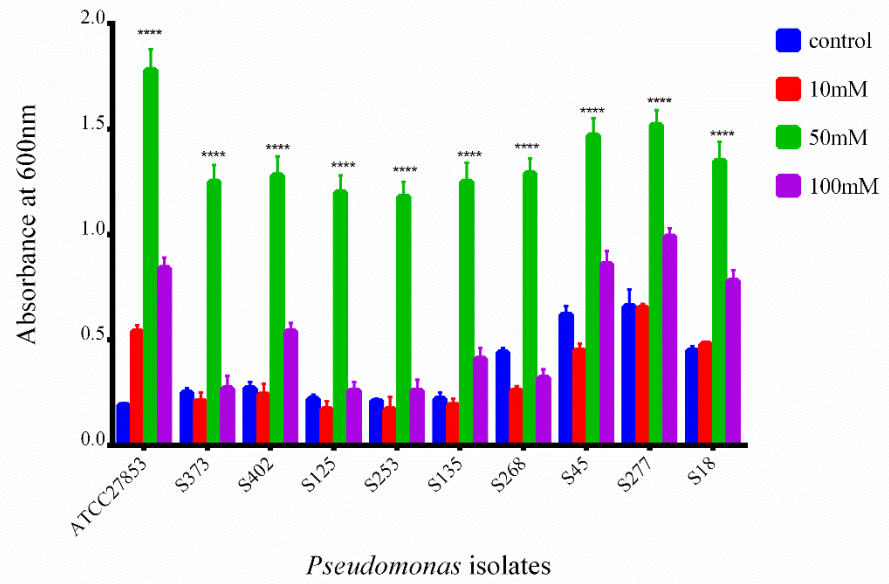

Fig.10: Effect of Iron Concentration on Biofilm formation: biofilm formation in the presence of varying concentrations of iron was quantified by crystal violet assay. 50mM concentration of iron increased biofilm formation. n=3, and statistical analysis was carried out by Students t-test ****p<0.0001.

4.1.6. Effect of glucose on biofilm formation by *Pseudomonas*

Glucose, a six-carbon sugar, is an essential source of carbon and energy for bacteria. The effect of glucose was assessed by quantifying the biofilms developed in a Davis minimal medium supplemented with varying glucose concentrations. The effect of glucose concentrations was strain-dependent (Fig 11).

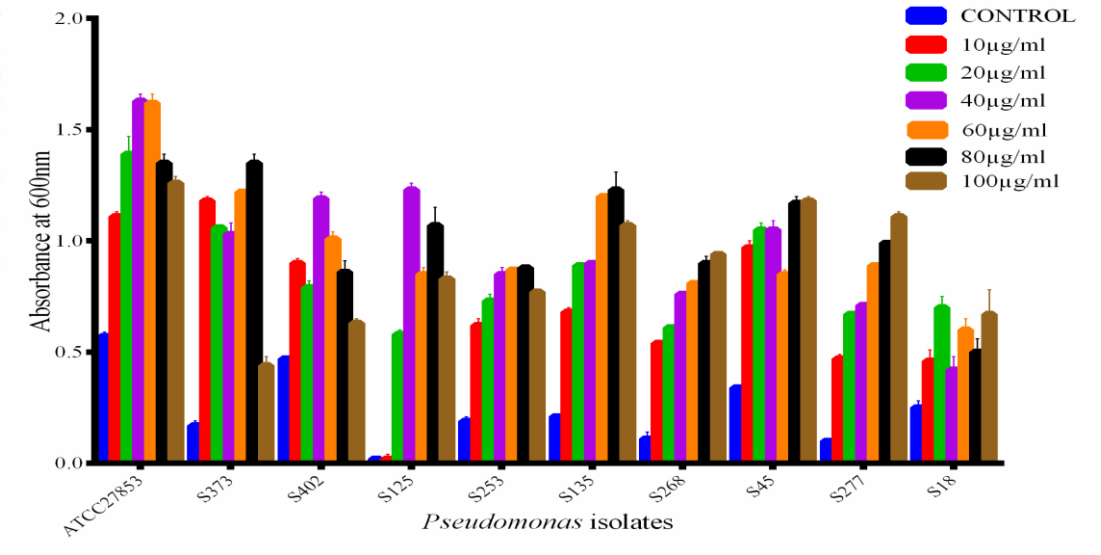

Fig.11: Effect of glucose on biofilm formation by *Pseudomonas* isolates. Biofilm formation at varying concentrations of glucose was assayed by crystal violet assay. N =3 or more and statistical analysis was carried out by Student's t-test. P<0.14

A concentration-dependent increase in biofilm formation in ATCC 27853 isolate was observed up to 40µg/ml and 60µg/ml, which educed at 80µg/ml and 100µg/ml (Fig 11). The clinical isolates did not show any significant increase in biofilm formation, with increasing glucose concentration. The presence of glucose did improve biofilm formation, but no substantial changes in biofilm formation were observed with respect to glucose concentration.

4.1.7. Effect of Antibiotics on biofilm formation by *Pseudomonas*

Antibiotics are the standard line of treatment for an infection. Ceftazidime, Gentamicin, and Norfloxacin are some of the common antibiotics used to treat *Pseudomonas* infections.

4.1.7.1.Effect of Ceftazidime on biofilm formation by *Pseudomonas*

Fig 12, Shows the effect of varying concentrations of Ceftazidime (7.5µg/ml, 15µg/ml, 30µg/ml, and 45µg/ml) on biofilm formation. It was observed that sub-inhibitory concentrations of Ceftazidime (7.5µg/ml and 15µg/ml) increased biofilm formation except in the S135 isolate. All the other clinical isolates and ATCC 27853 strains at sub–MIC showed increased biofilm formation. S253, S268, and S277 led to increased biofilm formation even at MIC (30µg/ml) and above MIC (45µg/ml).

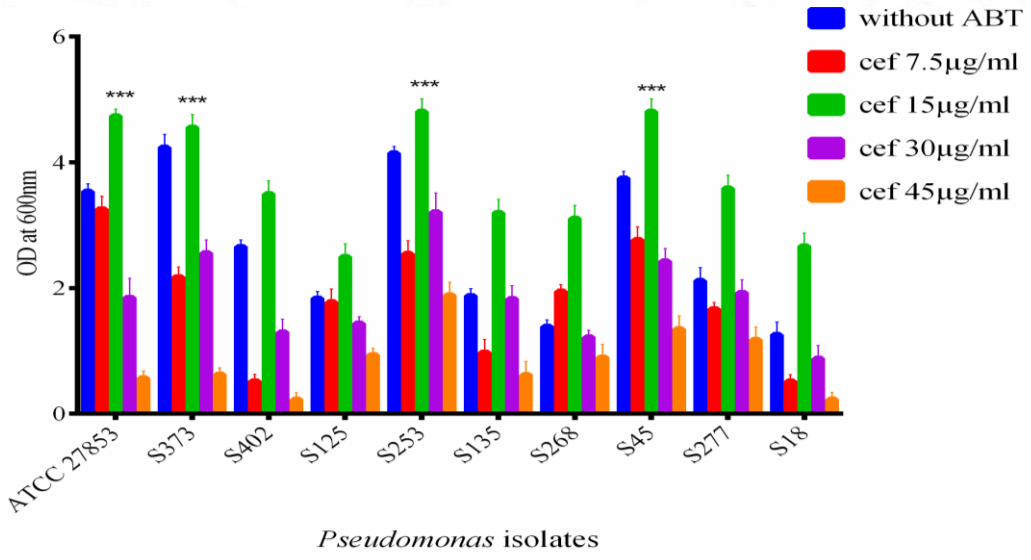

Fig 12: Effect of Ceftazidime on biofilm formation by *Pseudomonas* - Biofilms were developed in the presence of varying concentrations of ceftazidime (7.5µg/ml, 15µg/ml, 30µg/ml, and 45 µg/ml) and quantified at 48hr by crystal violet assay. N =3 or more and statistical analysis – Student's t-test and ***p<0.001 was considered significant.

4.1.7.2.Effect of Gentamicin on biofilm formation by *Pseudomonas*

Fig 13 shows the effect of varying co concentrations of Gentamicin (2.5µg/ml, 5µg/ml, 10µg/ml, and 15µg/ml) on biofilm formation by *Pseudomonas* isolates. Sub – inhibitory concentrations of gentamicin (2.5µg/ml and 5µg/ml) augmented biofilm formation by clinical isolates. On the other hand, no increase in biofilms was found in ATCC 27853 isolate. MIC and above MIC reduced biofilm formation in all the isolates.

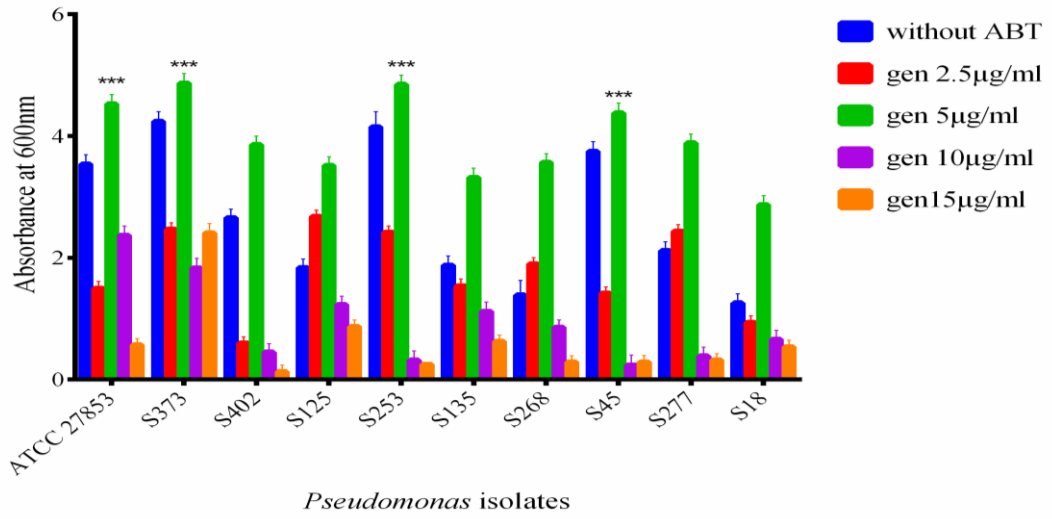

Fig.13: - Effect of Gentamicin on biofilm formation by *Pseudomonas*. Biofilms were developed in varying concentrations of ceftazidime and quantified at 48hr by crystal violet assay. n =3 or more and Statistical analysis – student's T-test. ***p<0.001 was considered significant

4.1.7.3.Effect of Norfloxacin on biofilm formation by *Pseudomonas*

Fig (14) depicts the effect of varying concentrations of Norfloxacin (2.5µg/ml, 5µg/ml, 10µg/ml and 15µg/ml) on biofilm formation by *Pseudomonas* isolates. Both ATCC 27853 and clinical isolates showed increased biofilm formation at sub-inhibitory concentrations (2.5µg/ml and 5µg/ml) of norfloxacin. S135, S277, and S18 showed increased biofilm formation even at MIC and above MIC (10µg/ml and 15µg/ml) concentrations of norfloxacin.

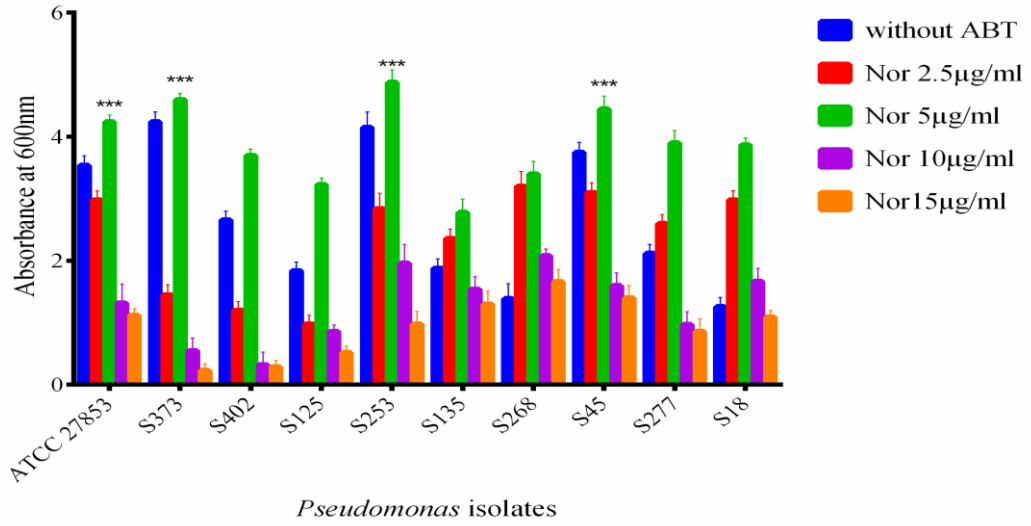

Fig 14: Effect of Norfloxacin on biofilm formation by *Pseudomonas*. Biofilms were developed in varying concentrations of Norfloxacin and quantified at 48hr by crystal violet assay. n=3 and Statistical analysis by Student's T-test. ***p<0.001.

4.1.8. Effect of antibiotics on eDNA release

eDNA is an integral part of the biofilm, which provides structural integrity and antibiotic resistance in biofilms. So, in our experiments eDNA was present in biofilms and this was positive control. bands corresponding to eDNA was absent in the planktonic groups (negative control). The effect of antibiotics on eDNA release within biofilms was analysed by agarose gel electrophoresis (0.7% agarose gels). The molecular weight of band was determined using DNA molecular weight marker in lane 'L' corresponding to ladder DNA 100bp to 1500bp. To compare the eDNA release between groups, the band intensities obtained on agarose gels were quantified using imageJ.

4.1.8.1. Effect of Ceftazidime on eDNA release in biofilms

It can be observed from Fig 15 A that only biofilms released eDNA, lanes 1, 7, 13, 19, 25, 31, 37, did not show any DNA band and were corresponding to planktonic cells. Fig 15 B shows the effect of Ceftazidime on eDNA release in biofilms of *Pseudomonas* isolates. No changes in eDNA release in biofilms were observed upon treatment with varying concentrations of ceftazidime.

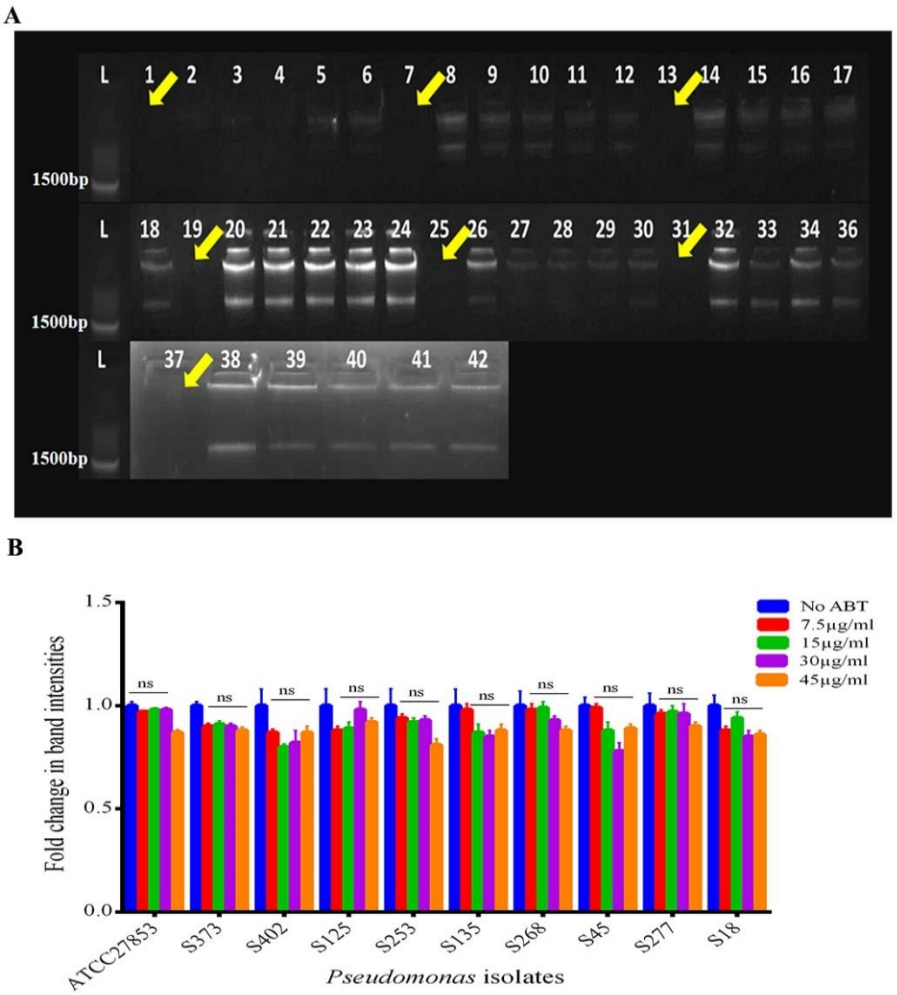

Fig 15: Effect of ceftazidime on eDNA release by *Pseudomonas* biofilms: A) Agarose Gel Electrophoresis of eDNA isolated from planktonic, non – treated (NT) biofilm and Biofilm treated with varying concentration of Ceftazidime. L – Ladder, 1. ATCC planktonic, 2. ATCC (NT) 3. ATCC 7.5µg/ml, 4. ATCC 15µg/ml, 5.ATCC 30µg/ml,6. ATCC 45µg/ml, 7. S373 planktonic, 8.S373 (NT),9. S373 7.5µg/ml,10. S373 15µg/ml,11. S373 30µg/ml, 12.S373 45µg/ml, 13. S253 planktonic,14. S253 (NT),15. S253 7.5µg/ml,16. S253 15µg/ml,17. S253 30µg/ml,18. S253 45µg/ml ,19. S241 planktonic,20. S241 (NT),21. S241 7.5µg/ml,22. S241 15µg/ml,23. S241 30µg/ml,24. S241 45µg/ml, 25. S268 planktonic, 26. S268 (NT), 27. S268 7.5µg/ml,28. S268 15µg/ml,29. S268 30µg/ml, 30. S268 45µg/ml, 31. S18 planktonic, 32. S18 (NT), 33.S18 7.5µg/ml,34. S18 15µg/ml,35. S18 30µg/ml,36. S18 45µg/ml,37. S45 planktonic 38. S45 biofilm (NT),),39. S45 7.5µg/ml, 40.S45 15µg/ml,41. S45 30µg/ml, 42.S45 45µg/ml. B) The band intensities obtained in Agarose gel electrophoresis were quantified by imageJ software. The band intensities of the antibiotic-treated group were normalized to that of the untreated control. N =3 and the statistical analysis used was the student's T-test. P<0.124

Most of the clinical isolates (S373, S402, S125, S135, S45, and S18) showed a reduction in eDNA release in biofilms compared to untreated control. No significant

increase was observed in eDNA release at a sub-inhibitory concentration of 7.5µg /ml of Ceftazidime.

4.1.8.2. Effect of Gentamicin on eDNA release in biofilms of *Pseudomonas*

An increase in eDNA release was observed in biofilm treated with half MIC (5µg/ml) gentamicin concentration (fig 16B). Surprisingly, sub-inhibitory concentration (2.5µg/ml) did not increase eDNA release in biofilms (Fig 16B). At the same time, MIC and above MIC decreased eDNA release in biofilms. S125, S135, S45, and S277 showed a significant increase in eDNA release at sub–MIC concentration.

4.1.8.3. Effect of Norfloxacin on eDNA release in *Pseudomonas* biofilms

Half MIC concentration of Norfloxacin increased eDNA release in biofilms except in S277. S125, S135, S268, S45, and S18 showed a significant increase in eDNA release in response to sub-MIC of Norfloxacin (Fig 17B). 2.5µg/ml of Norfloxacin increased eDNA only in S268 and S45. MIC and above MIC was found to reduce eDNA release in biofilms of *Pseudomonas.*

4.1.9. Assessment of virulence and pathogenicity of *Pseudomonas* isolates

Pyocyanin is one of the major virulence factors produced by *Pseudomonas*. Pyocyanin is known to play multiple roles in *Pseudomonas* pathogenesis. Pyocyanin production in various isolates of *Pseudomonas* was assessed. It can be observed that the ability to produce pyocyanin was strain-specific (Fig 18 A). Clinical isolates S253 and S45 showed increased expression of pyocyanin. ATCC 27853 and S125 showed reduced pyocyanin production among the isolates.

Rhamnolipids are virulence factors secreted by *Pseudomonas*, which play an important role in the early invasion of the airway epithelium. The rhamnolipid production was also observed to be strain specific. Clinical isolates S373, S253, and S45 showed increased production of rhamnolipids compared to the rest of the isolates (Fig 18 B). The clinical isolate S135 showed the least production of rhamnolipids.

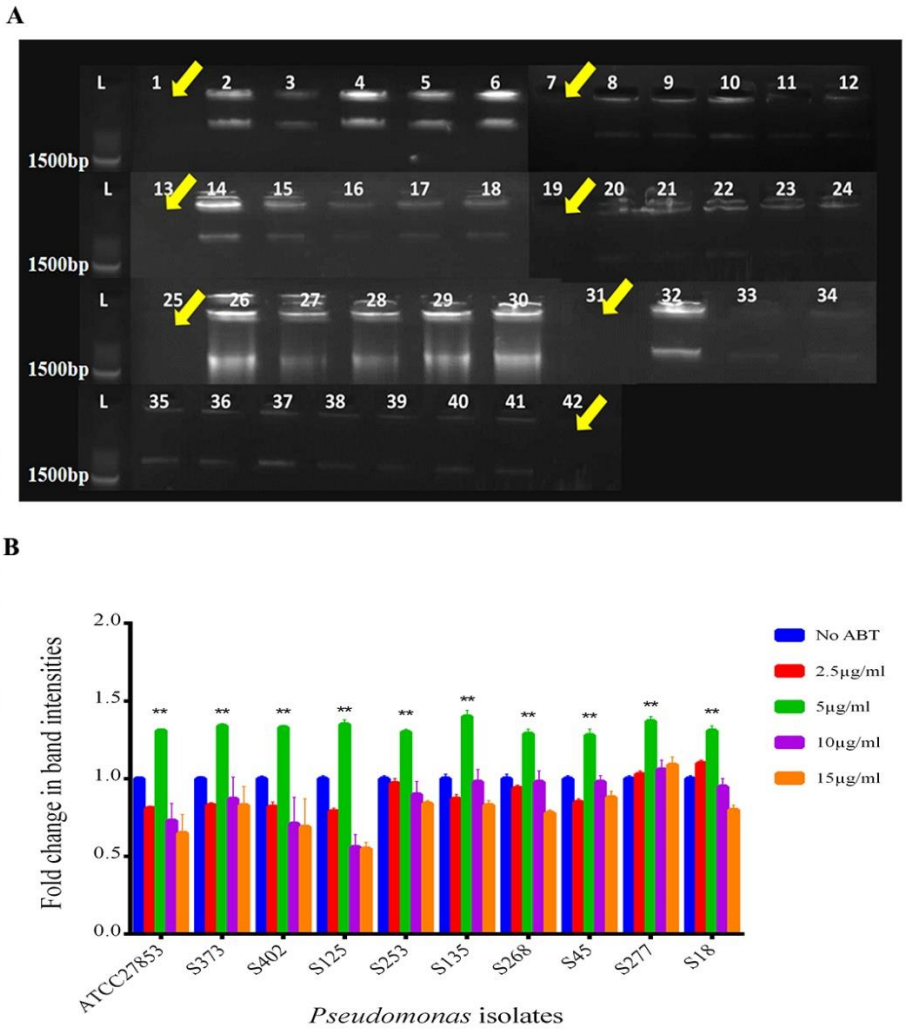

Fig 16: Effect of Gentamicin on eDNA release by *Pseudomonas* biofilm: Agarose Gel Electrophoresis of eDNA isolated from planktonic, non – treated (NT)biofilm and Biofilm treated with varying concentration of Gentamicin. L – Ladder, 1. ATCC planktonic, 2. ATCC (NT) 3. ATCC 2.5µg/ml, 4. ATCC 5µg/ml, 5.ATCC 10µg/ml,6. ATCC 15µg/ml, 7. S373 planktonic, 8.S373 (NT),9. S373 2.5µg/ml,10. S373 5µg/ml,11. S373 10µg/ml, 12.S37315µg/ml,13. S253 planktonic,14. S253 (NT),15. S253 2.5µg/ml,16. S253 5µg/ml,17. S253 10µg/ml,18. S253 15µg/ml ,19. S241 planktonic,20. S241 (NT),21. S241 2.5µg/ml,22. S241 5µg/ml,23. S241 10µg/ml,24. S24115µg/ml, 25. S268 planktonic,26. S268 (NT),27. S268 2.5µg/ml,28. S268 5µg/ml,29. S268 10µg/ml, 30. S26815µg/ml, 31. S18 planktonic, 32. S18 (NT), 33.S18 2.5µg/ml,34. S18 5µg/ml,35. S18 10µg/ml,36. S18 15µg/ml,37. S45 biofilm(NT),),38.S452.5µg/ml,39.S45 5µg/ml,40. S45 10µg/ml, 41.S45 15µg/ml, 42.S45 planktonic. B) The band intensities obtained in Agarose gel electrophoresis were quantified by imageJ software. The band intensities of the antibiotic-treated group were normalized to that of the untreated control. N =,3 and statistical analysis used was student's T-test, $p<0.01$ was considered significant.

A

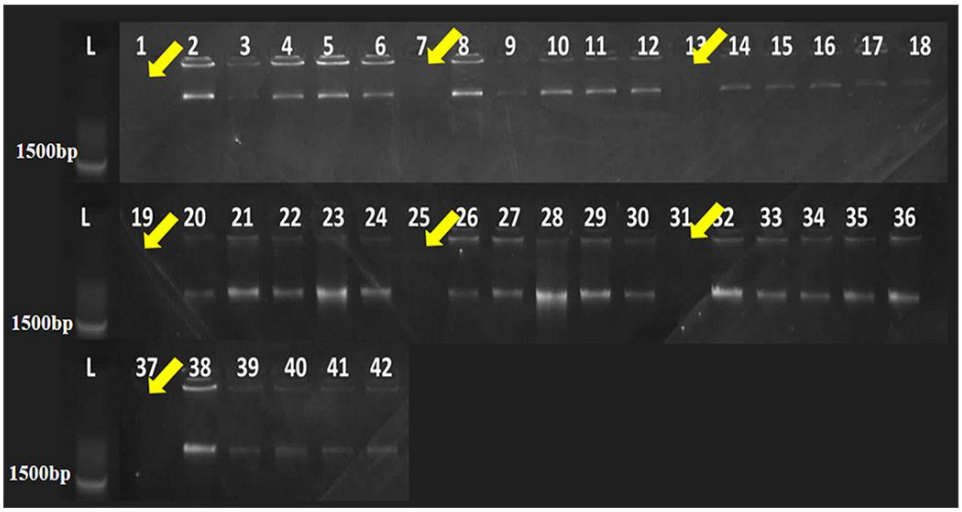

B

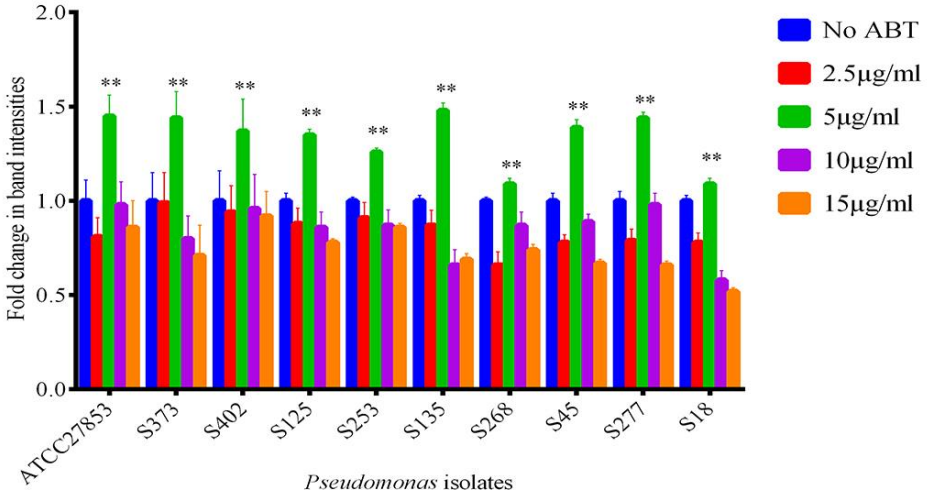

Fig 17: Effect of norfloxacin on eDNA release in *Pseudomonas* biofilms: A) Agarose Gel Electrophoresis of eDNA isolated from planktonic, non – treated (NT)biofilm and Biofilm treated with varying concentration of Norfloxacin. L – Ladder, 1. ATCC planktonic, 2. ATCC (NT) 3. ATCC 2.5µg/ml, 4. ATCC 5µg/ml, 5.ATCC 10µg/ml,6. ATCC 15µg/ml, 7. S373 planktonic, 8.S373 (NT),9. S373 2.5µg/ml,10. S373 5µg/ml,11. S373 10µg/ml, 12.S37315µg/ml,13. S253 planktonic,14. S253 (NT),15. S253 2.5µg/ml,16. S253 5µg/ml,17. S253 10µg/ml,18. S253 15µg/ml ,19. S241 planktonic,20. S241 (NT),21. S241 2.5µg/ml,22. S241 5µg/ml,23. S241 10µg/ml,24. S24115µg/ml, 25. S268 planktonic,26. S268 (NT),27. S268 2.5µg/ml,28. S268 5µg/ml,29. S268 10µg/ml, 30. S26815µg/ml, 31. S18 planktonic, 32. S18 (NT), 33.S18 2.5µg/ml,34. S18 5µg/ml,35. S18 10µg/ml,36. S18 15µg/ml,37. S45 planktonic, 38.S45 (NT),39. S452.5µg/ml,40. S455µg/ml,41. S45 10µg/ml, 42.S45 15µg/ml. B) The band intensities obtained in Agarose gel electrophoresis were quantified by imageJ software. The band intensities of the antibiotic-treated group were normalized to that of the untreated control. N =3 and statistical analysis used was Student's T-test, and $p<0.01$ was considered significant.

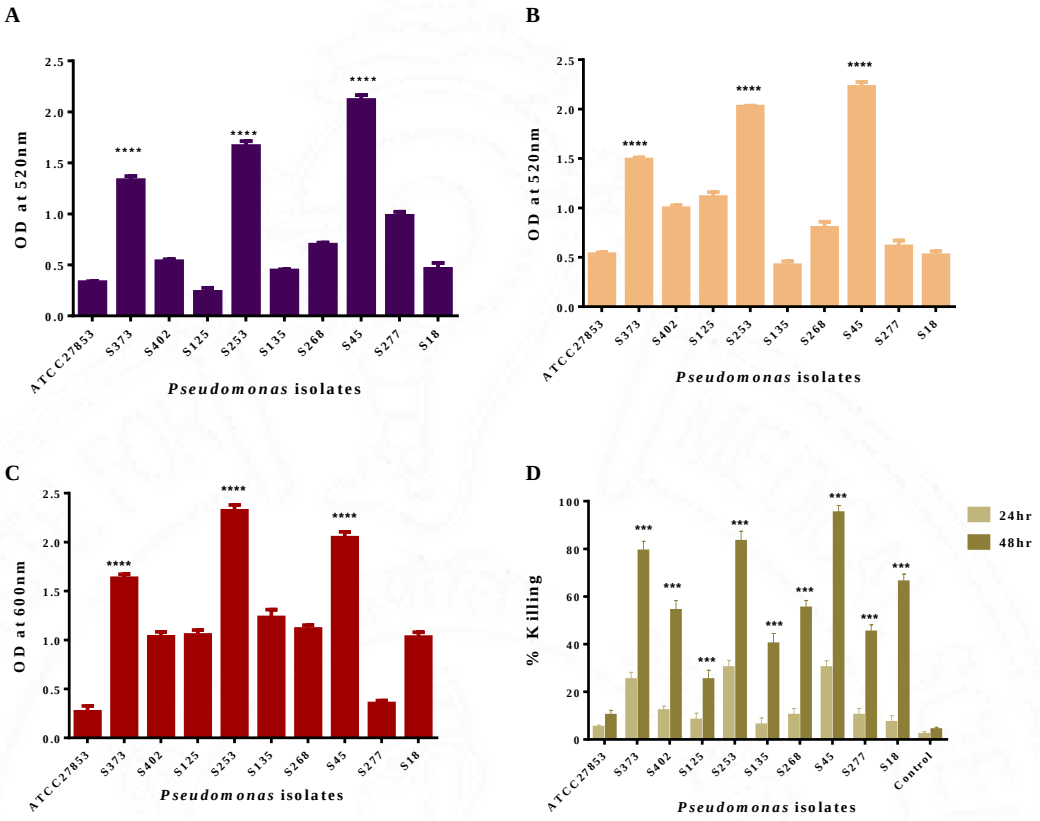

Fig.18: Assessment of virulence of *Pseudomonas* isolates: Estimation of virulence factors A) pyocyanin, B) Rhamnolipids and C) alkaline proteases in culture supernatants of ATCC 27853 and clinical isolates of *Pseudomonas*. D) *C. elegans* killing assay to assess virulence of *Pseudomonas* isolates. It can be observed that S373, S253, and S45 produced increased virulence factors. Clinical isolates induced increased killing of *C. elegans* S373, S253, and S45 induced the highest killing of *C. elegans* by 48hr.

Alkaline proteases play a crucial role in initiating and controlling tissue invasion by *Pseudomonas*. Strain-specific variation was found in alkaline protease expression. Most of the clinical isolates showed an increase in alkaline protease expression compared with ATCC 27853 isolate (Fig 18 C). S373, S253, and S45 showed higher alkaline protease production when compared with the rest of the isolates, while ATCC 27853 and S277 showed the least. *C. elegans* killing assay was used to assess the pathogenicity of the isolates. The graph indicates that the isolates differed in their pathogenicity. Most clinical isolates show increased pathogenicity compared with the ATCC 27853 isolate (Fig 18 D). S373, S253, and S45 showed 80%

killing, indicating increased virulence of the isolates. The percentage killing by ATCC 27853 was almost comparable with the control.

The data suggest that S373, S253, and S45 showed increased biofilm formation and were the most virulent among the isolates studied. These isolates showed increased expression of virulence factors and increased killing of *C. elegans.* Hence, these isolates were used to evaluate the epithelial and monocyte response to *Pseudomonas* biofilms.

4.2. Phase II

Phase II deals with establishing a suitable *in-vitro* system to study *Pseudomonas* sp. infection on airway epithelial cells. A549 are adenocarcinomic human alveolar basal epithelial cells. In the study, A549 cells were used as representative of type II alveolar epithelium to mimic *in-vivo* conditions.

4.2.1 Evaluation of submerged cultures

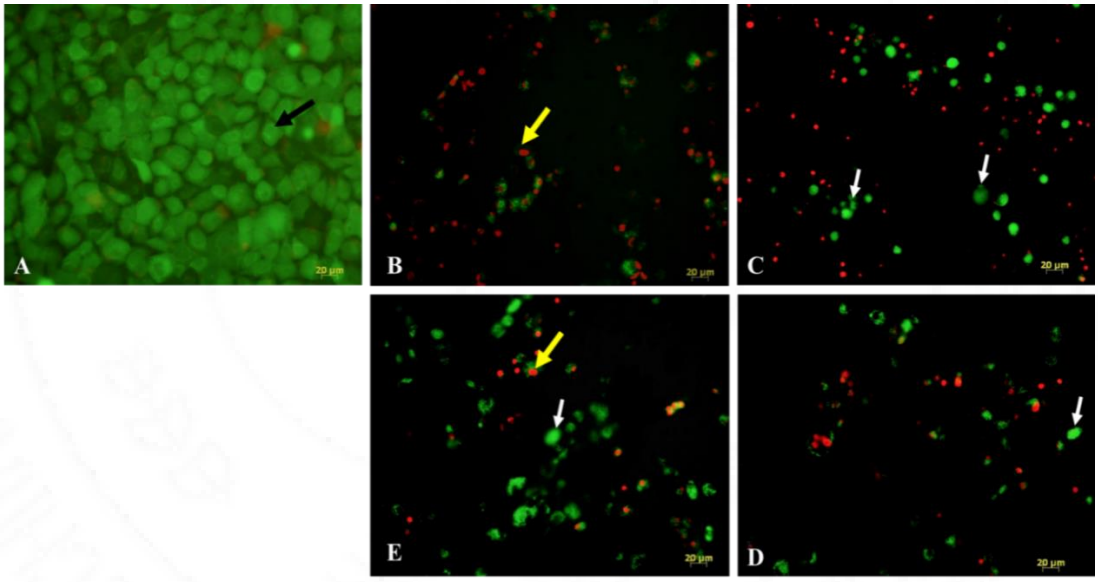

Fig 19: Evaluation of A549 submerged cultures as a *Pseudomonas* infection model. Live dead staining was performed to assess the viability of cells 4hr post-infection. A) Control (uninfected Cells), B) Cells infected with ATCC 27853, C) Cells infected with S373, D) Cells infected with S253, and E) Cells infected with S45. Live cells appear green in colour (White bold arrows). Dead cells appear red (bold yellow arrows). Scale bar 20µm, magnification 20x.

Submerged cultures were evaluated for cell viability following 4hr of infection. It was observed that *Pseudomonas* isolates induced cell extensive cell death in A549 submerged cultures. Both ATCC 27853 and clinical isolated induced cell death in A549 cells. A few viable cells were observed (Fig 19 white arrow) but lost their

epithelial morphology. The control cells maintained epithelial morphology and maintained almost 100% viability.

Nutrient broth and phosphate-buffered saline was *Pseudomonas* infection medium used. It was observed that when nutrient broth was used, *Pseudomonas* induced cell death in A549 cells as early as 2hr post-infection. Morphological changes also were observed in infected A549 cells. On the other hand, phosphate-buffered saline delayed infection of A549 cells by *Pseudomonas*. Even after 6hr post-infection, the epithelial morphology remained intact. A few cells were found to have altered morphology (Fig 20).

4.2.2. Evaluation of nutrient broth and PBS as a suitable medium for infection

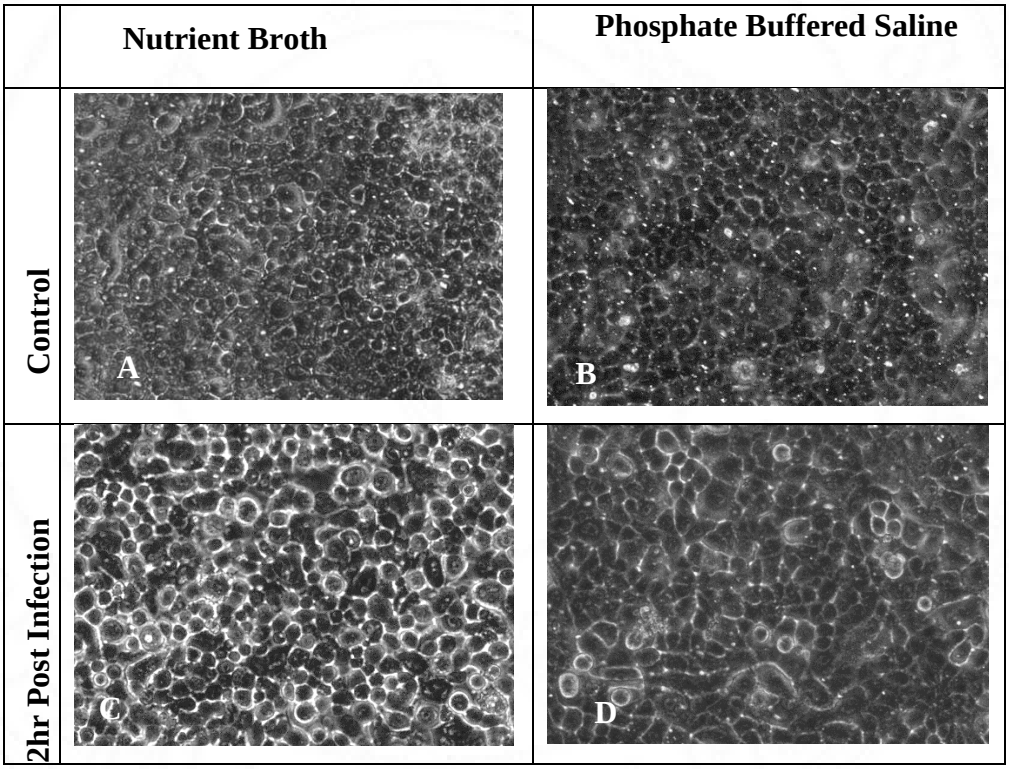

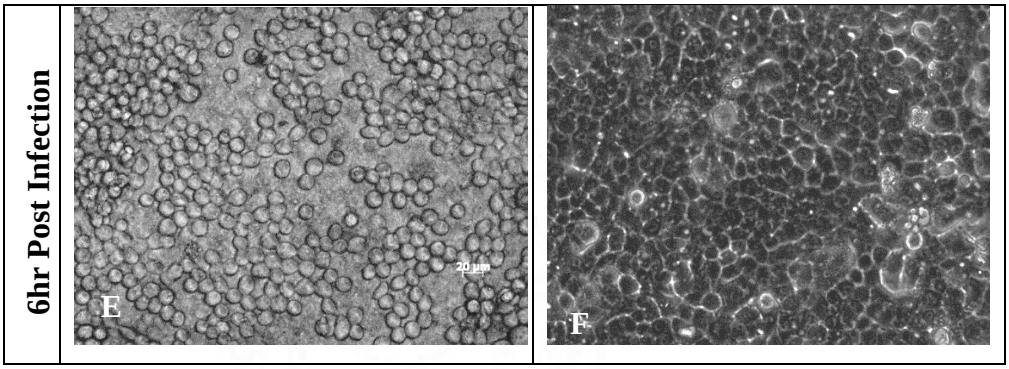

Fig 20: Establishment a suitable infection medium – A549 cells at Air-Liquid Interface were infected *Pseudomonas* re-suspended in nutrient broth (left panel) and phosphate-buffered saline (right panel) at a Multiplicity of Infection of 100:1. Morphological changes were evaluated by phase-contrast microscopy 2hr and 6hr PI. Magnification 20X

To better simulate the *in-vivo* conditions, A549 cells were cultured on Costar™ Transwell membranes and maintained at air-liquid interface cultures.

4.2.3. Evaluation of air liquid interface system

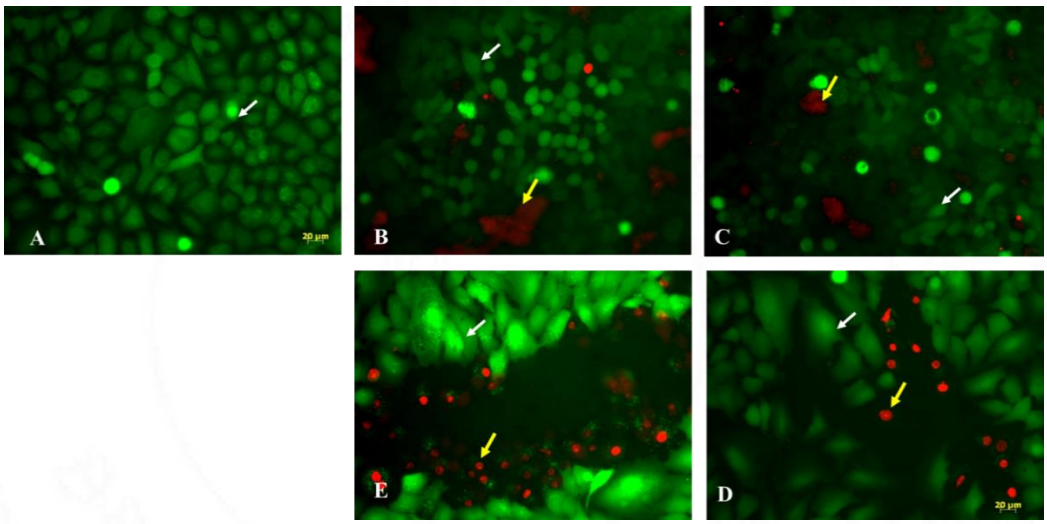

Fig. 21: Evaluation of A549 air-liquid interface system as a *Pseudomonas* infection model. Live dead staining was performed to assess the viability of cells 6hr post-infection. A) Control (uninfected Cells), B) Cells infected with ATCC 27853, C) Cells infected with S373, D) Cells infected with S253, and E) Cells infected with S45. Live cells appear green in colour (White bold arrows). Dead cells appear red, yellow bold arrows). Scale bar 20µm, magnification 20x

Air-liquid interface system was evaluated for cell viability after infection. The control cells remained viable and maintained epithelial morphology. More live cells were observed in air-liquid interface culture infected with *Pseudomonas* in PBS. Although changes were observed in cellular morphology, the cells appeared live. A few dead cells also appeared 6hr post-infection. Both ATCC 27853 (Fig 21B) and Clinical isolates S373 (Fig 21 C), S253 (Fig 21D), and S45 (Fig 21E) induced changes in changes in cellular morphology and cell death in A549 cells.

4.2.4. Evaluation of biofilm formed on Air-liquid interface system

Environmental Scanning Electron Microscopy was done to evaluate biofilms formed on A549 cells at the air-liquid interface system 6hr post-infection (Fig 22). The results show small bacterial aggregates on the surface of the membrane (Yellow arrows). Cellular blebbing also was observed on A549 cells post 6hr infection. No biofilm architecture was observed after 6hr of infection.

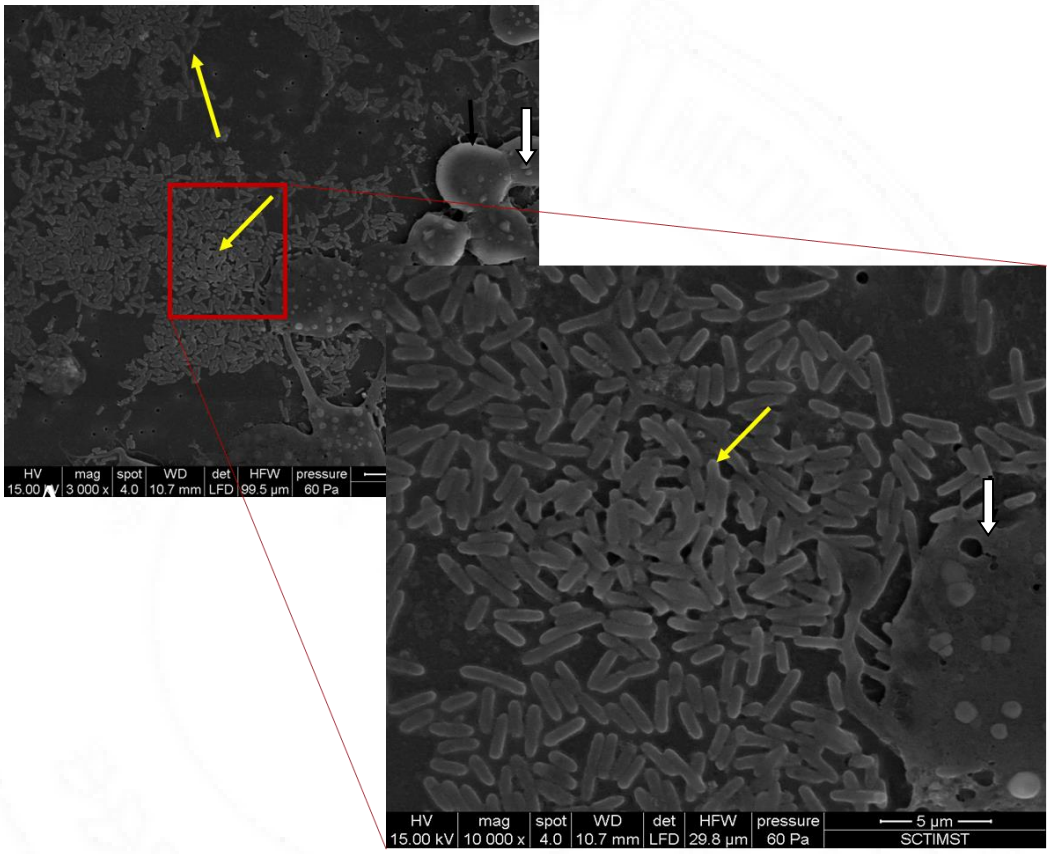

Fig 22: Environmental Scanning Electron Microscopic (ESEM) evaluation of biofilm structures formed on *Pseudomonas* infected ALI cultures of A549. A. Bacterial aggregates (yellow arrow) were observed on the surface of the membrane. B. magnified view of *Pseudomonas* aggregates. A549 cells on the membrane's surface were also visualized (white arrow). Magnification 10,000x scale bar 5µm

4.2.5. Evaluation of ALI system infected with biofilms developed on ETT tube

4.2.5.1. Evaluation of *Pseudomonas* biofilms formed on ETT

48hr old biofilms of *Pseudomonas* developed on the endotracheal tube (ETT) were evaluated by Crystal Violet staining (Fig 23 A and B) and Acridine orange staining (Fig 23 C and D). Crystal violet staining revealed *Pseudomonas* within the biofilms (bold black arrows). Crystal violet-stained exopolysaccharide matrix fibres

also were visualized. Acridine orange staining revealed aggregates of *Pseudomonas* on the surface of ETT.

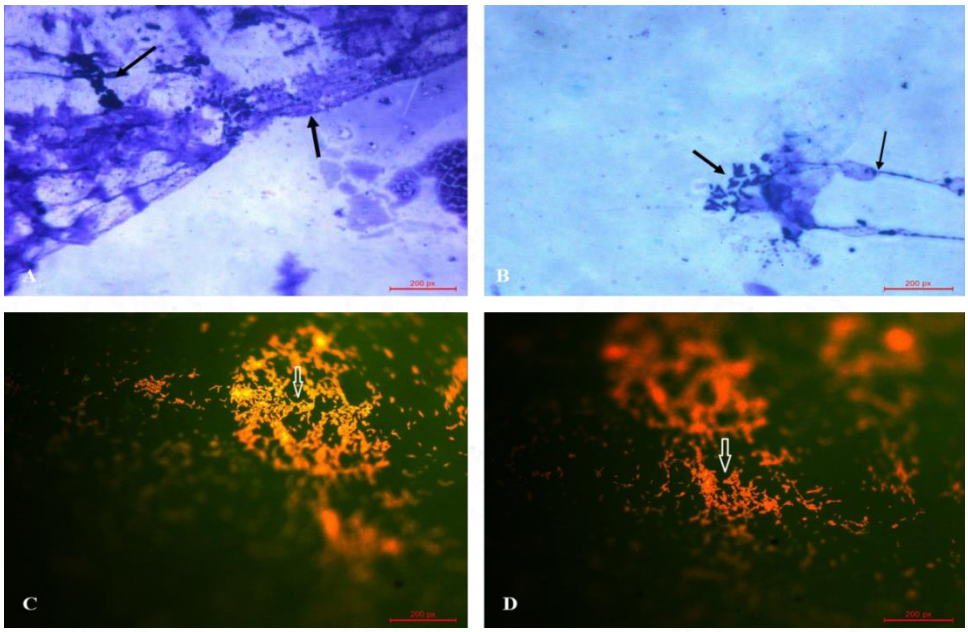

Fig 23: Evaluation of biofilms (48hr) developed on ETT pieces. A and B) crystal violet stained biofilm matrix (bold black arrows) and *Pseudomonas* within exopolysaccharide matrix. C and D) *Pseudomonas* aggregates (white arrows) on ETT visualized by Acridine orange staining. Scale bar 200px, Magnification 100x

4.2.5.2. Evaluation of A549 infection with biofilms developed on ETT as an infection model

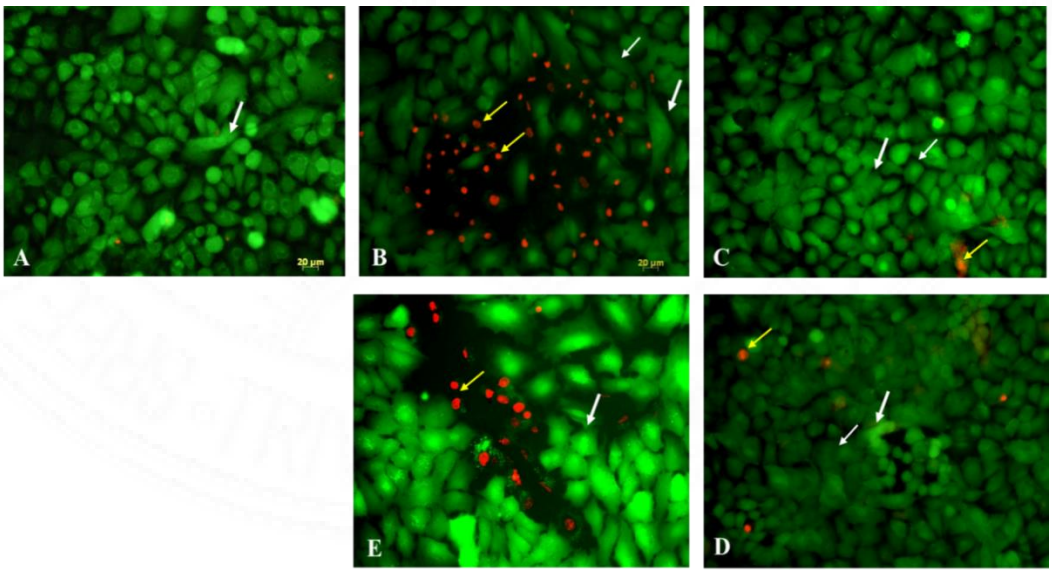

Fig. 24:. Evaluation of A549 air-liquid interface system as a *Pseudomonas* infection model. Live dead staining was performed to assess the viability of cells 6hr post-infection. A) Control

(uninfected Cells), B) Cells infected with ATCC27853, C) Cells infected with S373, D) Cells infected with S253, and E) Cells infected with S45. Live cells appear green in colour (White bold arrows). Dead cells appear red (bold yellow arrows). Scale bar 20µm, magnification 20x

A549 monolayers exposed to *Pseudomonas* biofilms on ETT pieces-maintained viability even after 8hr post-infection. Cells did show signs of infections like cellular blebbing and loss of epithelial morphology (Fig 24, B, C, D, and E). A few dead cells also were observed in cells infected with *Pseudomonas* biofilms. This system allowed the study of the interaction of epithelium with *Pseudomonas* biofilms and better mimicked an *in-vivo* condition and could be used to understand the epithelial interaction with biofilms.

4.3. Phase III

Phase III deals with understanding the epithelial and monocyte interaction with biofilms of *Pseudomonas*. Epithelia is the first line of defense for an organism; hence it is necessary to understand the interaction of epithelium with biofilms of *Pseudomonas*.

4.3.1. *Pseudomonas* infection-induced changes in barrier properties of the A549 epithelium.

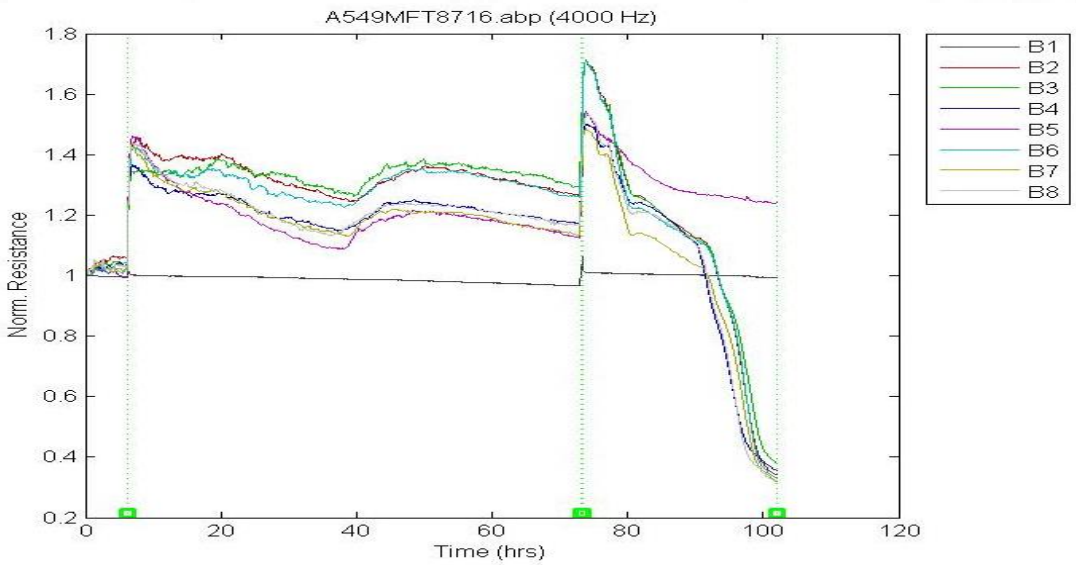

Fig 25: Normalized resistance vs. Time graph of A549 cells infected with *Pseudomonas* isolates (4000Hz). Resistance was measured at multiple frequencies. A decrease in resistance was observed as early as 2hr post-infection. Control (Pink line) did not show any significant changes in resistance measured. The infected cells showed a reduction in resistance measured.

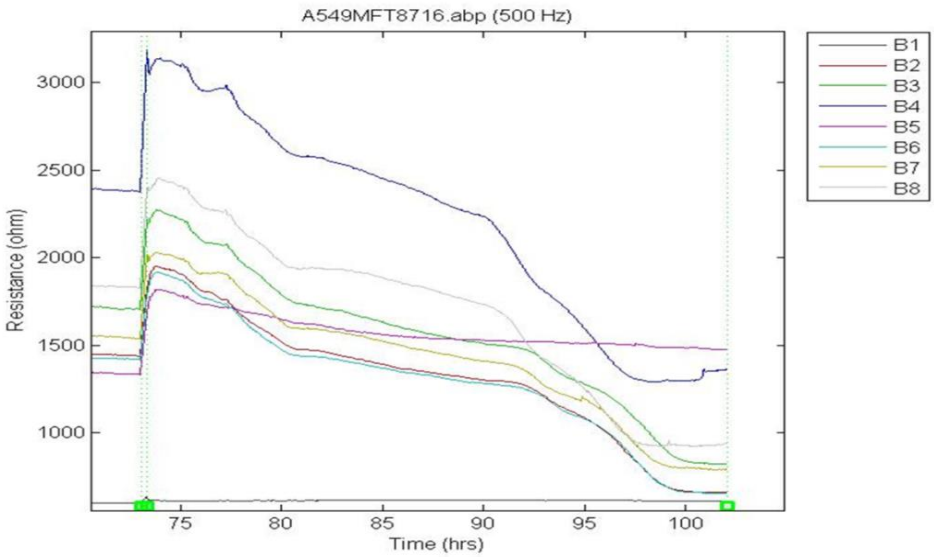

Fig 26: Normalized resistance vs. Time graph (500Hz) of A549 cells post-infection. Control cells (pink line) showed no significant changes in the impedance measurement. The infected cells showed a gradual reduction in resistance measured. Reduction in resistance was observed as early as 2hr PI.

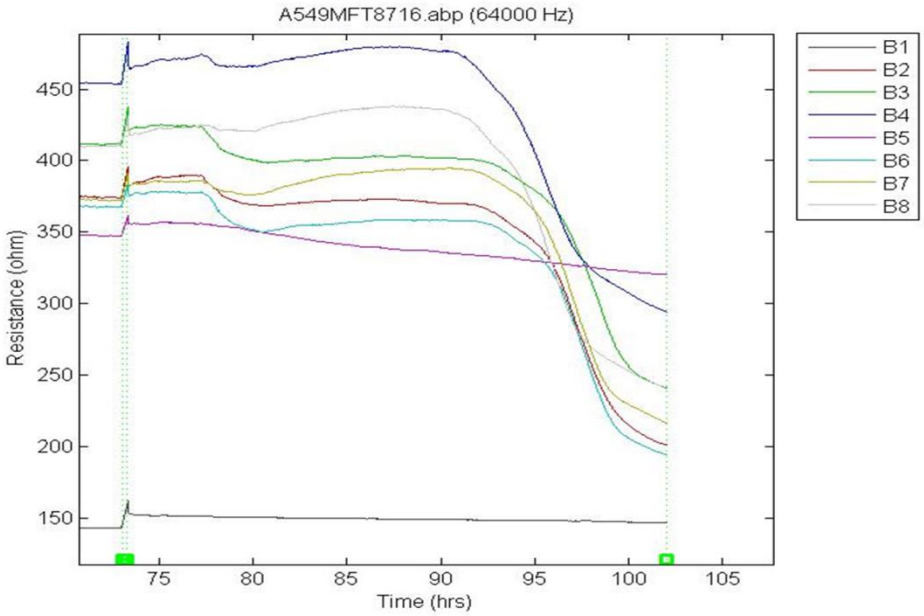

Fig 27: Normalized resistance vs. Time graph (64000Hz) of A549 cells post-infection. Control cells (pink line) showed no significant changes in the impedance measurement. The infected cells did not show any significant changes in the resistance measured till 10hr of infection. After which, a sudden decrease in resistance was observed.

The effect of *Pseudomonas* infection on the barrier properties of the A549 epithelium was assessed by Electrical Cell Substrate Impedance Sensing (ECIS). At

4000Hz (Fig 26), the reduction was observed in impedance following infection, indicating a decrease in barrier integrity of the monolayer. At 500Hz (Fig 27), current passes through the intercellular junctions and the focal adhesion points. This reveals the barrier properties of the monolayer. A gradual decrease was observed in barrier integrity of A549 monolayer infected with *Pseudomonas*. The decrease was observed as early as 2hr post-infection. No change in impedance was observed in uninfected cells throughout the experiment.

At 64000Hz (Fig 28), the applied current directly passes through the insulting membranes of the epithelial cells, revealing the changes in morphology and viability of cells. Change in the morphology of cells decreases the resistance offered by the cell to the flow of current. At 64000Hz, no changes in impedance were observed in A549 monolayers infected with *Pseudomonas*. 15hr post-infection.

4.3.2. Effect of Azithromycin on *Pseudomonas* infection of A549 cell

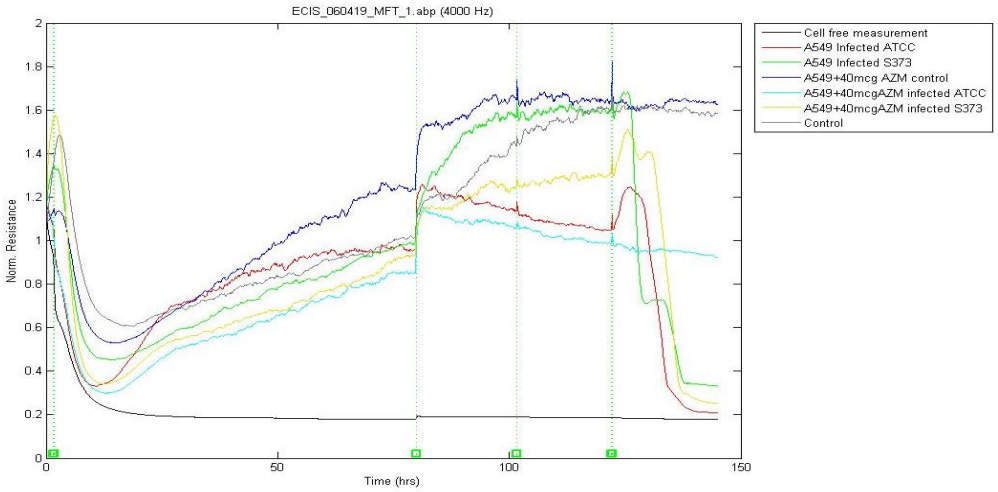

Fig 28: Effect of Azithromycin (AZM) pre-treatment on *Pseudomonas* infection of A549 cells - assessed by ECIS (4000Hz). Control wells did not show any significant reduction in resistance measured. Azithromycin pre-treated cells upon infection by *Pseudomonas* ATCC isolate showed no significant decrease in resistance measured till 8hrPI. AZM pre-treated cells infected with clinical isolate showed a delay in disease.

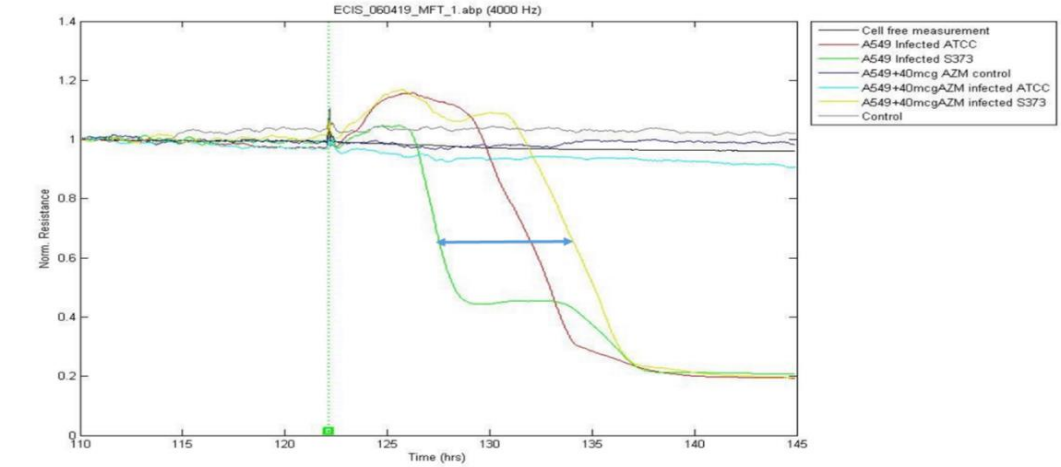

Fig 29: Effect of Azithromycin (AZM) pre-treatment on *Pseudomonas* infection of A549 cells - assessed by ECIS (4000Hz) hours post-infection. Control wells did not show any significant reduction in resistance measured. Azithromycin pre-treated cells upon infection by *Pseudomonas* ATCC isolate showed no significant reduction in resistance measured till 8hrPI. AZM pre-treated cells infected with clinical isolate showed a delay in infection.

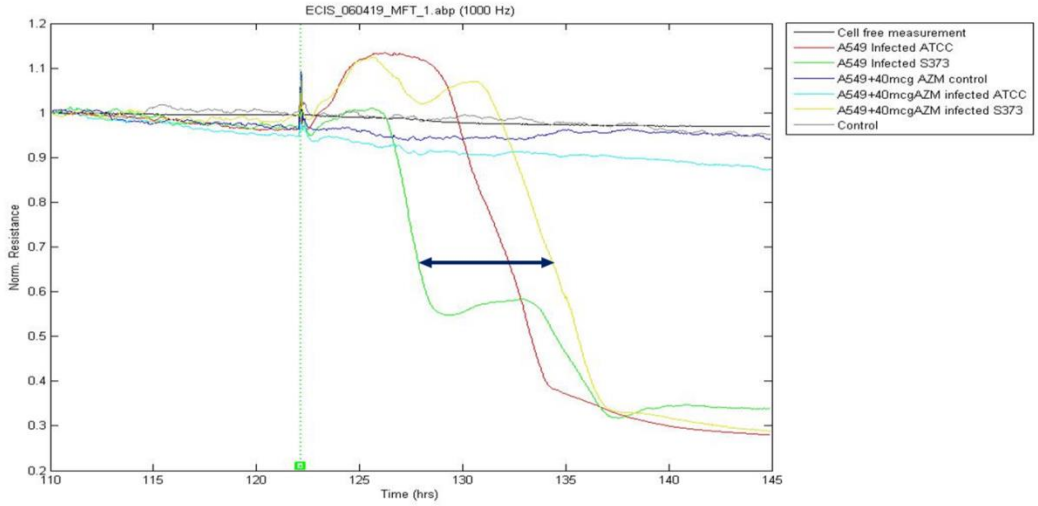

Fig 30: Effect of Azithromycin (AZM) pre-treatment on *Pseudomonas* infection of A549 cells - assessed by ECIS (1000Hz) hours post-infection. Control wells did not show any significant reduction in resistance measured. Azithromycin pre-treated cells upon infection by *Pseudomonas* ATCC isolate showed no significant reduction in resistance measured till 8hrPI. AZM pre-treated cells infected with clinical isolate showed a delay in infection.

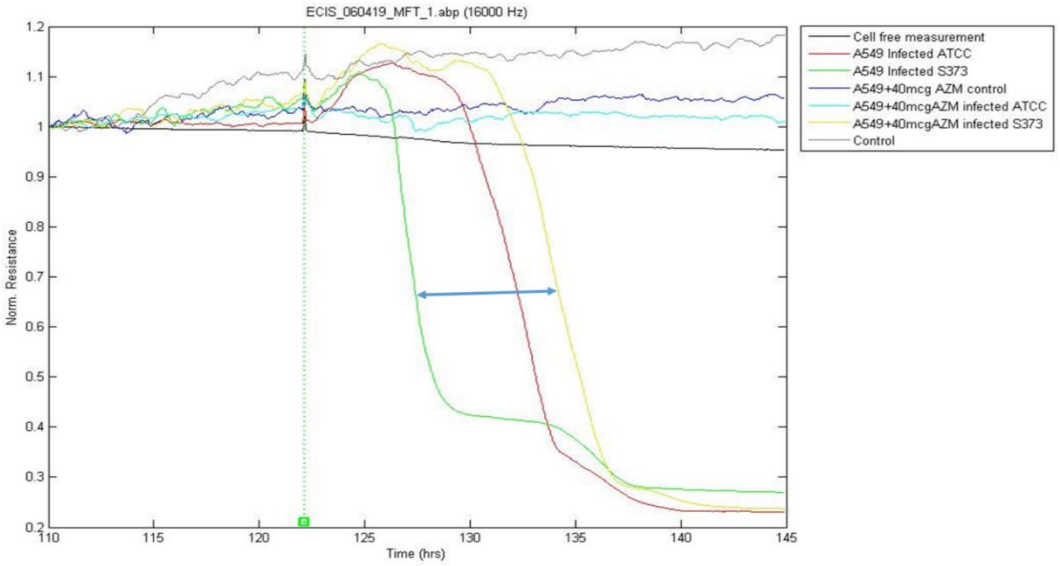

Fig 31: Effect of Azithromycin (AZM) pre-treatment on *Pseudomonas* infection of A549 cells - assessed by ECIS (16000Hz) hours post-infection. Control wells did not show any significant reduction in resistance measured. Azithromycin pre-treated cells upon infection by *Pseudomonas* ATCC isolate showed no significant reduction in resistance measured till 8hrPI. AZM pre-treated cells infected with clinical isolate showed a delay in infection.

The effect of azithromycin treatment on *Pseudomonas* infection of A549 cells was assessed by ECIS. Azithromycin (40µg/ml) pre-treatment was given to A549 cells for 5 days. A549 cells treated with azithromycin showed an increased impedance compared with the standard cell culture medium. Control cells did not show any changes in impedance. A decrease in impedance following infection with *Pseudomonas* was observed as early as three hours post-infection in cells grown in a standard cell culture medium (Fig 29 and 29a).

Pre-treatment of A549 cells with azithromycin resisted infection by *Pseudomonas* ATCC27853 isolate. At 1000Hz (fig 30), where the current passes through the intercellular junctions and focal adhesion points, the changes in impedance indicate that the azithromycin-treated wells showed a delay in changes in the barrier properties upon infection with clinical isolate S373. A 10hr delay was observed.

A similar observation was made at 16000Hz (fig 31), where the impedance measured indicates changes in cell morphology and viability of cells. A 10hr delay was observed in the time taken for morphology change in S373 infected cells pre-treated with AZM. At the same, AZM treatment resisted infection by ATCC27853.

4.3.3. Biofilms of *Pseudomonas* reduced reactive Oxygen species generation in A549 and THP1 cells.

Reactive Oxygen Species (ROS) generation is one of the early responses to stress. We assessed the ROS generation in A549 cells by the DCFHDA method. It was observed that, compared to the ATCC27853 isolate, the ROS generation in cells infected with clinical isolates was reduced (Fig.32A, B C, and D). ATCC isolate induced ROS production as early as 0hr post-infection. An increase in ROS generation in A549 infected with clinical isolates was observed only after 3hr post-infection (Fig 32 B, C, and D).

ROS generation by THP1 exposed to *Pseudomonas* planktonic and biofilm forms was assessed by the DCFHDA method. It was observed that planktonic cells induced an increase in ROS production (Fig 32 E-H). Biofilms reduced ROS production in monocytes. Planktonic *Pseudomonas* caused ROS production as early as 2hr PI. Even after 8hr of infection, biofilms failed to induce ROS production. Biofilms of both ATCC 27853 and clinical isolates reduced ROS production in monocytes (Fig 32 E-H).

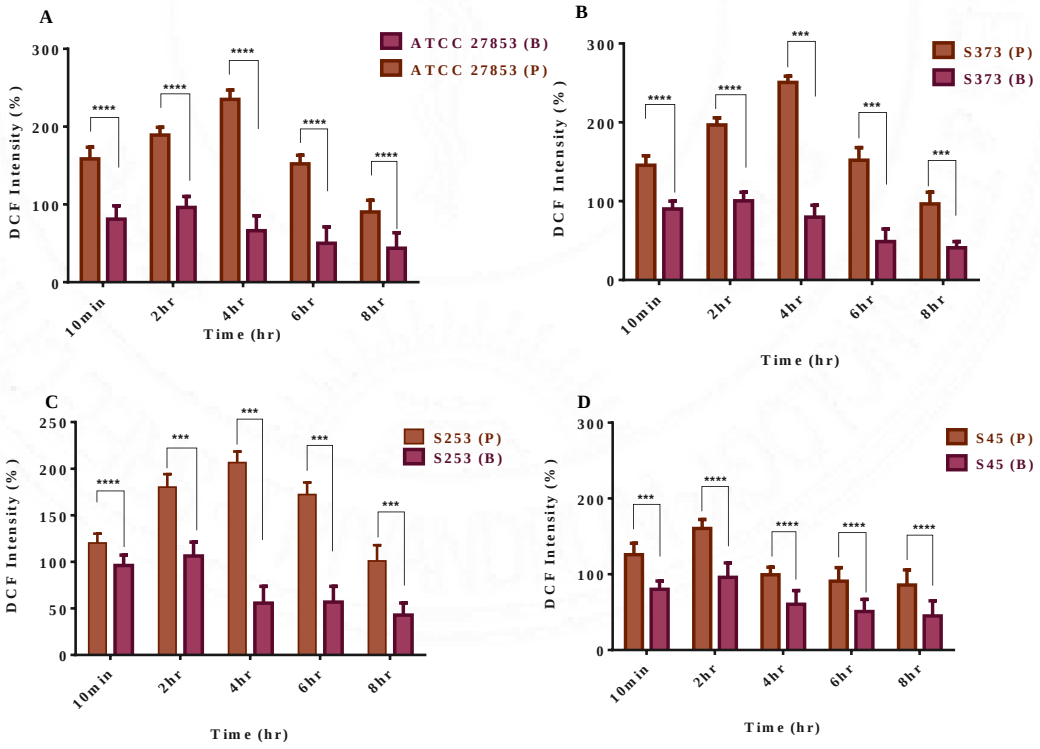

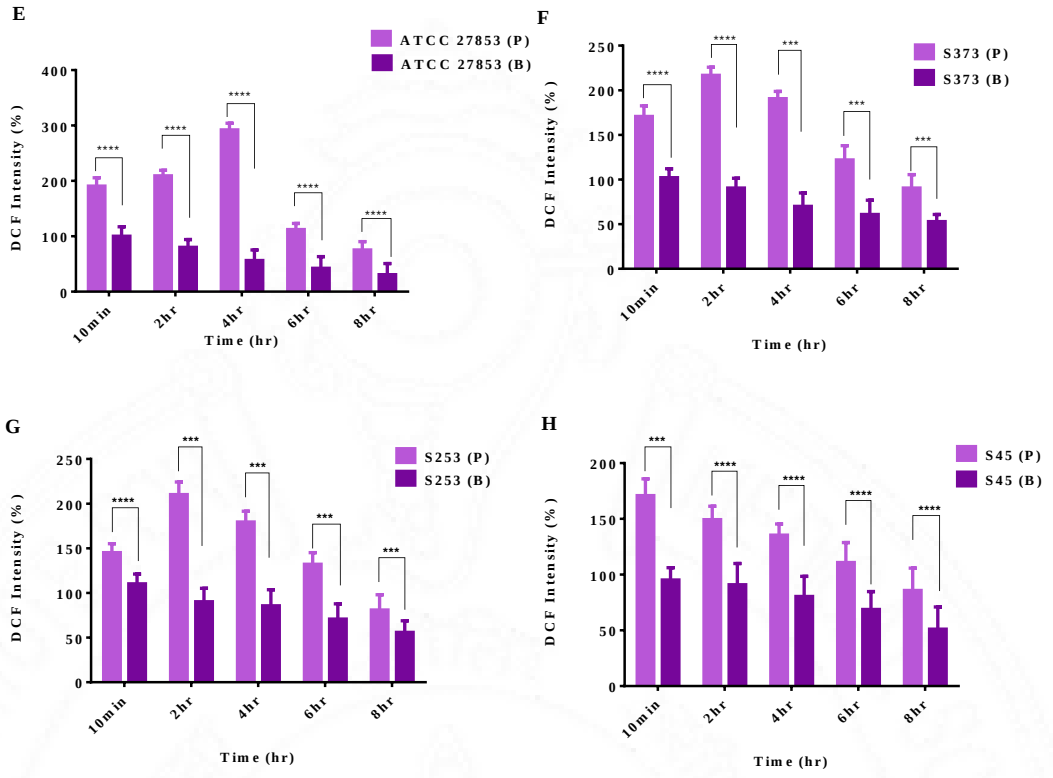

Fig 32: **Oxidative stress-induced by planktonic and biofilm forms of *Pseudomonas* on A549 and THP1 cells.** P- Planktonic and B- biofilms. The ROS generation in A549 cells (A-D) and THP1 cells (E-H) was assessed by the DCFDA method. Percentage DCF intensity (after normalisation with control) has been plotted. n=3, and statistical analysis was done by student's T-test. ****p<0.0001and p<0.001 were considered significant.

4.3.4. Biofilm *Pseudomonas* was less internalized than planktonic *Pseudomonas*

Phagocytosis is an essential mechanism of pathogen elimination by the innate immune system. Planktonic and biofilm bacterial internalization was analyzed by Gentamicin protection assay.

Monocytes exposed to planktonic *Pseudomonas* resulted in an increase in *Pseudomonas* internalization up to 3hr of infection. Biofilms bacteria reduced internalization by monocyte (Fig 33). Almost 50% reduction was observed in the internalization of biofilm bacteria

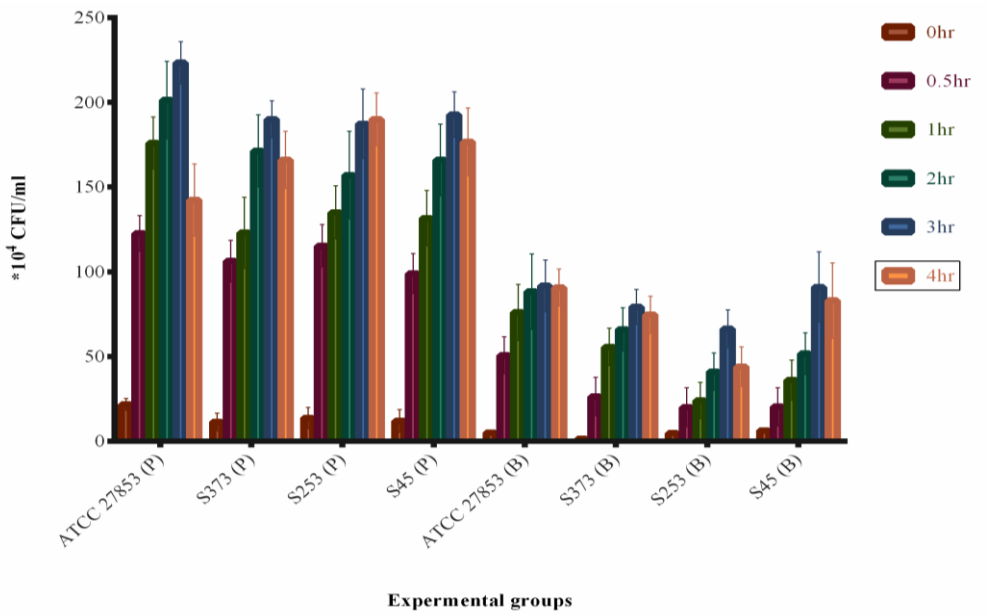

Fig 33: Gentamicin Protection Assay: Internalization of planktonic or biofilm forms of *Pseudomonas* by THP1 cells was assessed by gentamicin protection assay. Viable counts of internalized bacteria were obtained by gentamicin protection assay. Biofilm bacteria were less internalized than planktonic bacteria. No significant increase in biofilm bacteria internalization was observed over a period of 4hr. N =3 and statistical analysis was done using the student's t-test.

4.3.5. Biofilms infected A549, and THP1 cells showed both apoptotic and necrotic changes.

Fig. 34 depicts the acridine orange/propidium iodide-stained images of A549 cells infected with *Pseudomonas* planktonic and biofilm forms. Control cells stained green in color (Fig 34A). The cells showed an intact epithelial morphology. Planktonic *Pseudomonas* infected cells showed changes in cell morphology at 4hr post-infection. The cells appeared spherical (Fig 34 B to E). A decrease in cell membrane integrity, indicated by accumulation of propidium iodide in the cytoplasm, was noted in A549 cells 4hr post-infection ((Fig 34B to E). Such cells appeared yellow (red colour arrow).

8hr post-infection (Fig 35 F – I), more cells appeared to have changed morphologies. Excessive accumulation of propidium iodide (blue arrow) was observed in more cells. A few cells also appeared swollen, indicating a necrotic form of cell death. All these features observed indicate a necrotic form of cell death in A549 cells infected with planktonic forms of *Pseudomonas* (Fig 35 F – I).

The morphological changes in A549 cells infected with biofilms of *Pseudomonas* were assessed by acridine orange/ propidium iodide staining (Fig 35 A-I). 4hr post infections, A549 cells showed cellular blebbing (yellow arrows), indicating early stages of apoptosis (Fig 35B – E). Accumulation of propidium iodide was found in the cytoplasm of the cells indicating a loss of membrane integrity. Cells infected by biofilms of both ATCC 27853 strain and clinical isolates (S373, S253, and S45) showed cell swelling with excessive accumulation of propidium iodide. This was indicative of necrotic cell death (green arrows). Dead cells appeared red.

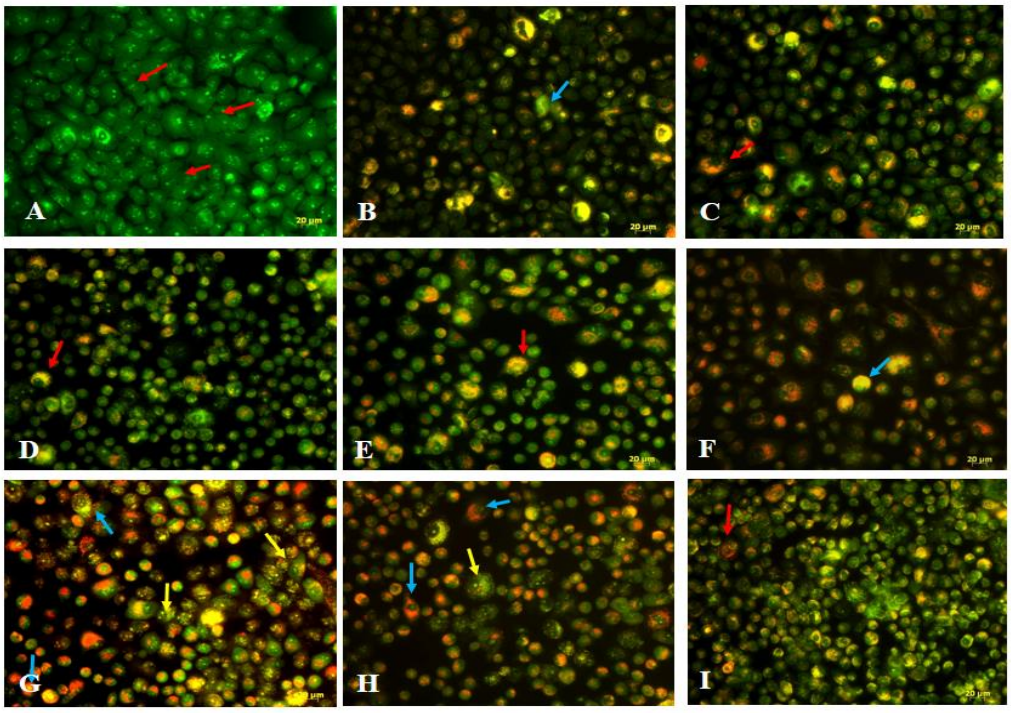

Fig 34: Assessment of mechanism of cells death. Acridine orange/Propidium Iodide-stained images of A549 cells infected with planktonic forms of *Pseudomonas* 4hr (B) ATCC 27853, C) S373, D) S253 and E) S45 and 8hr (F) ATCC 27853, G) S373, H) S253 and I) S45). A. Control (uninfected cells). The cells appeared to have PI accumulation in the cytoplasm, indicating the loss of membrane integrity (blue arrow). Scale bar 20µm and magnification 20X

At 8hr post-infection (Fig 35 F –I), most of the cells showed propidium iodide accumulation in the cytoplasm. Loss of membrane integrity and cellular swelling was the major observation at 8hr post-infection. Vacuolation was observed in cells infected with *Pseudomonas* biofilms (green arrows). Few cells appeared dead. Both apoptotic and necrotic cell death was observed in cells infected with biofilms of

Pseudomonas. Control cells appeared green with intact epithelial morphologies (Fig 35 A).

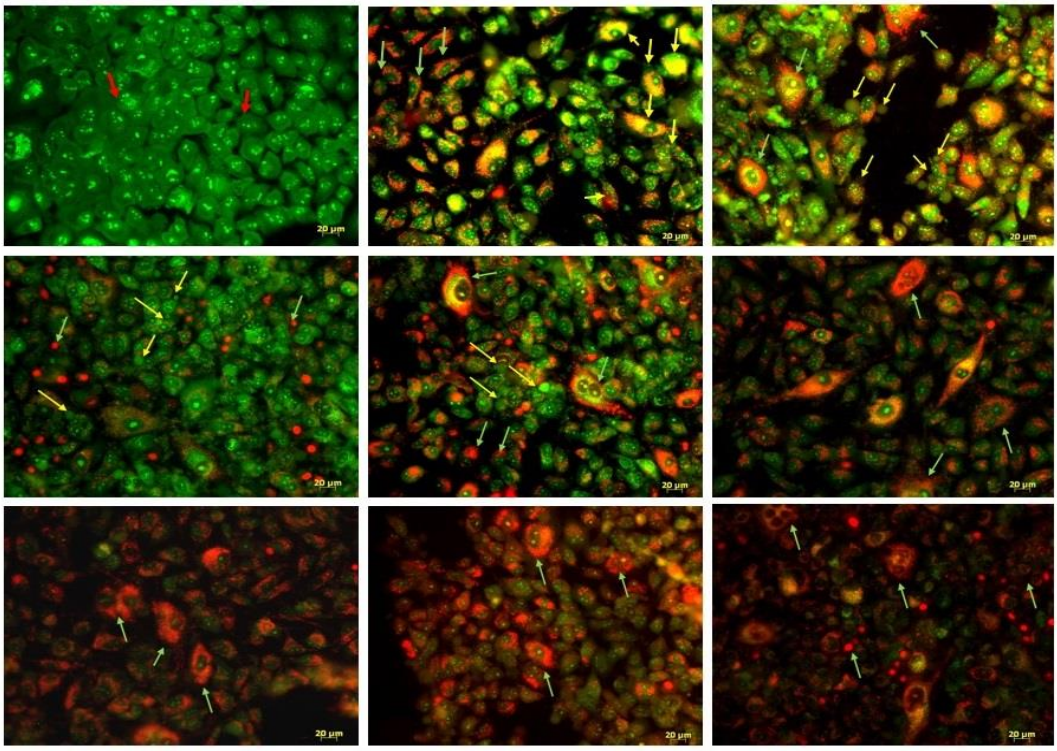

Fig 35: Assessment of mechanism of cell death induced by biofilms – Acridine orange/PI-stained images of A549 cells infected with biofilm forms of *Pseudomonas* 4hr (B) ATCC 27853, C) S373, D) S253 and E) S45 and 8hr (F) ATCC27853, G) S373, H) S253 and I) S45) post-infection. A. Control (uninfected cells). Cells with apoptotic morphologies like cellular blebbing (yellow arrows) and cell with excessive PI accumulation in the cytoplasm was observed (Green arrow). 8hr post-infection cells appeared to have lost membrane integrity (green arrow) and cellular swelling (green arrow). Scale bar 20µm and magnification 20X.

Morphological changes in THP1 monocytes were assessed by Acridine orange staining (Fig 36). It was observed that monocytes exposed to planktonic *Pseudomonas* showed necrotic cell death by 4hr post-infection (Fig 36 B – E).

On the other hand, monocytes exposed to biofilms (Fig 36 F - I) showed cellular blebbing. The cells lost their spherical morphology and showed altered morphologies. Monocytes were found entrapped in biofilms. The cells were also observed to have cytoplasmic fragmentation by 6hrs post-infection. 8hrs post-infection (Fig 36 F – I), the necrotic cells were found in abundance.

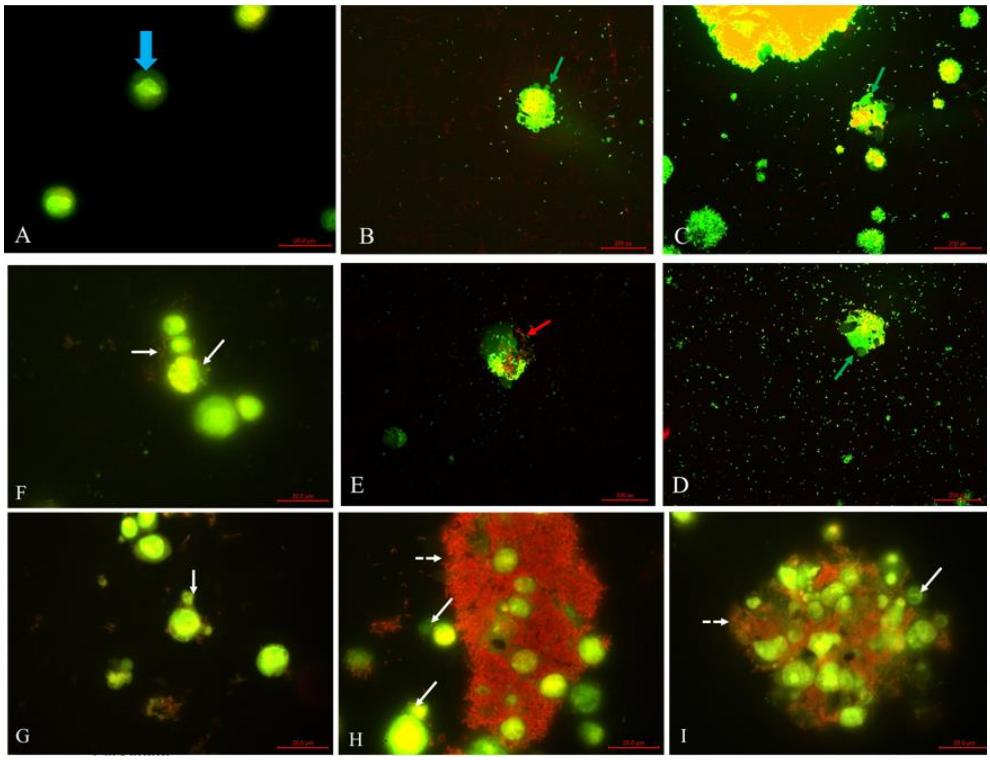

Fig 36: Assessment of cell death mechanism in THP1 cells induced by Planktonic and biofilm forms of *Pseudomonas*. THP1 cells infected with planktonic cells (B-E) showed changes in cell morphologies (arrowhead). Cells infected with biofilms of *Pseudomonas* (F-I) showed cellular blebbing (white arrows). THP1 cells were found entrapped within the biofilm (H and I) (white dashed arrows). Magnification 100X

Nuclear changes in A549 cells exposed to biofilms of *Pseudomonas* were assessed by staining with Hoechst 33342. Control cells showed intact nuclear morphology (Fig.37 A). ATCC27853 (Fig 37B), S373 (Fig 37C), S253 (Fig 37D), and S45 (Fig 37E) biofilm infected cells showed nuclear fragmentation with an intact nuclear membrane (yellow arrow). Multiple fragments (stained as blue dots) were observed in most cells. A few cells also appeared to have condensed nuclei, indicative of apoptosis. Nuclear fragmentation is one of the key features of apoptotic cells. In apoptotic cells, nuclear fragmentation is accompanied by the dissolution of the nuclear membrane. The nuclear membrane remained intact in the cells infected by *Pseudomonas* biofilms. (Fig 37B – E)

Nuclear changes were assessed by Hoechst 33342 staining. Like what was observed in epithelial cells, nuclear fragmentation with an intact nuclear membrane (Fig 37A – E).

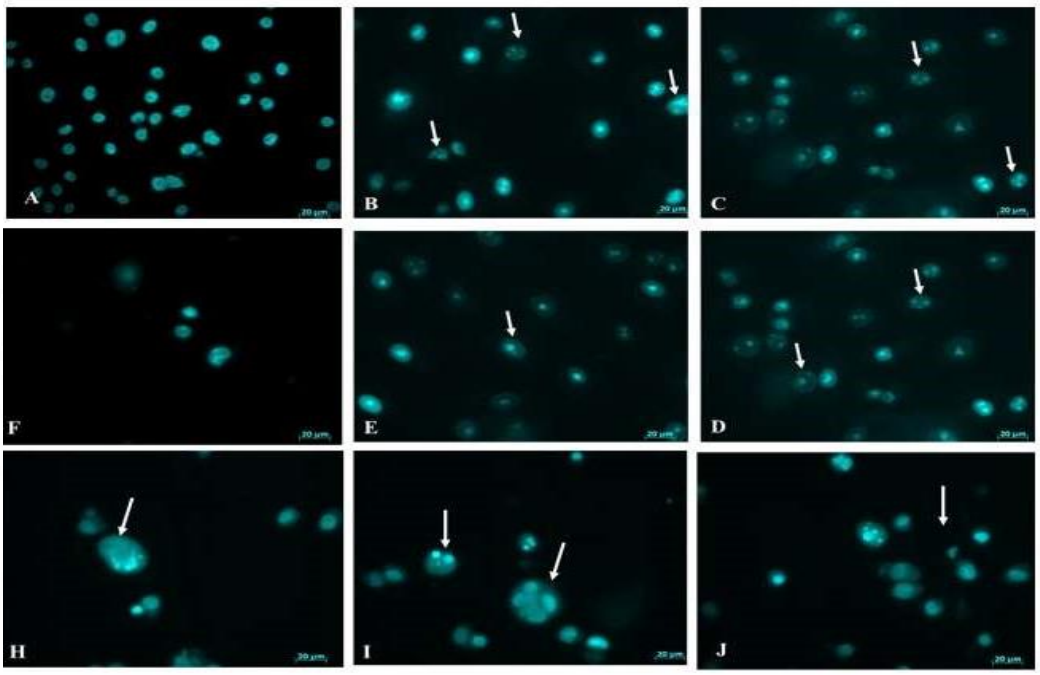

Fig 37: Assessment of nuclear change in A549 cells and THP1 infected with biofilms of *Pseudomonas*. Hoechst 33342 stained nucleus of A549 (A-E) cells and THP1 (F – J) infected with biofilms of *Pseudomonas* ATCC (B and G), S373 (C and H), S253 (D and I), and S45 (E and J). White arrows indicate DNA fragmentation with the intact nuclear membrane. A and F A549 control and THP1 Control respectively. Control cells show intact nuclei. Scale bar 20µm and magnification 20X.

4.3.6. Immune modulations

4.3.6.1. Epithelial responses: Biofilms of *Pseudomonas* upregulated TNFα in epithelial cells

TNFα is involved in the antimicrobial defense of the host. They are produced by epithelial cells, Monocytes/Macrophages during an acute response. They play important role in the immune response to bacterial pathogens.

TNFα gene expression in epithelial cells was evaluated by RT-PCR. As seen in fig: 38A – D, A549 cells exposed to planktonic forms of *Pseudomonas* (both ATCC 27853 and Clinical isolates) showed an up-regulation in TNFα gene expression. A time-dependent increase was observed till 6hrs post when challenged with planktonic *Pseudomonas,* followed by a decrease at 8hr PI, and this increase was 5-fold. ATCC

27853 biofilms also induced an up-regulation in TNFα gene expression in A549 cells, up to 4hr PI, followed by a decrease at 6hr and 8hr (Fig 38A). It can also be observed that biofilms downregulated the TNFα expression compared to the planktonic forms of ATCC 27853.

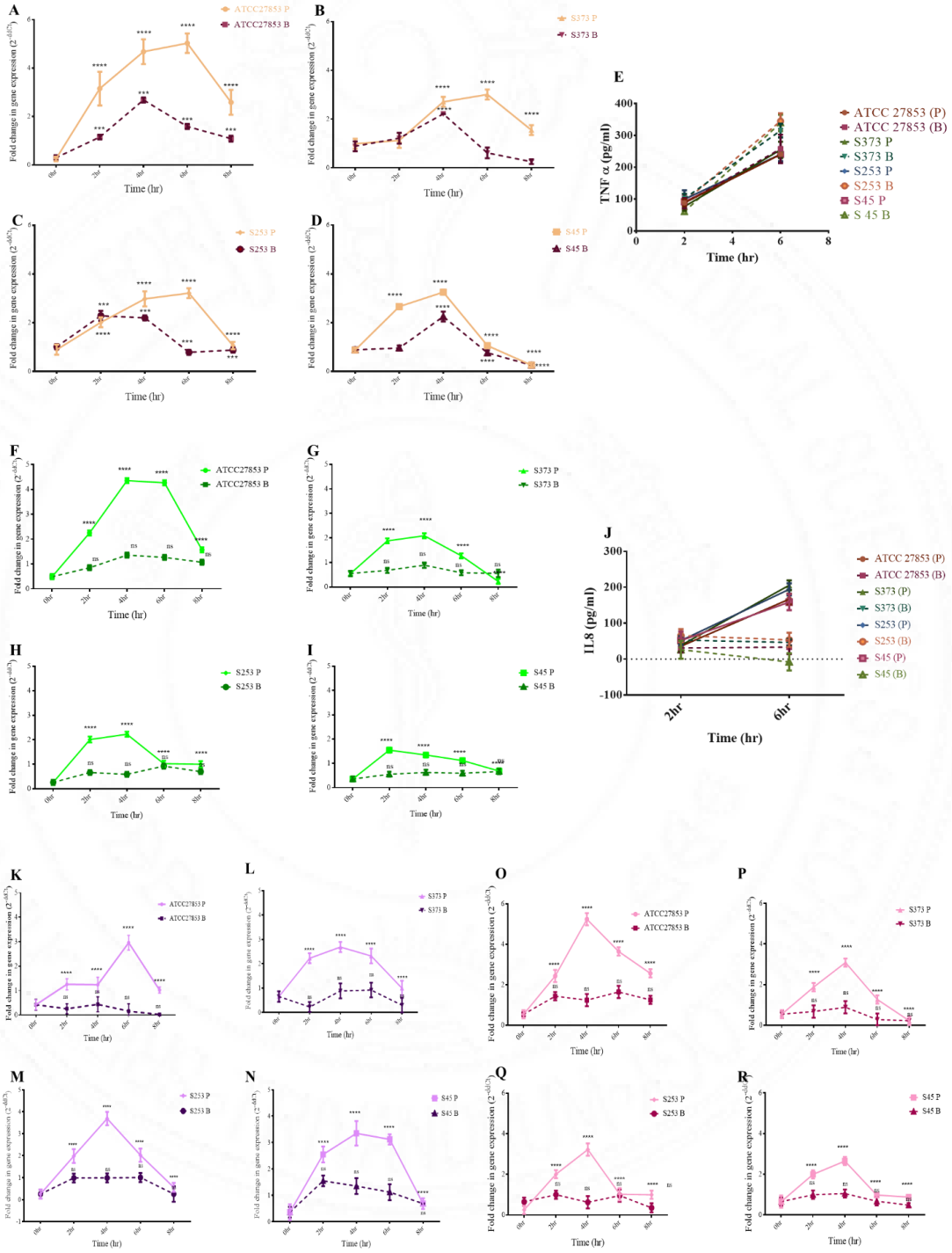

Fig. 38: Proinflammatory cytokine expression in A549 cells exposed to planktonic (P) and Biofilm (B) forms of *Pseudomonas*. Proinflammatory cytokine gene expression in A549 cells exposed to planktonic and biofilm forms of *Pseudomonas* was assessed by real-time – quantitative PCR. Fold change in gene expression ($2^{(-\Delta\Delta Ct)}$) has been plotted. TNFα gene expression in A549 cells exposed to A. ATCC 27853 B. S373, C. S253, and D S45. IL8 gene expression in A549 cells exposed to F. ATCC 27853 G. S373, H. S253, and I.S45. IL6 gene expression in A549 cells exposed to K. ATCC 27853 L. S373, M. S253, and N. S45. iNOS gene expression in A549 cells exposed to O. ATCC 27853 P. S373, R. S253, and S S45. TNFα (E) and IL8 (J) released into the culture medium were quantified by ELISA. N=3 and statistical analysis were carried out by ANOVA. $P<0.0001$ and $p< 0.001$ were considered significant. Ns – not significant.

Clinical isolates also showed similar cytokine profiles (Fig 38 B-D). The planktonic forms of S373 (Fig 38 B) and S253 (Fig 38 C) induced α up-regulation in A549 cells up to 6hr post-infection, followed by a decrease at 8hr (Fig 38 B, C, and D). The TNFα gene expression in A549 cells infected with planktonic forms of S45 (Fig 38D) isolates peaked at 4hr PI, followed by a decrease at 6hr and 8hr.

Biofilms of clinical isolates also showed a time-dependent up-regulation in TNFα gene expression up to 6hr PI and then decreased (Fig 38 B, C, and D). A significant down-regulation in TNFα gene expression was noted in A549 cells exposed to biofilm forms compared with the planktonic forms. This was noted in the case of both the ATCC 27853 isolate and the clinical isolate S373, S253, and S45 (Fig 38 A-D).

IL8 is a pro-inflammatory cytokine, also known as neutrophil chemo attractant protein. The major function of IL8 involves the recruitment of neutrophils and their activation and therefore plays an important role in pathogen clearance.

ATCC 27853 planktonic forms induced upregulation of IL8 gene expression in A549 cells up to 6hr post-infection, which reduced at 8hr (Fig.38F). A 4.5-fold increase was observed at 4hr and 6hr PI. Planktonic forms of clinical isolates S373 (Fig 38G), S253 (Fig 38H), and S45 (Fig 38I)) also showed a time-dependent increase in IL8 expression in A549 cells up to 4hr (Fig. 38F-I). A decrease in IL8 gene expression was observed at 6hr and 8hr PI. IL8 gene expression in A549 cells exposed to planktonic forms of S45 isolates peaked at 2hr (Fig 38I), followed by a decrease. When compared with the ATCC 27853 planktonic forms, the planktonic forms of clinical isolates reduced IL8 production in A549 cells.

Biofilms of *Pseudomonas* (both ATCC 27853 and clinical isolates) did not induce a significant up-regulation in IL8 gene expression. Biofilms reduced IL8 expression by A549 cells, and no time-dependent increase in IL8 gene expression was observed till 8hr PI.

IL6 is a multifunctional cytokine involved in acute phase responses of the host. Planktonic forms of ATCC 27853 (Fig 38K) isolate induced an up-regulation in IL6 expression at 6hr post-infection. A 3fold increase was obtained at 6hr followed by a decrease at 8hr. A549 cells exposed to planktonic forms of *Pseudomonas* clinical isolates showed a time-dependent increase (Fig 42 K-N) in IL6 gene expression up to 4hr PI, followed by reduction at 6hr and 8hr PI. S373 (Fig 42L) showed a 2.8-fold increase at 4hr, S253 (Fig 42M) and S45 (Fig 42N) showed a 3.8- and 3.5-fold increase respectively at 4hr PI.

On the other hand, Biofilms failed to induce a significant upregulation in IL6 expression by A549 cells. Biofilms of ATCC 27853 and clinical isolates reduced IL6 expression in A549 cells.

Induced Nitric oxide synthase is involved in synthesizing Nitric Oxide, which is one of the major antibacterial molecules produced in response to an infection. Nitric Oxide (NO) is a pro-inflammatory molecule involved in the redox mediated killing of bacterial pathogens. Planktonic forms of ATCC 27853 (Fig 42 O-R) isolate induced a time-dependent increase in iNOS gene expression up to 4hr PI, followed by a decrease at 6hr and 8hr PI. The planktonic forms of clinical isolates S373 (Fig 42P), S253 (Fig 42 Q), and S45 (Fig 42 R) also showed a time-dependent increase up to 4hr post-infection, which was followed by a decrease. ATCC 27853 isolate induced a 5.5-fold increase in iNOS gene expression, whereas clinical isolates S373, S253, and S45 induced a 3.0-, 3.2-, and 3.6-fold increase, respectively.

Biofilms of both ATCC 27853 and clinical isolates failed to induce upregulation of iNOS gene expression in A549 cells up to 8hr PI.

In concordance with the gene expression results, TNFα protein expression also increased A549 cells infected with planktonic and biofilm forms of *Pseudomonas*. A significant increase in TNFα expression was observed at 6hr PI (Fig 38E). On the other

hand, IL8 protein expression showed a significant change only in THP1 cells infected with planktonic forms of *Pseudomonas*. Biofilm reduced IL8 protein expression in A549 cells (Fig 38J).

4.3.6.2. Monocytes responses - Biofilms of *Pseudomonas* upregulated TNFα expression in monocytes

The TNF α gene expression in THP1 cells exposed to planktonic and biofilm forms *Pseudomonas* was evaluated. A time-dependant increase in TNFα gene expression was observed in THP1 cells infected with planktonic forms of ATCC27853 (Fig 39 A) isolate ($p<0.0001$). The expression peaked at 4hr post-infection. A decrease in TNFα gene expression was observed at 6hr and 8hr. This could be due to cell death induced in THP1 cells. A 4.5-fold increase was observed.

THP1 cells exposed to biofilms of *Pseudomonas* also showed an upregulation in TNFα gene expression (***$p<0.001$). A 3.7-fold increase was observed at 4hr PI. At 6hr and 8hr post-infection, TNFα expression reduced (Fig 39 A-D). The planktonic forms of clinical isolate S373 (Fig 39 B) and S45 (Fig 39 D) also induced significant upregulation in TNFα gene expression up to 4hr post-infection. In S253, TNFα expression peaked at 6hr (Fig 39 C).

Biofilms of clinical isolates also upregulated TNFα gene expression in THP1 cells (Fig 39 A-D). A time-dependent increase was observed in S373 and S45 isolates, which Peaked at 4hr followed by a decrease at 6hr and 8hr. A 3.9-to-4-fold increase was observed at 4hr PI in TNFα induced by S373 (Fig 39 B) and S45 (Fig 39 D). Biofilms of S253 (Fig 39C), on the other hand, induced a significant increase in TNFα expression only at 4hr and 6hr PI. A 3.8- and 4.3-fold increase was observed at 4hr and 6hr PI.

A time-dependent increase in IL8 gene expression was observed up to 4hr in THP1 cells infected with planktonic ATCC27853 isolate (Fig 39 F – I). A 5.3-fold increase was observed at 4hr. Planktonic forms of clinical isolates also induced a time-dependent increase in IL8 gene expression inTHP1 cells up to 4hr PI. S373 (Fig 39G), S45 (Fig39H), and S45 (Fig 39 I) induced a 4.2-, 4-, and 3.3-fold increase in IL8 gene expression, respectively. Planktonic forms of ATCC27853 and clinical isolates

significantly reduced IL8 gene expression in THP1 cells 8hr PI due to cell death due to infection.

Biofilms of *Pseudomonas* significantly reduced IL8 expression by THP1 cells. No time-dependent increase in IL8 expression was observed in IL8 gene expression in THP1 cells exposed to biofilm (both ATCC 27853 and clinical isolates).

Planktonic forms of ATCC27853 and clinical isolates induced upregulation in IL6 gene expression in THP1 in a time-dependent manner. IL6 gene expression in ATCC27853 (Fig 39K) infected cells peaked at 6hr PI (4.3-fold). In S373 (Fig 39L), S253 (Fig 39M), and S45 (Fig 39N), the peak was observed at 4hr with a fold increase of 3.8, 3.0, and 3.6, respectively. A significant decrease in IL6 expression was observed at 8hr due to cell death induced by infection.

On the other hand, biofilms of both ATCC 27853 and clinical isolates failed to induce IL6 expression in THP1 cells. Up to 8hr PI, no time-dependent change was observed in IL6 expression in THP1 cells exposed to biofilms.

Both ATCC 27853 and clinical isolates induced a time-dependent increase in iNOS expression in THP1 cells up to 4hr PI, followed by a decrease at 6hr and 8hr PI (Fig 39 O). ATCC 27853 isolates induced a maximum of 5.5-fold increase in iNOS expression, whereas S373 (Fig 39P), S253 (Fig 39Q), and S45 (Fig 39R) induced only 3.8, 4.1 and 3.4.

Fold increase in iNOS expression. A significant reduction in iNOS expression was observed at 8hr PI due to cell death due to infection.

It was observed that iNOS expression was reduced in THP1 cells exposed to biofilms of *Pseudomonas* (both ATCC 27853 and clinical isolates). No time-dependent change in iNOS expression was observed till 8hr PI.

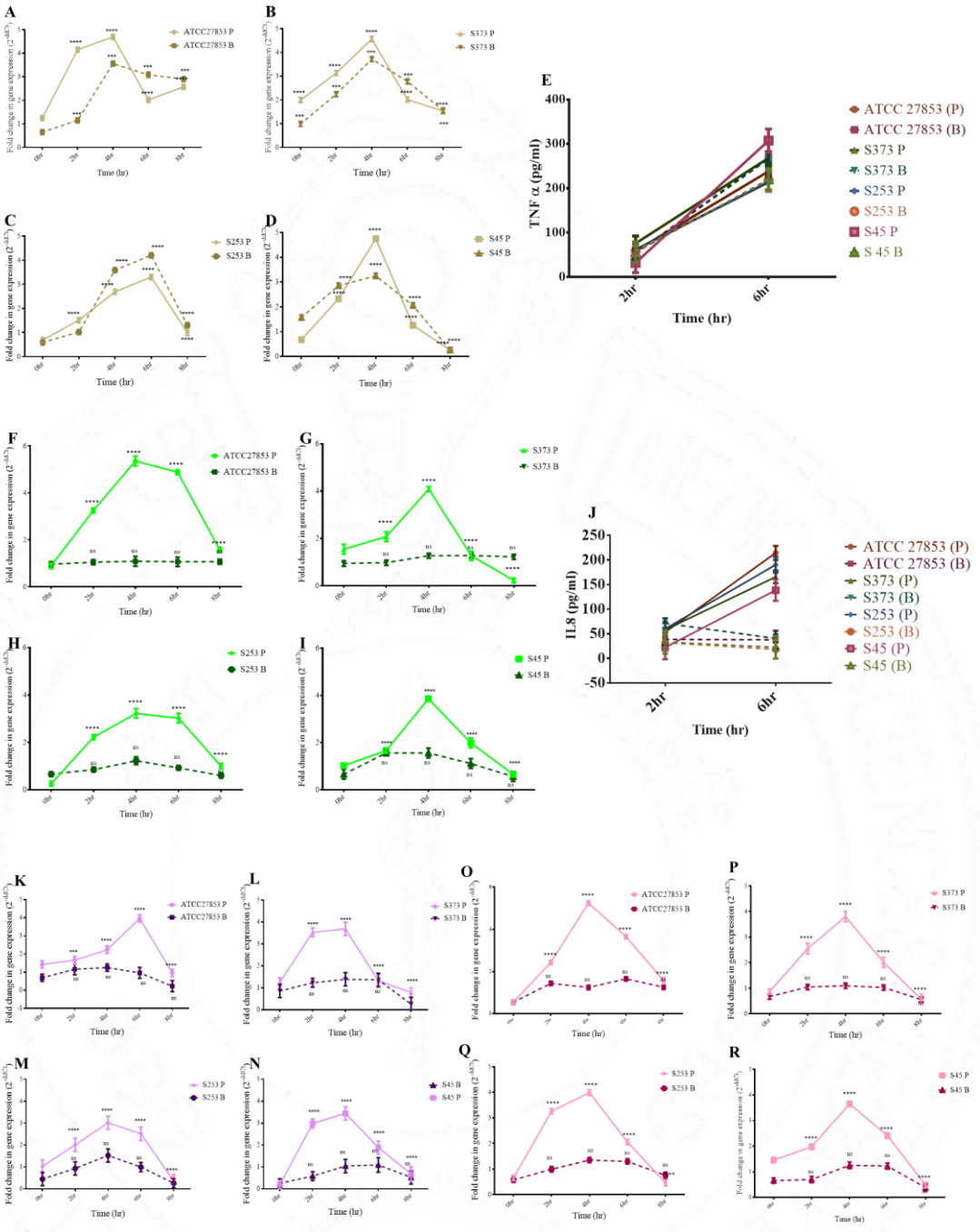

Fig 39: Proinflammatory cytokine expression in THP1 cells exposed to planktonic (P) and Biofilm (B) forms of *Pseudomonas*. Proinflammatory cytokine gene expression in THP1 cells exposed to planktonic and biofilm forms of *Pseudomonas* was assessed by real-time – quantitative PCR. Fold change in gene expression ($2^{(-\Delta\Delta Ct)}$) has been plotted. TNFα gene expression in THP1 cells exposed to A. ATCC 27853 B. S373, C. S253, and D S45. IL8 gene expression in THP1 cells exposed to F. ATCC 27853 G. S373, H. S253, and I.S45. IL6 gene expression in THP1 cells exposed to K. ATCC 27853 L. S373, M. S253, and N. S45. iNOS gene expression in THP1 cells exposed to O. ATCC 27853 P. S373, R. S253, and S S45. TNFα (E) and IL8 (J) released by THP1 cells was quantified by ELISA n=3, and statistical analysis was done by ANOVA; **** p<0.0001 and ***p<0.001 were considered significant, ns – not significant.

In concordance with the gene expression results, TNFα protein expression also increased THP1 cells infected with planktonic and biofilm forms of *Pseudomonas*. A significant increase in TNFα expression was observed at 6hr PI (Fig 39E). On the other hand, IL8 protein expression showed a significant change only in THP1 cells infected with planktonic forms of *Pseudomonas*. Biofilm reduced IL8 protein expression in THP1 cells (Fig 39J).

4.3.6.3. Co-culture responses - Biofilms of *Pseudomonas* upregulated TNFα expression in epithelial monocyte co-cultures

The effect of *Pseudomonas* infection on cytokine gene expression in A549:THP1 co-cultures was assessed. Planktonic forms of ATCC 27853 and clinical isolates induced a time-dependent upregulation in TNFα gene expression (Fig43 A - D). A 5.5-fold upregulation was observed as early as 2hr PI in ATCC 27853 infected cells (Fig 43A). S373 (3.5-fold) (Fig 43 B) and S45 (4.4-fold) (Fig 40D) showed maximum TNFα gene expression at 4hr. S253 (4.4) showed maximum upregulation at 6hr post-infection (Fig 43C). A significant reduction in TNFα expression was observed at 8hr due to cell death induced by infection.

Co-cultures exposed to biofilms showed an increase in TNFα gene expression (Fig 40A-D). A time-dependent increase in TNFα gene expression was observed. Biofilms of both ATCC 27853 and clinical isolates increased TNFα expression. An increase in TNFα protein expression also was observed in co-cultures exposed to planktonic and biofilm forms of *Pseudomonas* (Fig 40E).

A significant increase in IL8 expression was observed in co-cultures in a time-dependent manner. A 6.2-fold increase was induced by ATCC 27853 (Fig 40 F) planktonic forms at 4hr PI. S373 (Fig40G), S253 (Fig 40 H), and S45 (Fig 40I) induced 4.5-, 4.4-, and 4.8-fold increases at 4hr, respectively. A decrease was observed in IL8 gene expression at 8hr PI. A reduction in cell numbers due to cell death reduced IL8 expression at 8hr. IL8 gene expression in A549 cells, THP1 cells, and co-cultures exposed to biofilms of *Pseudomonas* did not show a time-dependent increase.

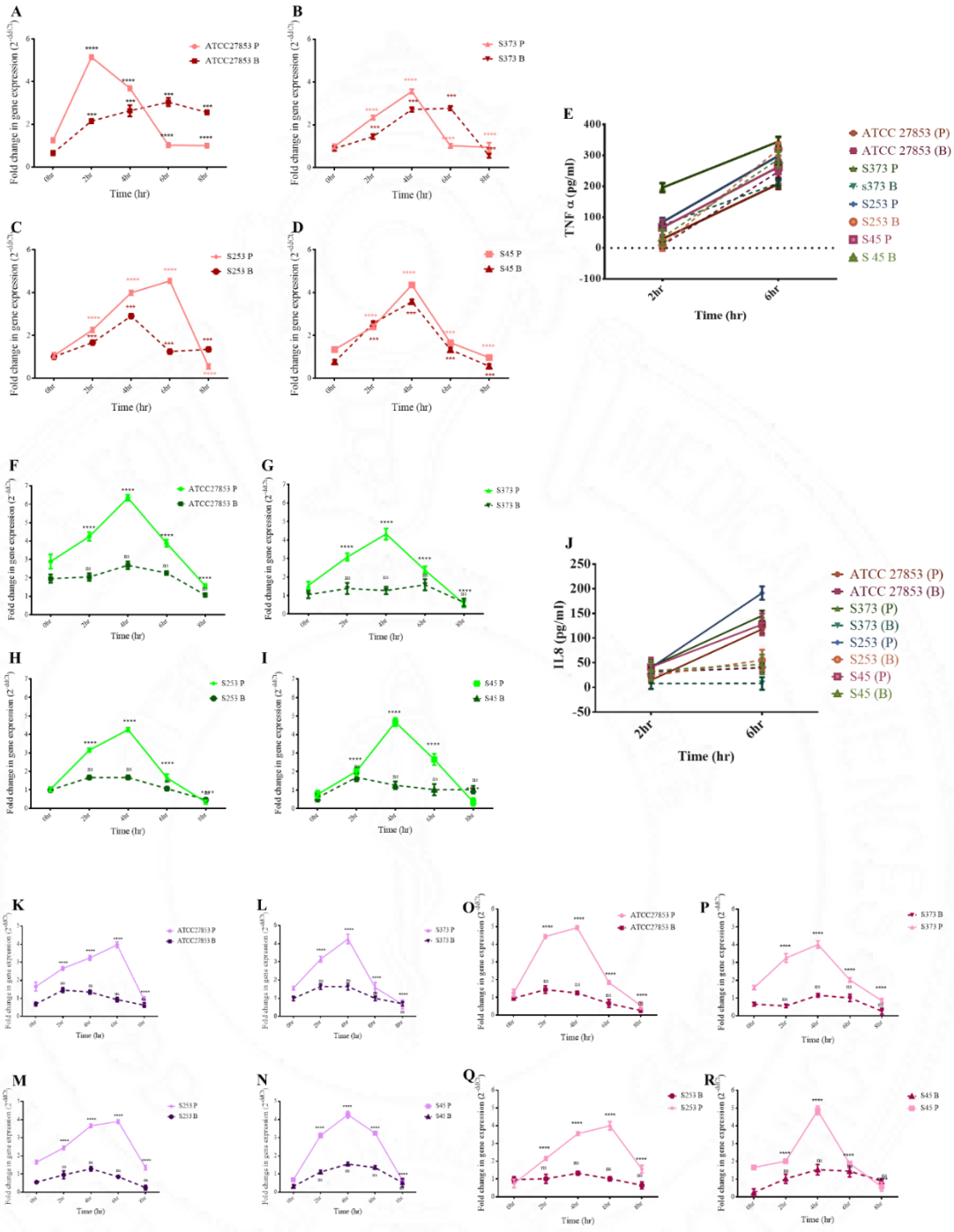

Fig 40: Proinflammatory cytokine expression in A549:THP1 co-cultures on exposure to planktonic (P) and Biofilm (B) forms of *Pseudomonas*. Proinflammatory cytokine gene expression in A549:THP1 cells exposed to planktonic and biofilm forms of *Pseudomonas* was assessed by real-time – quantitative PCR. Fold change in gene expression ($2^{(-\Delta\Delta Ct)}$) has been plotted. TNFα gene expression in A549:THP1 cells exposed to A. ATCC 27853 B. S373, C. S253, and D S45. IL8 gene expression in A549:THP1 cells exposed to F. ATCC 27853 G. S373, H. S253, and I.S45. IL6 gene expression in A549:THP1 cells exposed to K. ATCC 27853 L. S373, M. S253, and N. S45. iNOS gene expression in A549:THP1 cells exposed to O. ATCC 27853 P. S373, R. S253, and S S45. TNFα (E) and IL8 released by A549:THP1 coculture in the medium were quantified by ELISA. N =3, statistical

analysis was carried out by ANOVA, ****p<0.0001 and ***p<0.001was considered significant, ns – not significant.

Biofilms of ATCC 27853 and clinical isolates reduce IL8 expression in co-cultures exposed to *Pseudomonas* biofilms. In concordance with the gene expression data, IL8 protein expression also was found to be reduced in co-cultures exposed to biofilms.

IL6 expression in *Pseudomonas* infected A549:THP1 co-cultures were assessed. A time-dependent increase in IL6 was observed in co-cultures infected with planktonic forms of ATCC 27853 (Fig 40K). The increase was observed up to 6hr PI; A 4.1-fold increase was observed at 6hr PI, followed by a decrease. S373 (4.5-fold) (Fig 40L) and S45 (4.3-fold) (Fig 40N) showed an increase at 4hr. S253 (3.95) (Fig 40M) showed an increase at 6hr PI. A significant decrease was observed in 8hr PI. This was due to the decrease in cell numbers because of cell death.

On the other hand, biofilms significantly reduced IL6 expression in co-cultures. No time-dependent change was observed till 8hr PI.

Planktonic forms of the isolates induced iNOS gene expression in co-cultures. Planktonic ATCC 27853 (Fig 40 O) induced a significant upregulation was observed at 2hr and 4hr PI. A 5-fold increase was observed. S373 (Fig 40P) and S45 (Fig 40R) induced increased expression at 4hr and showed 4.5- and 5.1-fold increase, respectively. S253 (Fig 40Q) showed an increase at 6hr post-infection. A 4.2-fold increase was observed. 8hr PI significantly reduced the iNOS gene expression as a result of cell death due to infection.

Biofilms reduced iNOS gene expression in co-cultures. No significant change in IL8 expression was observed till 8hrPI.

4.3.6.4. Biofilms of *Pseudomonas* upregulate inflammasome markers:

Inflammasomes are cytosolic multiprotein oligomers of the innate immune system responsible for activating inflammatory responses. The assembly and activation of the inflammasome promote proteolytic cleavage, maturation, and secretion of pro-inflammatory cytokines interleukin 1β (IL-1β). Induce a pro-inflammatory form of programmed cell death distinct from apoptosis, referred to as pyroptosis.

The inflammasome gene expression in A549 cells exposed to biofilms of *Pseudomonas* was evaluated. Caspase 1, IL 1β, and Caspase 3 are essential modulators of inflammasome response. Fig 41 shows that A time-dependent increase in Caspase 1 and IL1β gene expression was observed in A549 cells exposed to biofilms of both ATCC 27853 (Fig 41A) and clinical isolates (Fig 41B, C, and D). Caspase 3, which is the executioner caspase in the apoptotic pathway, was found to be expressed only at basal levels.

IL1β protein expression also significantly increased at 2hr and 6hr post-infection in A549 cells (Fig 41E). The protein expression correlated with the gene expression data. The planktonic infection did not significantly increase IL1β. Only basal level of IL1β protein expression was observed.

The influence of biofilms on inflammasome in THP1 cells also was evaluated. It was observed that biofilms significantly increased IL1β and caspase 1 expression. A 5-to-6-fold upregulation of IL1β and Caspase 1 was observed (Fig 41 F-I). Biofilms of both ATCC 27853 and clinical isolates showed similar responses. A significant increase in IL1β protein expression was observed at 6hrPI in biofilm infected THP1 cells. Caspase 3 expression was found only at basal levels in the cells exposed to biofilms of *Pseudomonas*. No significant increase in caspase 3 was observed in THP1 cells exposed to clinical isolates.

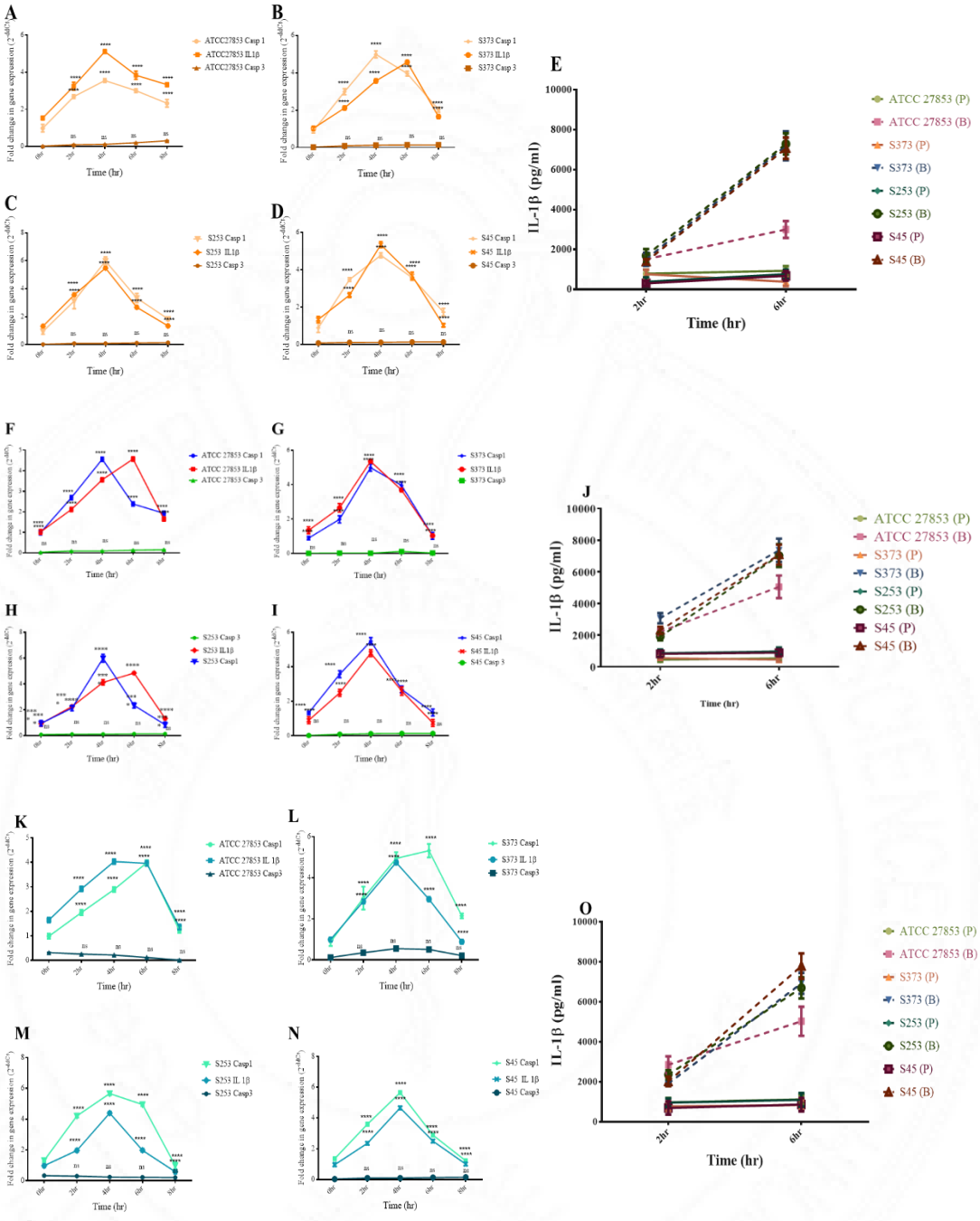

Fig 41: Inflammasome markers in A549 cells, THP1 cells, and co-cultures exposed to biofilms of *Pseudomonas*: Caspase 1, IL1β, and caspase3 expression in A549 cells infected with planktonic (P) and Biofilm (B) forms of *Pseudomonas* was assessed by real-time quantitative PCR and the fold change in gene expression ($2^{-\Delta\Delta Ct}$) has been plotted. A. ATCC 27853, B. S373, C S253, and D. S45. Caspase 1, IL1β, and caspase3 expression in THP1 cells infected with planktonic (P) and Biofilm (B) forms of F. ATCC 27853, G. S373, H S253, and I. S45. Caspase 1, IL1β, and caspase3 expression in A549:THP1 co-cultures infected with planktonic (P) and Biofilm (B) forms of K. ATCC 27853, L. S373, M. S253, and N. S45. IL1β cytokine released into the medium was quantified by ELISA E. A549, J. THP1, and O. A549:THP1 co-culture.

IL1β expression in THP1 cells exposed to biofilm showed an increase at 6hrPI; on the other hand, planktonic forms of *Pseudomonas* failed to induce IL1β production in THP1 cells (Fig 41J).

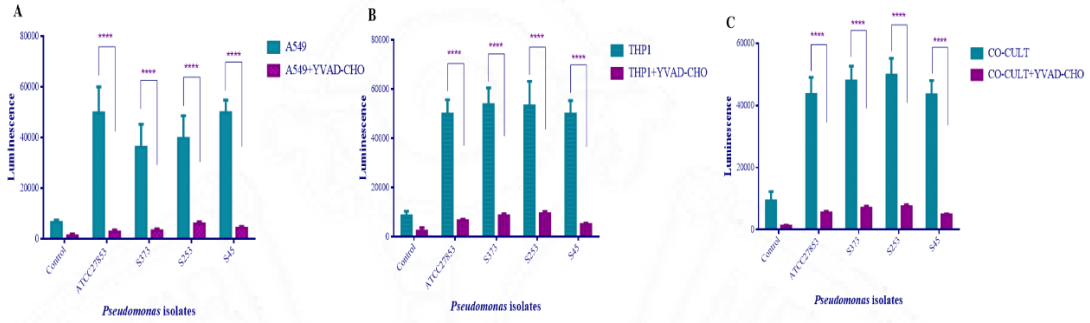

Fig 42: Analysis of Caspase 1 activity in cells infected with biofilms of *Pseudomonas*. The functional assay for Caspase 1 was assessed in A549 monolayers (A), THP1 cells (B) and A549:THP1 co-cultures (C) exposed to biofilm of *Pseudomonas*. YVAD-CHO was the caspase 1 inhibitor used to confirm the caspase 1 activity.

A549:THP1 cocultures showed an increase in caspase 1 and IL1β expression. ATCC27853 biofilms induced a 3-to-5-fold increase in IL1β expression and a four-fold increase in caspase 1 expression (Fig 41 K-N). On the other hand, clinical isolates induced a 5 – 6-fold increase in Caspase 1 and IL1β expression. IL1β protein expression was concordant with the gene expression data (Fig41O).

No significant changes were observed in caspase 3 expression in A549:THP1 co-cultures infected with *Pseudomonas* biofilms up to 8hr PI. A significant decrease was observed in Caspase 1 and IL1β expression at 8hrPI. This could be due to a reduction in cells numbers due to infection.

Functional assays for caspase 1 were assayed in A549 monolayers, THP1 cells, and A549:THP1 co-cultures exposed to biofilms of *Pseudomonas*. A significant increase was observed in caspase1 activity in the cells exposed to biofilms of *Pseudomonas* ATCC 27853 and clinical isolates (Fig 42)

5. DISCUSSION

The ability of *Pseudomonas* to colonise medical devices and human tissues forming biofilms, leading to chronic infections recalcitrant to antibiotic therapy is a global health concern. Bacterial biofilms are the predominant mode of life although two phenotypically different bacterial lifestyles exist – the free-floating "planktonic" form and the sessile colonial form the "biofilms." Biofilms are defined as a structured consortium of bacteria at interfaces embedded in a self-produced exopolysaccharide matrix consisting of polysaccharides, proteins, and DNA (Karygianni et al., 2020). One of the most intriguing facts about biofilm is its increased antibiotic resistance and host immune tolerance compared to its planktonic counterparts (Zhang et al., 2020). More than 60% of infections in humans are due to biofilms (Jamal et al., 2018). Biofilm infections are usually chronic in nature. Chronic infections are slow in progression compared to acute infections.

Pseudomonas is one of the model organisms used in understanding biofilms. *Pseudomonas* is an opportunistic pathogen capable of infecting a wide variety of hosts, including humans. It is the fourth most frequently isolated multidrug-resistant isolate from infections (Pachori et al., 2019). Biofilms in general confer survival advantage and *Pseudomonas* biofilms in chronic infections are impervious to the host immune response and high doses of antibiotics. Direct tissue infections (for, e.g., Infections in Cystic Fibrosis lung) and device-related infections (e.g., Ventilator-associated Pneumonia (VAP), infection on contact lenses, etc.) are all caused by *Pseudomonas*. In fact, it is the leading cause of Gram-Negative ventilator-associated pneumonia, with a mortality rate of 34% to 68%. Tsay et al. observed that mice that received mechanical ventilation followed by nasal instillation of *Pseudomonas* increased lung injury. Large quantities of *Pseudomonas* were observed in the trachea of the ventilated animals. Under such conditions, the alveoli and the surrounding parenchyma appeared swollen (Tsay et al., 2016). Mechanism underlying *Pseudomonas* ventilator-associated pneumonia-induced lung injury remains elusive. Most of the elucidated immune evasion mechanisms are good for acute infection caused by planktonic bacteria (Hänsch, 2012).

In this work, an effort has been made to delineate the molecular mechanisms underlying the interactions of alveolar epithelial cells and monocytes with

Pseudomonas biofilms. Epithelial cells by virtue of their position in an organ or tissue form the first line of defence to an insult or injury and monocytes and macrophages are among the first immune cells to respond to an insult or injury. These cell types have been used in the development of an *in vitro* system to understand the complex interactions in the development and persistence of *Pseudomonas* biofilms.

5.1. Phase I - Understanding the dynamics of biofilm formation by *Pseudomonas* isolates:

The study used ATCC 27853 and clinical isolates of *Pseudomonas* for the analysis. The antibiotic susceptibility profiles were analyzed in both ATCC 27853 and clinical isolates. All the clinical isolates showed resistance to Ceftazidime, a third-generation cephalosporin. Except for S373, all the other isolates were sensitive to Gentamicin- an aminoglycoside. S373 and S253 isolates showed resistance to Norfloxacin – a fluoroquinolone.

The effect of factors influencing biofilm formation lead to the conclusion that in both ATCC 27853 and clinical isolates maximum biofilm formation was at 48hr followed by its reduction by72hr. Physiological temperature (37ºC) and pH (7.4) supported maximum biofilm formation by all strains ATCC 27853 and the clinical isolates of *Pseudomonas* which was in agreement with earlier observations of Hostacká et al., 2010 and Kannan & Gautam, 2015). She et al. had observed an increase in biofilm formation on the addition of exogenous glucose which was in contrast to the present study and did not show any significant increase in biofilm formation in response to glucose concentration (She et al., 2019) (Fig 8-11).

Antibiotics are the first line of treatment for bacterial infections. Hence, the effect of antibiotics on biofilm formation was assessed. Third-generation cephalosporins, aminoglycosides, and fluoroquinolones are the three major classes of antibiotics used to treat *Pseudomonas* infection (Bassetti et al., 2018). Hoffman et al. were among the earliest reports on the effect of a sub-inhibitory concentration of antibiotics on biofilms formation (Hoffman et al., 2005). Numerous studies have reported that sub-inhibitory concentrations of antibiotics induce biofilm formation (Wright et al., 2013). Our data also suggests that sub-inhibitory concentrations of the antibiotics augmented biofilm formation by *Pseudomonas*. The sub-inhibitory

concentration of Ceftazidime, Gentamicin, and Norfloxacin increased biofilm formation (Fig 12-14).

eDNA is an integral part of the biofilms and plays a critical role in the attachment, aggregation and maintenance of the 3D architecture of biofilms (Lewenza, 2013). Sub – inhibitory concentration of ceftazidime failed to increase eDNA release in *Pseudomonas* biofilms. Table1 shows that the clinical isolates were resistant to ceftazidime and did not induce cell death. It was observed that aminoglycoside antibiotic gentamicin and Fluoroquinolone norfloxacin caused an increase in eDNA release in the biofilms of *Pseudomonas* (Fig 15-17). Mulcahy, Charron and Lewenza reported that eDNA chelates cations and acts as a shield against aminoglycosides and antimicrobial peptides (Mulcahy et al., 2008). The increase in eDNA release in response to aminoglycosides is a protective mechanism in *Pseudomonas*, as observed in Fig 6b, which showed an increase in biofilm formation at sub-inhibitory concentrations of gentamicin. The present study showed an increased eDNA release in response to sub-inhibitory concentrations of norfloxacin. It was observed by Wilton et al that eDNA acidifies *Pseudomonas* biofilms (Wilton et al., 2016). At the same time, norfloxacin which is zwitterionic at neutral pH acquires a positive charge at acidic pH, causing sequestration by eDNA in the biofilm (Cama et al., 2016; Purushothaman et al., 2016).

Alternatively, the increase in eDNA could also be due to cell death by autolysis, microbial fratricide, or membrane vesicle formation and transport of chromosomal DNA to the outside (Campoccia et al., 2021b). The released eDNA in the EPS protects the inner layers of biofilm from the action of antibiotics (Campoccia et al., 2021b; Uruén et al., 2021).

In the clinical scenario, bacteria are exposed to sub-inhibitory concentrations of antibiotics during the beginning and end stages of therapy (Chen et al., 2021). Bacteria within the biofilm are continuously exposed to sub-inhibitory concentrations of antibiotics (Singh et al., 2021). Our studies revealed that bacterial exposure to a low concentration of antibiotics induces biofilm formation and eDNA release which ensures stabilization of biofilms. This could be the mechanism by which *Pseudomonas* biofilms resist antibiotic action and persist within the host leading to chronic biofilm-related infections in medical devices.

Pyocyanin, rhamnolipids, and proteases are some of the essential virulence factors secreted by *Pseudomonas*. They play vital roles in biofilm formation and pathogenesis of *Pseudomonas* (Gellatly & Hancock, 2013). The expression of these virulence factors was higher in *Pseudomonas* clinical compared to the ATCC27853 isolate. The isolates differed in their ability to produce virulence factors. Amongst the clinical isolates, S373, S253, and S45 produced higher amounts of virulence factors (Fig 18).

C.elegans is a widely accepted model to study host-pathogen interaction (Marsh & May, 2012). Tan et al. have described the use of *C. elegans* killing assay as a method to assess the pathogenicity of *Pseudomonas* isolates (Tan et al., 1999). The current study used this model to determine the virulence of *Pseudomonas* clinical isolates. S373, S253, and S45 exhibited increased virulence (fig 18.D). These isolates also exhibited increased virulence factor expression. Tan et al. showed a significant correlation between the virulence factors expressed and virulence (Tan et al., 1999).

S373, S253, and S45 clinical isolates showed increased biofilm formation, virulence factor expression, and *C. elegans* killing. Hence, S373, S253, and S45 isolates were used to study the interaction of *Pseudomonas* biofilms with the alveolar epithelium and its effects on monocytes.

5.2. Phase II Establishment of a suitable *in-vitro* system to study the interaction of *Pseudomonas* biofilms with alveolar epithelium.

Phase II of the study focused at establishing a suitable *in-vitro* system to study the interaction of biofilms with the alveolar epithelium. The study used human lung adenocarcinoma cell line A549 to simulate the alveolar epithelial cells. A549 cells are reported to retain some properties of Type II alveolar epithelial cells and produce surfactants proteins A, B, C, and D and Phospholipids essential for the alveolar functions and host defenses.

Two different culture systems were tested.

1. A549 in submerged cultures
2. A549 at air-liquid interface cultures.

A549 monolayers in multi-well plates were used as submerged models. Infection of such monolayers resulted in excessive cell death by 4hr post-infection. Changes in A549 cell morphology appeared as early as 2hr post-infection. Significantly few viable cells were observed after 4hr PI. Therefore, it was not possible to study the effect of A549 cells with *Pseudomonas* biofilms (Fig 19).

In the air liquid interface culture system, A549 cells were grown on Costar™ Transwell membrane and lifted to an air-liquid interface system. Phosphate buffered saline was the suitable medium to introduce infection at a multiplicity of infection of 100:1 (Fig 20,21). *Pseudomonas* suspended in Phosphate buffered saline was used to infect A459 monolayer at a multiplicity of infection of 100:1 a method followed in line with the experiments of Woodworth et al. who had also used PBS to produce *Pseudomonas* infection model and observed that PBS reduced cell death and maintained the viability of nasal epithelial cells (Woodworth et al., 2008). Such an infection model at air-liquid interface in this study reduced the intensity of infection. In addition, ESEM analysis showed loss of A549 cell morphology and presence of small aggregates of *Pseudomonas* on the membrane (Fig 22). ALI systems supported improved expression of tight junctions and Moreau-Marquis et al. (2008) opined that they could be used for long-term studies on bacterial -cell monolayer interactions (Moreau-Marquis et al., 2009). But the system failed to develop mature 3D biofilms; therefore, it could not be used for understanding the interaction of biofilms with epithelium. An alternative model was established.

For this initially, *Pseudomonas* biofilms were developed on ETT by the method described by (Pericolini et al., 2018). In phase I studies, it was observed that all the isolates produced maximum biofilms at 48hr. Therefore, we evaluated the biofilm formation by ATCC 27853, S373, S253, and S45 isolates on ETT tube pieces 48hr post-exposure (Fig 23). Crystal violet staining and Acridine orange staining revealed the presence of exopolysaccharide matrix and rod-shaped *Pseudomonas* within the biofilms. This was in concordance with the observations of Pericolini et al. (Pericolini et al., 2018).

These developed *Pseudomonas* biofilms on ETTs were added to the apical side of a confluent A549 ALI culture. A549 cells exposed to these biofilms showed changes in morphology at 8hr post-infection (PI). Changes in morphology observed, indicated infection progress. A successful biofilm infection model was ascertained by live-dead staining which revealed many viable cells and few dead cells at 8hr PI (fig 24). Such a system could be used to simulate in vivo situation invitro and was considered representative of presence of *Pseudomonas* as seen in the alveoli of ventilated patients (El Solh et al., 2008). Costerton, Stewart, and Greenberg suggested that the colonization of ETT during the initial phases contributes to infection of airway epithelial cells and alveolar epithelium. The developed model attempts to replicate the *in-vivo* scenario (Costerton et al., 1999).

5.3. Phase III - Understanding the epithelial and monocytes responses to biofilms

Electrical cell surface impedance system (ECIS) as a method to understand pathogenicity dynamics, i.e., bacterial infection of epithelial cells in vitro in real-time was explored. The study of bacterial-cell interactions to delineate intricate mechanisms involved in pathogenicity is often hampered by the lack of suitable non-destructive methods, which are label-free and in real-time. Our data suggest that contrary to endpoint analysis ECIS provides a unique platform for understanding cellular interactions, cell–material, and microbial-cell interactions, which are discrete, nuanced, and multiparametric. ECIS helps understand early changes in the cell-cellular morphology, cytoskeletal changes, and intracellular junctional changes, which are usually forerunners of endpoint observations. We could observe marked differences in the impedance patterns using a different multiplicity of infections and different frequencies and record the changes over time. It can also be observed that, during the infection process, *Pseudomonas* disrupts the barrier integrity during the early phase of infection, as early as 2hr PI (Fig 25-27). Holldorsson et al., suggest that a reduction of barrier integrity, facilitates bacterial invasion of the epithelium, increasing its susceptibility to infection (Halldorsson et al., 2010).

Azithromycin pre-treatment helped preserve barrier integrity and changes due to infection with *Pseudomonas*, were delayed. The ability of Azithromycin to improve barrier properties of broncho-epithelial cells was described by Holldorsson et al. The

study revealed an up-regulation in the tight junctional proteins in the airway epithelium on treatment with Azithromycin (Halldorsson et al., 2010). In addition, we observed that pre-treatment of 40µg/ml azithromycin significantly delayed infection by the clinical isolate S373 and inhibited the progression of infection by ATCC 27853 (Fig 28-31). This could be due to the upregulation in the tight junctional protein expression by A549 cells or the prevention of degradation of these TJ proteins due to azithromycin treatment.

Our study suggests the feasibility of the use of ECIS to study the changes in barrier integrity due to any stimuli. ECIS specifically measures nanoscale morphological changes in challenged adherent cell monolayers and thus is a more sensitive tool than assessment of morphology by light microscopy or by fixing and staining infected cells or doing end-point analysis.

When taking a closer look at the normalised ECIS data, we observed early spikes in impedance measurement following infection with *Pseudomonas*. These could be due to the physical manipulation of the cells monolayer cultures required to add the bacteria or control medium, which results in transient temperature and pH changes. Indeed, a small spike is typically observed following any manipulation of wells in an ECIS experiment. But the major limitations of the ECIS technique is that it is applicable only on adherent monolayers and does not provide direct information of molecular-level changes, an endpoint assay.

On taking a closer look at the normalized ECIS data, we observed early spikes in impedance measurement following infection with *Pseudomonas*. These could be due to the physical manipulation of the cell's monolayer cultures required to add the bacteria or control medium, which results in transient temperature and pH changes. Indeed, a small spike is typically observed following any manipulation of wells in an ECIS experiment. But the major limitation of the ECIS technique is that it is applicable only to adherent monolayers and does not provide direct information on molecular-level changes, an endpoint assay.

Our data delineated the epithelial responses to biofilms of *Pseudomonas*. Reactive oxygen species generation is one of the major mechanisms of pathogen

elimination by the epithelia and the cells of the immune system. A reduction in ROS response was noted in A549cells exposed to *Pseudomonas* biofilms, both ATCC 27853 and clinical isolates (Fig 32 A-D). This reduction could be due to the ROS scavenging properties of the exopolysaccharide matrix of the biofilm (Rybtke et al., 2020). Alginate, a major component of the biofilm exopolysaccharide matrix, was capable of scavenging superoxide molecules and other free radicals released by neutrophils and activated macrophages *in-vitro* (Limoli et al., 2015; Rybtke et al., 2020). *Pseudomonas* is also known to express superoxide dismutase (Hassett et al., 1995; Martins et al., 2018). The superoxide dismutase and exopolysaccharide matrix together contributed to the reduction in ROS responses in A549 cells.

Planktonic cells induced necrotic cell death in A549 cells. WhereasA549 cells exposed to biofilms showed features of both apoptosis and necrosis. Cellular blebbing and nuclear fragmentation were the key apoptotic features observed in A549 cells exposed to biofilms. Few cells also showed necrotic changes like loss of membrane integrity and cellular swelling (Fig 34,35). Biofilms induced an up-regulation of TNFα alone and IL8, IL6, and IL1β. The nuclear changes revealed the presence of fragmented nuclei within an intact nuclear membrane, which was atypical of both apoptosis and necrosis and is indicative of a pyroptotic mechanism of cell death.

Biochemical features: Inflammasome-mediated activation of caspase 1 leading to the upregulation of IL1β is the key identification feature of pyroptotic cells death. Upon evaluation, both Casp 1 and IL1β were upregulated in A549 cells infected with a biofilm of both ATCC27853 and Clinical isolates. Caspase 3, the executioner caspase in apoptosis, and Pi3K, an inflammasome inhibitor, were expressed only at a basal level (Fig 41,42).

Hence our study provided insights into the mechanism of cells death in biofilms infected cells - Pyroptosis. Pyroptosis also plays a prominent role in chronic inflammatory diseases (Bergsbaken et al., 2009; T. Li et al., 2021). Hence, we believe that this could be the underlying reason behind chronic inflammation observed in biofilm infections.

The epithelium is an organism's first line of defense against an insult or injury. Studying the epithelial responses helps understand the immediate or primary innate immune response to invading pathogens. Neutrophil responses involving the immune system are the second line of defence against pathogens like *Pseudomonas* and were reviewed by Pestrak et al. The study reported respiratory burst, penetration, phagocytosis, production of cytokines of biofilm bacteria (Pestrak et al., 2018). This review details the innate immune mechanism that is activated in biofilm infection but due to inherent defects cannot bring around the elimination of biofilms. The failing bactericidal and phagocytic activity is also due the virulence factor rhamnolipids which in turn protects the biofilm from the action of neutrophils – an activity absent in planktonic forms (Pestrak et al., 2018).

Monocyte interaction with *Pseudomonas* biofilms was studied by exposing 48hr biofilms to monocyte cultures. The biochemical, morphological, and molecular changes in the infected cells were analyzed.

Free radical generation is a host response to environmental stress, including bacterial invasion (Fang et al., 2016). Planktonic cells of *Pseudomonas* increased ROS responses in THP1 cells. On the other hand, a reduction was observed in ROS generation in THP1 cells upon exposure to biofilms forms of *Pseudomonas* but was higher than the positive control (10mM H_2O_2) (Fig 32 E-H). The ROS scavenging properties of the alginate in the exopolysaccharide matrix and superoxide dismutase expressed by *Pseudomonas* significantly reduced ROS generation in THP1 cells (Hassett et al., 1995; Rybtke et al., 2020). Biofilm bacteria were less internalized than planktonic bacteria by THP1 cells (Fig 33). Phagocytosis is one of the major antibacterial mechanisms. Lied describes phagocytosis to be ineffective against biofilms (J. Leid, 2009) . THP1 cells used in the study showed reduced internalization of *Pseudomonas* biofilms bacteria. Over a period, no significant increase in internalized bacteria was observed. Pradeep Singh et al. revealed that alginate, an integral part of the exopolysaccharide matrix, protects the bacteria from internalization and phagocytosis by neutrophils and macrophages. The absence of alginate in the EPS matrix was found to make the bacteria susceptible to internalization, phagocytosis, and enhances killing by antibiotics (Alkawash et al., 2006; J. G. Leid et al., 2005). The

mechanism of cell death induced by planktonic *Pseudomonas* was observed to be necrosis. It was observed by Okuda et al., that virulence factors secreted by *Pseudomonas* disrupt cell membrane integrity and induced necrotic cell death. The study revealed that ExoS binding with Kinesin-like protein 7 (KIF7) induces significant cell death by necrosis in human bronchial epithelial cells (Okuda et al., 2014). On the other hand, biofilm exposed THP1 cells showed signs of both apoptosis (cellular blebbing and DNA fragmentation) and necrosis (loss of membrane integrity and cell swelling). Some atypical features of apoptosis also were observed. The nuclear fragmentation showed no changes in the nuclear membrane.

Upregulation was observed only in TNFα gene expression. IL6, IL8, and iNOS gene expression were found to be reduced (Fig 38-40). Thurlow et al., demonstrated a reduction in pro-inflammatory gene expression in macrophages exposed to *S.aureus* biofilms *in-vitro* (Thurlow et al., 2011). In the current study, monocytes exposed to *Pseudomonas* biofilms showed a reduction in IL6 and IL8 gene expression. Wight and Potter-Perigo observed that ECM molecules could significantly reduce pro-inflammatory responses (Wight & Potter-Perigo, 2011). A reduction in iNOS expression also was observed in THP1 cells exposed to biofilms of *Pseudomonas* in the present study, which was in concordance with the observations of Thurlow et al. (Thurlow et al., 2011).

Evaluation of Inflammasome markers revealed the upregulation of caspase 1 and IL1β. Executioner caspase3 was found to be expressed only at basal levels indicating that biofilms did not induce cell death via apoptosis (Fig 41,42). Wang, Eagen, and Lee observed that extracellular vesicles of *Staphylococcus aureus* induce upregulation of caspase 1 and IL1β in monocytes resulting in inflammasome mediated pyroptotic cell death (Wang et al., 2020).

Caspase 1 activation results in the production of inflammatory cytokines and are characterized by rapid cell death induced by plasma membrane rupture and acceleration of inflammation. Pores formed in the plasma membrane disturb the osmotic balance of the cells and result in cellular swelling. In the present study, we observed an increase in the size of cells and a loss of membrane integrity (marked by

the accumulation of propidium iodide in the cytoplasm of the cells). Fragmentation of DNA is indicative of apoptotic cells death. DNA fragmentation in pyroptosis is marked by the presence of an intact nuclear membrane. Similar observations were made in A549 and THP1 cells exposed to the biofilm of *Pseudomonas.* These data strongly suggest the involvement of the pyroptotic mechanism of cell death in biofilm-infected cells.

Our data suggest that biofilms reduce IL8 expression in epithelium and monocytes resulting in a reduction in the recruitment of neutrophils and other innate immune cells. An increase in caspase 1 and IL1β is indicative of the pyroptotic mechanism of cell death. In conclusion, our study is the first to report that biofilms of *Pseudomonas* induce pyroptotic cell death in Alveolar epithelial cells and monocytes. Further studies could provide insights into the mechanism of biofilm inducing pyroptotic cell death.

5.4. Limitations of the study

- *In-vivo* studies are necessary to validate the effect of biofilm-induced pyroptotic cell death in the development of chronic infections and the persistence of biofilms within the host.
- Therapeutic strategies to prevent biofilm infections, disruption of biofilms and possible mechanisms for reversal of deleterious effects of such infections need to be focused on for societal benefit of this work.

6. SUMMARY AND CONCLUSIONS

This work focuses on the trigonal interaction between bacteria, material, and host. *Pseudomonas*, when exposed to material surfaces like the endotracheal tube, form biofilms on them. These biofilms interact with the epithelial layer of the organ in contact and lead to a cascade of interaction. The cascade is initiated by the epithelium, which recruits the immune cells to the site. The study details these interactions using in-vitro systems. Thus, the significant outcomes of the study are:

- At physiological conditions of temperature (37ºC), pH 7.4, and iron concentrations, *Pseudomonas* produced maximum biofilm formation at 48hr. Temperature below 37ºC (physiological temperature) also promoted biofilm formation to a limited extent, while higher temperatures were unfavorable.
- Iron concentration beyond the optimal concentration did not promote biofilm formation.
- Our studies suggested that exposure of *Pseudomonas* to a low concentration of antibiotics induced biofilm formation and eDNA release. These were suggestive of the mechanism adopted by *Pseudomonas* biofilms to antibiotic challenge and persist within the host.
- The *C.elegans* killing assay helped in understanding the degree of virulence among various isolates of *Pseudomonas* and led to the selection of highly virulent isolates.
- Electrical cell-substrate impedance sensing has proven to be a non–invasive, nondestructive method for understanding the early changes of pathogenesis in real-time.
- Our ECIS data suggests that during the infection process, *Pseudomonas* disrupts the epithelial integrity during the early stages of infection.
- The barrier protection property of Azithromycin was demonstrated using ECIS. 40µg/ml concentration helped in preserving the tight junctional integrity of the A549 monolayer when evaluated by ECIS at 500Hz.
- The ECIS technique also helped in establishing that AZM at 40µg/ml concentration (below MIC) was capable of delaying the process of infection when analyzed at 1000Hz and 64000Hz.

- In the understanding of immune modulation, it was established that the epithelia represented by A549 monolayers used in the study initiated the immune response.
- An increase was observed in TNFα alone in A549 cells infected with biofilms of *Pseudomonas*, while *Pseudomonas* in the planktonic state was capable of upregulating TNFα, IL8, IL6, and iNOS. IL8 and IL6 are chemoattractants and facilitate the recruitment of neutrophils and monocytes to the site of infection, while iNOS builds oxidative stress in bacteria leading to death and these mechanisms were operational only in the case of planktonic forms.
- The study clearly shows that biofilms cause immune modulations in the host preventing the innate immune mechanism from being operated and facilitating the persistence of infection.

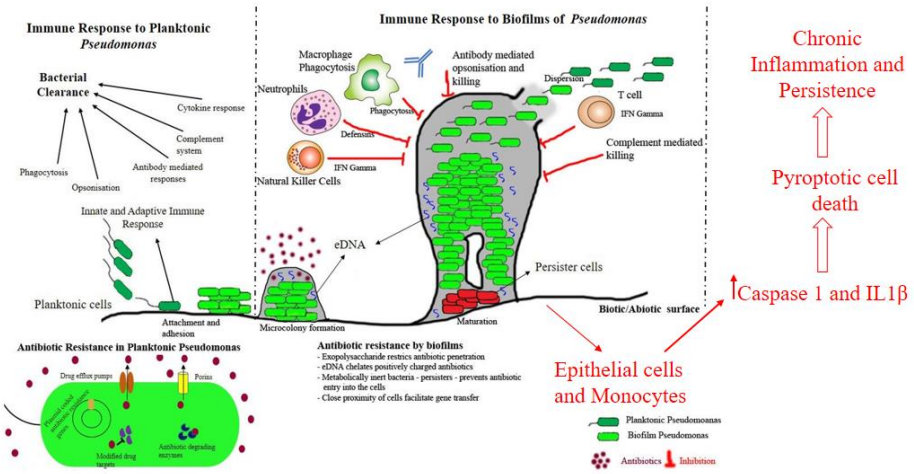

Fig 43: Mechanism of *Pseudomonas* biofilm persistence in the host. Planktonic *Pseudomonas are* cleared by the immature immune system. But biofilm persists despite the activation of both innate and adaptive immune responses. Our data suggest that biofilms induce inflammasome-mediated pyroptotic cell death in epithelial cells and monocytes by upregulating caspase 1 and IL1β resulting in chronic inflammation and persistence of biofilms.

- The study also explains the **mechanism of cell death** induced by biofilm to be of the **pyroptotic type**, denoted by an increase in caspase 1 and IL1β and down-regulation of caspase 3. This mechanism is not observed in the acute phase of the infection, which is caused by planktonic bacteria, again pointing to the development of persistence leading to chronic infections (fig 43).

7. References

1. Abd El-Baky, R. M., Masoud, S. M., Mohamed, D. S., Waly, N. G., Shafik, E. A., Mohareb, D. A., Elkady, A., Elbadr, M. M., & Hetta, H. F. (2020). Prevalence and Some Possible Mechanisms of Colistin Resistance Among Multidrug-Resistant and Extensively Drug-Resistant *Pseudomonas aeroginosa*. *Infection and Drug Resistance*, *13*, 323–332. https://doi.org/10.2147/IDR.S238811
2. Abisado, R. G., Benomar, S., Klaus, J. R., Dandekar, A. A., & Chandler, J. R. (n.d.). Bacterial Quorum Sensing and Microbial Community Interactions. *MBio*, *9*(3), e02331-17. https://doi.org/10.1128/mBio.02331-17
3. Acosta, N., Waddell, B., Heirali, A., Somayaji, R., Surette, M. G., Workentine, M. L., Rabin, H. R., & Parkins, M. D. (2020). Cystic Fibrosis Patients Infected With Epidemic *Pseudomonas aeroginosa* Strains Have Unique Microbial Communities. *Frontiers in Cellular and Infection Microbiology*, *10*. https://www.frontiersin.org/article/10.3389/fcimb.2020.00173
4. Alav, I., Sutton, J. M., & Rahman, K. M. (2018). Role of bacterial efflux pumps in biofilm formation. *Journal of Antimicrobial Chemotherapy*, *73*(8), 2003–2020. https://doi.org/10.1093/jac/dky042
5. Alkawash, M. A., Soothill, J. S., & Schiller, N. L. (2006). Alginate lyase enhances antibiotic killing of mucoid *Pseudomonas aeroginosa* in biofilms. *APMIS: Acta Pathologica, Microbiologica, et Immunologica Scandinavica*, *114*(2), 131–138. https://doi.org/10.1111/j.1600-0463.2006.apm_356.x
6. Amador, C. I., Stannius, R. O., Røder, H. L., & Burmølle, M. (2021). High-throughput screening alternative to crystal violet biofilm assay combining fluorescence quantification and imaging. *Journal of Microbiological Methods*, *190*, 106343. https://doi.org/10.1016/j.mimet.2021.106343
7. Amaral, L., Martins, A., Spengler, G., & Molnar, J. (2014). Efflux pumps of Gram-negative bacteria: What they do, how they do it, with what and how to deal with

them. *Frontiers in Pharmacology*, *4*. https://www.frontiersin.org/article/10.3389/fphar.2013.00168

8. Banin, E., Vasil, M. L., & Greenberg, E. P. (2005). Iron and *Pseudomonas aeroginosa* biofilm formation. *Proceedings of the National Academy of Sciences, 102*(31), 11076–11081. https://doi.org/10.1073/pnas.0504266102
9. Barrett, T. C., Mok, W. W. K., Murawski, A. M., & Brynildsen, M. P. (2019). Enhanced antibiotic resistance development from fluoroquinolone persisters after a single exposure to antibiotic. *Nature Communications*, *10*(1), 1177. https://doi.org/10.1038/s41467-019-09058-4
10. Barron, S. L., Saez, J., & Owens, R. M. (2021). In Vitro Models for Studying Respiratory Host–Pathogen Interactions. *Advanced Biology*, *5*(6), 2000624. https://doi.org/10.1002/adbi.202000624
11. Bassetti, M., Vena, A., Croxatto, A., Righi, E., & Guery, B. (2018). How to manage *Pseudomonas aeroginosa* infections. *Drugs in Context*, *7*, 212527. https://doi.org/10.7573/dic.212527
12. Bergsbaken, T., Fink, S. L., & Cookson, B. T. (2009). Pyroptosis: Host cell death and inflammation. *Nature Reviews. Microbiology*, *7*(2), 99–109. https://doi.org/10.1038/nrmicro2070
13. Bermudez-Brito, M., Plaza-Díaz, J., Fontana, L., Muñoz-Quezada, S., & Gil, A. (2013). In vitro cell and tissue models for studying host-microbe interactions: A review. *The British Journal of Nutrition, 109 Suppl 2,* S27-34. https://doi.org/10.1017/S0007114512004023
14. Bjarnsholt, T., Alhede, M., Alhede, M., Eickhardt-Sørensen, S. R., Moser, C., Kühl, M., Jensen, P. Ø., & Høiby, N. (2013). The in vivo biofilm. *Trends in Microbiology*, *21*(9), 466–474. https://doi.org/10.1016/j.tim.2013.06.002

15. Bjarnsholt, T., Jensen, P. Ø., Jakobsen, T. H., Phipps, R., Nielsen, A. K., Rybtke, M. T., Tolker-Nielsen, T., Givskov, M., Høiby, N., & Ciofu, O. (2010). Quorum Sensing and Virulence of *Pseudomonas aeroginosa* during Lung Infection of Cystic Fibrosis Patients. *PLoS ONE*, *5*(4), e10115. https://doi.org/10.1371/journal.pone.0010115

16. Blanco, P., Hernando-Amado, S., Reales-Calderon, J. A., Corona, F., Lira, F., Alcalde-Rico, M., Bernardini, A., Sanchez, M. B., & Martinez, J. L. (2016). Bacterial Multidrug Efflux Pumps: Much More Than Antibiotic Resistance Determinants. *Microorganisms*, *4*(1), E14. https://doi.org/10.3390/microorganisms4010014

17. Cai, Y., Wang, R., An, M.-M., & Liang, B.-B. (2010). Iron-Depletion prevents biofilm formation in *Pseudomonas aeroginosa* through twitching mobility and quorum sensing. *Brazilian Journal of Microbiology*, *41*(1), 37–41. https://doi.org/10.1590/S1517-83822010000100008

18. Cama, J., Schaich, M., Al Nahas, K., Hernández-Ainsa, S., Pagliara, S., & Keyser, U. F. (2016). Direct Optofluidic Measurement of the Lipid Permeability of Fluoroquinolones. *Scientific Reports*, *6*(1), 32824. https://doi.org/10.1038/srep32824

19. Campoccia, D., Mirzaei, R., Montanaro, L., & Arciola, C. R. (2019). Hijacking of immune defences by biofilms: A multifront strategy. *Biofouling*, *35*(10), 1055–1074. https://doi.org/10.1080/08927014.2019.1689964

20. Campoccia, D., Montanaro, L., & Arciola, C. R. (2021a). Extracellular DNA (eDNA). A Major Ubiquitous Element of the Bacterial Biofilm Architecture. *International Journal of Molecular Sciences*, *22*(16), 9100. https://doi.org/10.3390/ijms22169100

21. Campoccia, D., Montanaro, L., & Arciola, C. R. (2021b). Tracing the origins of extracellular DNA in bacterial biofilms: Story of death and predation to community benefit. *Biofouling*, *37*(9–10), 1022–1039. https://doi.org/10.1080/08927014.2021.2002987

22. Caruso, R., Warner, N., Inohara, N., & Núñez, G. (2014). NOD1 and NOD2: Signaling, Host Defense, and Inflammatory Disease. *Immunity*, *41*(6), 898–908. https://doi.org/10.1016/j.immuni.2014.12.010

23. Chaplin, D. D. (2010). Overview of the Immune Response. *The Journal of Allergy and Clinical Immunology*, *125*(2 Suppl 2), S3-23. https://doi.org/10.1016/j.jaci.2009.12.980

24. Chavan, R., De, A., & Baveja, S. (2017). Study on the Role of Efflux Pump in Drug Resistance of *Pseudomonas aeroginosa*. *International Journal of Current Microbiology and Applied Sciences*, *6*(12), 1944–1955. https://doi.org/10.20546/ijcmas.2017.612.222

25. Chen, J., Zhou, H., Huang, J., Zhang, R., & Rao, X. (2021). Virulence alterations in staphylococcus aureus upon treatment with the sub-inhibitory concentrations of antibiotics. *Journal of Advanced Research*, *31*, 165–175. https://doi.org/10.1016/j.jare.2021.01.008

26. Choi, K.-Y. G., Wu, B. C., Lee, A. H.-Y., Baquir, B., & Hancock, R. E. W. (2020). Utilizing Organoid and Air-Liquid Interface Models as a Screening Method in the Development of New Host Defense Peptides. *Frontiers in Cellular and Infection Microbiology*, *10*. https://www.frontiersin.org/article/10.3389/fcimb.2020.00228

27. Chong, H., & Li, Q. (2017). Microbial production of rhamnolipids: Opportunities, challenges and strategies. *Microbial Cell Factories*, *16*(1), 137. https://doi.org/10.1186/s12934-017-0753-2

28. Ciofu, O., & Tolker-Nielsen, T. (2019). Tolerance and Resistance of *Pseudomonas aeroginosa* Biofilms to Antimicrobial Agents—How P. aeruginosa Can Escape Antibiotics. *Frontiers in Microbiology*, *10*, 913. https://doi.org/10.3389/fmicb.2019.00913

29. Cornelis, P., & Dingemans, J. (2013). *Pseudomonas aeroginosa* adapts its iron uptake strategies in function of the type of infections. *Frontiers in Cellular and Infection Microbiology*, *3*, 75. https://doi.org/10.3389/fcimb.2013.00075

30. Costerton, J. W., Stewart, P. S., & Greenberg, E. P. (1999). Bacterial biofilms: A common cause of persistent infections. *Science (New York, N.Y.)*, *284*(5418), 1318–1322. https://doi.org/10.1126/science.284.5418.1318

31. Crabbé, A., Ledesma, M. A., & Nickerson, C. A. (2014). Mimicking the host and its microenvironment in vitro for studying mucosal infections by *Pseudomonas aeroginosa*. *Pathogens and Disease*, *71*(1), 1–19. https://doi.org/10.1111/2049-632X.12180

32. Crandon, J. L., Schuck, V. J., Banevicius, M. A., Beaudoin, M.-E., Nichols, W. W., Tanudra, M. A., & Nicolau, D. P. (2012). Comparative In Vitro and In Vivo Efficacies of Human Simulated Doses of Ceftazidime and Ceftazidime-Avibactam against *Pseudomonas aeroginosa*. *Antimicrobial Agents and Chemotherapy*, *56*(12), 6137–6146. https://doi.org/10.1128/AAC.00851-12

33. Das, T., Ibugo, A. I., Klare, W., & Manefield, M. (2016). Role of Pyocyanin and Extracellular DNA in Facilitating *Pseudomonas aeroginosa* Biofilm Formation. In *Microbial Biofilms—Importance and Applications*. IntechOpen. https://doi.org/10.5772/63497

34. Das, T., & Manefield, M. (2012). Pyocyanin promotes extracellular DNA release in *Pseudomonas aeroginosa*. *PloS One*, *7*(10), e46718. https://doi.org/10.1371/journal.pone.0046718

35. Das, T., Sharma, P. K., Busscher, H. J., van der Mei, H. C., & Krom, B. P. (2010). Role of Extracellular DNA in Initial Bacterial Adhesion and Surface Aggregation. *Applied and Environmental Microbiology*, *76*(10), 3405–3408. https://doi.org/10.1128/AEM.03119-09

36. Devaraj, A., Buzzo, J. R., Mashburn-Warren, L., Gloag, E. S., Novotny, L. A., Stoodley, P., Bakaletz, L. O., & Goodman, S. D. (2019). The extracellular DNA lattice of bacterial biofilms is structurally related to Holliday junction recombination intermediates. *Proceedings of the National Academy of Sciences*, *116*(50), 25068–25077. https://doi.org/10.1073/pnas.1909017116

37. Diabaté, S., Armand, L., Murugadoss, S., Dilger, M., Fritsch-Decker, S., Schlager, C., Béal, D., Arnal, M.-E., Biola-Clier, M., Ambrose, S., Mülhopt, S., Paur, H.-R., Lynch, I., Valsami-Jones, E., Carriere, M., & Weiss, C. (2021). Air–Liquid Interface Exposure of Lung Epithelial Cells to Low Doses of Nanoparticles to Assess Pulmonary Adverse Effects. *Nanomaterials*, *11*(1), 65. https://doi.org/10.3390/nano11010065

38. Donlan, R. M., & Costerton, J. W. (2002). Biofilms: Survival Mechanisms of Clinically Relevant Microorganisms. *Clinical Microbiology Reviews*, *15*(2), 167–193. https://doi.org/10.1128/CMR.15.2.167-193.2002

39. Dössel, J., Meyer-Hoffert, U., Schröder, J.-M., & Gerstel, U. (2012). *Pseudomonas aeroginosa*-derived rhamnolipids subvert the host innate immune response through manipulation of the human beta-defensin-2 expression. *Cellular Microbiology*, *14*(9), 1364–1375. https://doi.org/10.1111/j.1462-5822.2012.01801.x

40. Drenkard, E., & Ausubel, F. M. (2002). *Pseudomonas* biofilm formation and antibiotic resistance are linked to phenotypic variation. *Nature*, *416*(6882), 740–743. https://doi.org/10.1038/416740a

41. El Solh, A. A., Akinnusi, M. E., Wiener-Kronish, J. P., Lynch, S. V., Pineda, L. A., & Szarpa, K. (2008). Persistent infection with *Pseudomonas aeroginosa* in ventilator-associated pneumonia. *American Journal of Respiratory and Critical Care Medicine*, *178*(5), 513–519. https://doi.org/10.1164/rccm.200802-239OC

42. El-Mowafy, S. A., Abd El Galil, K. H., El-Messery, S. M., & Shaaban, M. I. (2014). Aspirin is an efficient inhibitor of quorum sensing, virulence and toxins in *Pseudomonas aeroginosa*. *Microbial Pathogenesis*, *74*, 25–32. https://doi.org/10.1016/j.micpath.2014.07.008

43. Essar, D. W., Eberly, L., Hadero, A., & Crawford, I. P. (1990). Identification and characterization of genes for a second anthranilate synthase in *Pseudomonas aeroginosa*: Interchangeability of the two anthranilate synthases and evolutionary implications. *Journal of Bacteriology*, *172*(2), 884–900. https://doi.org/10.1128/jb.172.2.884-900.1990

44. Fang, F. C., Frawley, E. R., Tapscott, T., & Vázquez-Torres, A. (2016). Bacterial Stress Responses during Host Infection. *Cell Host & Microbe*, *20*(2), 133–143. https://doi.org/10.1016/j.chom.2016.07.009

45. Fisher, R. A., Gollan, B., & Helaine, S. (2017). Persistent bacterial infections and persister cells. *Nature Reviews. Microbiology*, *15*(8), 453–464. https://doi.org/10.1038/nrmicro.2017.42

46. Fung, D. K. C., Chan, E. W. C., Chin, M. L., & Chan, R. C. Y. (2010). Delineation of a bacterial starvation stress response network which can mediate antibiotic tolerance development. *Antimicrobial Agents and Chemotherapy*, *54*(3), 1082–1093. https://doi.org/10.1128/AAC.01218-09

47. García-Contreras, R. (2016). Is Quorum Sensing Interference a Viable Alternative to Treat *Pseudomonas aeroginosa* Infections? *Frontiers in Microbiology*, *7*. https://www.frontiersin.org/article/10.3389/fmicb.2016.01454

48. Gellatly, S. L., & Hancock, R. E. W. (2013). *Pseudomonas aeroginosa*: New insights into pathogenesis and host defenses. *Pathogens and Disease*, *67*(3), 159–173. https://doi.org/10.1111/2049-632X.12033

49. Gestel, J. van, Vlamakis, H., & Kolter, R. (2015). Division of Labor in Biofilms: The Ecology of Cell Differentiation. *Microbiology Spectrum*. https://doi.org/10.1128/microbiolspec.MB-0002-2014

50. Giaever, I., & Keese, C. R. (1991). Micromotion of mammalian cells measured electrically. *Proceedings of the National Academy of Sciences*, *88*(17), 7896–7900. https://doi.org/10.1073/pnas.88.17.7896

51. González, J. F., Hahn, M. M., & Gunn, J. S. (2018). Chronic biofilm-based infections: Skewing of the immune response. *Pathogens and Disease*, *76*(3). https://doi.org/10.1093/femspd/fty023

52. Guilhen, C., Forestier, C., & Balestrino, D. (2017). Biofilm dispersal: Multiple elaborate strategies for dissemination of bacteria with unique properties. *Molecular Microbiology*, *105*(2), 188–210. https://doi.org/10.1111/mmi.13698

53. Günther, J., & Seyfert, H.-M. (2018). The first line of defence: Insights into mechanisms and relevance of phagocytosis in epithelial cells. *Seminars in Immunopathology*, *40*(6), 555–565. https://doi.org/10.1007/s00281-018-0701-1

54. Ha, D.-G., & O'Toole, G. A. (2015). c-di-GMP and its Effects on Biofilm Formation and Dispersion: A *Pseudomonas aeroginosa* Review. *Microbiology Spectrum*, *3*(2), MB-0003-2014. https://doi.org/10.1128/microbiolspec.MB-0003-2014

55. Hajdamowicz, N. H., Hull, R. C., Foster, S. J., & Condliffe, A. M. (2019). The Impact of Hypoxia on the Host-Pathogen Interaction between Neutrophils and Staphylococcus aureus. *International Journal of Molecular Sciences*, *20*(22), 5561. https://doi.org/10.3390/ijms20225561

56. Hall, C. W., & Mah, T.-F. (2017). Molecular mechanisms of biofilm-based antibiotic resistance and tolerance in pathogenic bacteria. *FEMS Microbiology Reviews*, *41*(3), 276–301. https://doi.org/10.1093/femsre/fux010

57. Hall, S., McDermott, C., Anoopkumar-Dukie, S., McFarland, A. J., Forbes, A., Perkins, A. V., Davey, A. K., Chess-Williams, R., Kiefel, M. J., Arora, D., & Grant, G. D. (2016). Cellular Effects of Pyocyanin, a Secreted Virulence Factor of *Pseudomonas aeroginosa*. *Toxins*, *8*(8). https://doi.org/10.3390/toxins8080236

58. Halldorsson, S., Gudjonsson, T., Gottfredsson, M., Singh, P. K., Gudmundsson, G. H., & Baldursson, O. (2010). Azithromycin Maintains Airway Epithelial Integrity during *Pseudomonas aeroginosa* Infection. *American Journal of Respiratory Cell and Molecular Biology*, *42*(1), 62–68. https://doi.org/10.1165/rcmb.2008-0357OC

59. Hamzah, N., Kasmuri, N., Tao, W., Singhal, N., Padhye, L., & Swift, S. (2020). Effect of rhamnolipid on the physicochemical properties and interaction of bacteria and fungi. *Brazilian Journal of Microbiology*, *51*(3), 1317–1326. https://doi.org/10.1007/s42770-020-00295-0

60. Hänsch, G. M. (2012). Host Defence against Bacterial Biofilms: "Mission Impossible"? *ISRN Immunology*, *2012*, 853123. https://doi.org/10.5402/2012/853123

61. Harrison, J. J., Ceri, H., Yerly, J., Stremick, C. A., Hu, Y., Martinuzzi, R., & Turner, R. J. (2006). The use of microscopy and three-dimensional visualization to evaluate the structure of microbial biofilms cultivated in the Calgary Biofilm Device. *Biological Procedures Online*, *8*, 194–215. https://doi.org/10.1251/bpo127

62. Hassett, D. J., Schweizer, H. P., & Ohman, D. E. (1995). *Pseudomonas aeroginosa* sodA and sodB mutants defective in manganese- and iron-cofactored superoxide dismutase activity demonstrate the importance of the iron-cofactored form in

aerobic metabolism. *Journal of Bacteriology*, *177*(22), 6330–6337. https://doi.org/10.1128/jb.177.22.6330-6337.1995

63. Henrichfreise, B., Wiegand, I., Pfister, W., & Wiedemann, B. (2007). Resistance Mechanisms of Multiresistant *Pseudomonas aeroginosa* Strains from Germany and Correlation with Hypermutation. *Antimicrobial Agents and Chemotherapy*, *51*(11), 4062–4070. https://doi.org/10.1128/AAC.00148-07
64. Hoffman, L. R., D'Argenio, D. A., MacCoss, M. J., Zhang, Z., Jones, R. A., & Miller, S. I. (2005). Aminoglycoside antibiotics induce bacterial biofilm formation. *Nature*, *436*(7054), 1171–1175. https://doi.org/10.1038/nature03912
65. Hooper, D. C., & Jacoby, G. A. (2016). Topoisomerase Inhibitors: Fluoroquinolone Mechanisms of Action and Resistance. *Cold Spring Harbor Perspectives in Medicine*, *6*(9), a025320. https://doi.org/10.1101/cshperspect.a025320
66. Horcajada, J. P., Montero, M., Oliver, A., Sorlí, L., Luque, S., Gómez-Zorrilla, S., Benito, N., & Grau, S. (n.d.). Epidemiology and Treatment of Multidrug-Resistant and Extensively Drug-Resistant *Pseudomonas aeroginosa* Infections. *Clinical Microbiology Reviews*, *32*(4), e00031-19. https://doi.org/10.1128/CMR.00031-19
67. Hostacká, A., Ciznár, I., & Stefkovicová, M. (2010). Temperature and pH affect the production of bacterial biofilm. *Folia Microbiologica*, *55*(1), 75–78. https://doi.org/10.1007/s12223-010-0012-y
68. Hughes, G., & Webber, M. A. (2017). Novel approaches to the treatment of bacterial biofilm infections. *British Journal of Pharmacology*, *174*(14), 2237–2246. https://doi.org/10.1111/bph.13706
69. Huynh, T. T., McDougald, D., Klebensberger, J., Al Qarni, B., Barraud, N., Rice, S. A., Kjelleberg, S., & Schleheck, D. (2012). Glucose Starvation-Induced

Dispersal of *Pseudomonas aeroginosa* Biofilms Is cAMP and Energy Dependent. *PLoS ONE*, *7*(8), e42874. https://doi.org/10.1371/journal.pone.0042874

70. Ibáñez de Aldecoa, A. L., Zafra, O., & González-Pastor, J. E. (2017). Mechanisms and Regulation of Extracellular DNA Release and Its Biological Roles in Microbial Communities. *Frontiers in Microbiology*, *8*. https://doi.org/10.3389/fmicb.2017.01390
71. Jamal, M., Ahmad, W., Andleeb, S., Jalil, F., Imran, M., Nawaz, M. A., Hussain, T., Ali, M., Rafiq, M., & Kamil, M. A. (2018). Bacterial biofilm and associated infections. *Journal of the Chinese Medical Association: JCMA*, *81*(1), 7–11. https://doi.org/10.1016/j.jcma.2017.07.012
72. Jensen, E. T., Kharazmi, A., Lam, K., Costerton, J. W., & Høiby, N. (1990). Human polymorphonuclear leukocyte response to *Pseudomonas aeroginosa* grown in biofilms. *Infection and Immunity*, *58*(7), 2383–2385. https://doi.org/10.1128/iai.58.7.2383-2385.1990
73. Jensen, P. Ø., Givskov, M., Bjarnsholt, T., & Moser, C. (2010). The immune system vs. *Pseudomonas aeroginosa* biofilms. *FEMS Immunology and Medical Microbiology*, *59*(3), 292–305. https://doi.org/10.1111/j.1574-695X.2010.00706.x
74. Jones, E. M., Cochrane, C. A., & Percival, S. L. (2015). The Effect of pH on the Extracellular Matrix and Biofilms. *Advances in Wound Care*, *4*(7), 431–439. https://doi.org/10.1089/wound.2014.0538
75. Jurado-Martín, I., Sainz-Mejías, M., & McClean, S. (2021). *Pseudomonas aeroginosa*: An Audacious Pathogen with an Adaptable Arsenal of Virulence Factors. *International Journal of Molecular Sciences*, *22*(6), 3128. https://doi.org/10.3390/ijms22063128

76. Kang, D., & Kirienko, N. V. (2018). Interdependence between iron acquisition and biofilm formation in *Pseudomonas aeroginosa*. *Journal of Microbiology (Seoul, Korea)*, *56*(7), 449–457. https://doi.org/10.1007/s12275-018-8114-3

77. Kannan, A., & Gautam, P. (2015). A quantitative study on the formation of *Pseudomonas aeroginosa* biofilm. *SpringerPlus*, *4*(1), 379. https://doi.org/10.1186/s40064-015-1029-0

78. Kaplan, J. B. (2010). Biofilm Dispersal. *Journal of Dental Research*, *89*(3), 205–218. https://doi.org/10.1177/0022034509359403

79. Kaplan, J. B., Izano, E. A., Gopal, P., Karwacki, M. T., Kim, S., Bose, J. L., Bayles, K. W., & Horswill, A. R. (2012). Low Levels of β-Lactam Antibiotics Induce Extracellular DNA Release and Biofilm Formation in Staphylococcus aureus. *MBio*, *3*(4), e00198-12. https://doi.org/10.1128/mBio.00198-12

80. Karygianni, L., Ren, Z., Koo, H., & Thurnheer, T. (2020). Biofilm Matrixome: Extracellular Components in Structured Microbial Communities. *Trends in Microbiology*, *28*(8), 668–681. https://doi.org/10.1016/j.tim.2020.03.016

81. Khatoon, Z., McTiernan, C. D., Suuronen, E. J., Mah, T.-F., & Alarcon, E. I. (2018). Bacterial biofilm formation on implantable devices and approaches to its treatment and prevention. *Heliyon*, *4*(12), e01067. https://doi.org/10.1016/j.heliyon.2018.e01067

82. King, A. J. (2012). The use of animal models in diabetes research. *British Journal of Pharmacology*, *166*(3), 877–894. https://doi.org/10.1111/j.1476-5381.2012.01911.x

83. Kntayya, S. B., Ibrahim, M. D., Mohd Ain, N., Iori, R., Ioannides, C., & Abdull Razis, A. F. (2018). Induction of Apoptosis and Cytotoxicity by Isothiocyanate Sulforaphene in Human Hepatocarcinoma HepG2 Cells. *Nutrients*, *10*(6), 718. https://doi.org/10.3390/nu10060718

84. Köhler, T., Guanella, R., Carlet, J., & van Delden, C. (2010). Quorum sensing-dependent virulence during *Pseudomonas aeroginosa* colonisation and pneumonia in mechanically ventilated patients. *Thorax*, *65*(8), 703–710. https://doi.org/10.1136/thx.2009.133082

85. Kokare, C. R., Chakraborty, S., Khopade, A. N., & Mahadik, K. R. (2009). Biofilm: Importance and applications. *INDIAN J BIOTECHNOL*, 10.

86. Kon, Y., Tsukada, H., Hasegawa, T., Igarashi, K., Wada, K., Suzuki, E., Arakawa, M., & Gejyo, F. (1999). The role of *Pseudomonas aeroginosa* elastase as a potent inflammatory factor in a rat air pouch inflammation model. *FEMS Immunology & Medical Microbiology*, *25*(3), 313–321. https://doi.org/10.1111/j.1574-695X.1999.tb01356.x

87. Kostakioti, M., Hadjifrangiskou, M., & Hultgren, S. J. (2013). Bacterial Biofilms: Development, Dispersal, and Therapeutic Strategies in the Dawn of the Postantibiotic Era. *Cold Spring Harbor Perspectives in Medicine*, *3*(4), a010306. https://doi.org/10.1101/cshperspect.a010306

88. Kostylev, M., Kim, D. Y., Smalley, N. E., Salukhe, I., Greenberg, E. P., & Dandekar, A. A. (2019). Evolution of the *Pseudomonas aeroginosa* quorum-sensing hierarchy. *Proceedings of the National Academy of Sciences*, *116*(14), 7027–7032. https://doi.org/10.1073/pnas.1819796116

89. Lebeaux, D., Ghigo, J.-M., & Beloin, C. (2014). Biofilm-Related Infections: Bridging the Gap between Clinical Management and Fundamental Aspects of Recalcitrance toward Antibiotics. *Microbiology and Molecular Biology Reviews : MMBR*, *78*(3), 510–543. https://doi.org/10.1128/MMBR.00013-14

90. Lee, J., & Zhang, L. (2015). The hierarchy quorum sensing network in *Pseudomonas aeroginosa*. *Protein & Cell*, *6*(1), 26–41. https://doi.org/10.1007/s13238-014-0100-x

91. Lee, K., & Yoon, S. S. (2017). *Pseudomonas aeroginosa Biofilm, a Programmed Bacterial Life for Fitness*. *27*(6), 1053–1064. https://ir.ymlib.yonsei.ac.kr/handle/22282913/160946

92. Leid, J. (2009). Bacterial Biofilms Resist Key Host Defenses. *Microbe*, *4*, 66–70.

93. Leid, J. G., Willson, C. J., Shirtliff, M. E., Hassett, D. J., Parsek, M. R., & Jeffers, A. K. (2005). The exopolysaccharide alginate protects *Pseudomonas aeroginosa* biofilm bacteria from IFN-gamma-mediated macrophage killing. *Journal of Immunology (Baltimore, Md.: 1950)*, *175*(11), 7512–7518. https://doi.org/10.4049/jimmunol.175.11.7512

94. Lempp, M., Lubrano, P., Bange, G., & Link, H. (2020). Metabolism of non-growing bacteria. *Biological Chemistry*, *401*(12), 1479–1485. https://doi.org/10.1515/hsz-2020-0201

95. Lewenza, S. (2013). Extracellular DNA-induced antimicrobial peptide resistance mechanisms in *Pseudomonas aeroginosa*. *Frontiers in Microbiology*, *4*. https://doi.org/10.3389/fmicb.2013.00021

96. Li, T., Zheng, G., Li, B., & Tang, L. (2021). Pyroptosis: A promising therapeutic target for noninfectious diseases. *Cell Proliferation*, *54*(11), e13137. https://doi.org/10.1111/cpr.13137

97. Li, X.-H., & Lee, J.-H. (2019). Quorum sensing-dependent post-secretional activation of extracellular proteases in *Pseudomonas aeroginosa*. *The Journal of Biological Chemistry*, *294*(51), 19635–19644. https://doi.org/10.1074/jbc.RA119.011047

98. Limoli, D. H., Jones, C. J., & Wozniak, D. J. (2015). Bacterial Extracellular Polysaccharides in Biofilm Formation and Function. *Microbiology Spectrum*, *3*(3), 10.1128/microbiolspec.MB-0011–2014. https://doi.org/10.1128/microbiolspec.MB-0011-2014

99. Liu, C., Sun, D., Zhu, J., Liu, J., & Liu, W. (2020). The Regulation of Bacterial Biofilm Formation by cAMP-CRP: A Mini-Review. *Frontiers in Microbiology*, *11*. https://www.frontiersin.org/article/10.3389/fmicb.2020.00802

100. Mah, T.-F. (2012). Biofilm-specific antibiotic resistance. *Future Microbiology*, *7*(9), 1061–1072. https://doi.org/10.2217/fmb.12.76

101. Marsh, E. K., & May, R. C. (2012). Caenorhabditis elegans, a Model Organism for Investigating Immunity. *Applied and Environmental Microbiology*, *78*(7), 2075–2081. https://doi.org/10.1128/AEM.07486-11

102. Marshall, J. S., Warrington, R., Watson, W., & Kim, H. L. (2018). An introduction to immunology and immunopathology. *Allergy, Asthma, and Clinical Immunology: Official Journal of the Canadian Society of Allergy and Clinical Immunology*, *14*(Suppl 2), 49. https://doi.org/10.1186/s13223-018-0278-1

103. Martins, D., McKay, G., Sampathkumar, G., Khakimova, M., English, A. M., & Nguyen, D. (2018). Superoxide dismutase activity confers (p)ppGpp-mediated antibiotic tolerance to stationary-phase *Pseudomonas aeroginosa*. *Proceedings of the National Academy of Sciences of the United States of America*, *115*(39), 9797–9802. https://doi.org/10.1073/pnas.1804525115

104. Maurice, N. M., Bedi, B., & Sadikot, R. T. (2018). *Pseudomonas aeroginosa* Biofilms: Host Response and Clinical Implications in Lung Infections. *American Journal of Respiratory Cell and Molecular Biology*, *58*(4), 428–439. https://doi.org/10.1165/rcmb.2017-0321TR

105. Merritt, J. H., Kadouri, D. E., & O'Toole, G. A. (2005). Growing and Analyzing Static Biofilms. *Current Protocols in Microbiology*, *0 1*, Unit-1B.1. https://doi.org/10.1002/9780471729259.mc01b01s00

106. Mittal, R., Sharma, S., Chhibber, S., & Harjai, K. (2006). Effect of macrophage secretory products on elaboration of virulence factors by planktonic and biofilm

cells of *Pseudomonas aeroginosa*. *Comparative Immunology, Microbiology and Infectious Diseases*, *29*(1), 12–26. https://doi.org/10.1016/j.cimid.2005.11.002

107. Mittal, R., Sharma, S., Chhibber, S., & Harjai, K. (2009). Evaluation of tumour necrosis factor-alpha and interleukin-1beta in an experimental pyelonephritis model induced with planktonic and biofilms cells of *Pseudomonas aeroginosa*. *The Canadian Journal of Infectious Diseases & Medical Microbiology*, *20*(3), e35–e42. https://www.ncbi.nlm.nih.gov/pmc/articles/PMC2770315/
108. Mogensen, T. H. (2009). Pathogen Recognition and Inflammatory Signaling in Innate Immune Defenses. *Clinical Microbiology Reviews*, *22*(2), 240–273. https://doi.org/10.1128/CMR.00046-08
109. Moradali, M. F., Ghods, S., & Rehm, B. H. A. (2017). *Pseudomonas aeroginosa* Lifestyle: A Paradigm for Adaptation, Survival, and Persistence. *Frontiers in Cellular and Infection Microbiology*, *7*. https://www.frontiersin.org/article/10.3389/fcimb.2017.00039
110. Moreau-Marquis, S., O'Toole, G. A., & Stanton, B. A. (2009). Tobramycin and FDA-approved iron chelators eliminate *Pseudomonas aeroginosa* biofilms on cystic fibrosis cells. *American Journal of Respiratory Cell and Molecular Biology*, *41*(3), 305–313. https://doi.org/10.1165/rcmb.2008-0299OC
111. MOSER, C., JENSEN, P. O., KOBAYASHI, O., HOUGEN, H. P., SONG, Z., RYGAARD, J., KHARAZMI, A., & HØIBY, N. (2002). Improved outcome of chronic *Pseudomonas aeroginosa* lung infection is associated with induction of a Th1-dominated cytokine response. *Clinical and Experimental Immunology*, *127*(2), 206–213. https://doi.org/10.1046/j.1365-2249.2002.01731.x
112. Moser, C., Jensen, P. Ø., Pressler, T., Frederiksen, B., Lanng, S., Kharazmi, A., Koch, C., & Høiby, N. (2005). Serum concentrations of GM-CSF and G-CSF correlate with the Th1/Th2 cytokine response in cystic fibrosis patients with

chronic *Pseudomonas aeroginosa* lung infection. *APMIS: Acta Pathologica, Microbiologica, et Immunologica Scandinavica*, *113*(6), 400–409. https://doi.org/10.1111/j.1600-0463.2005.apm_142.x

113. Moser, C., Jensen, P. Ø., Thomsen, K., Kolpen, M., Rybtke, M., Lauland, A. S., Trøstrup, H., & Tolker-Nielsen, T. (2021). Immune Responses to *Pseudomonas aeroginosa* Biofilm Infections. *Frontiers in Immunology*, *12*, 625597. https://doi.org/10.3389/fimmu.2021.625597
114. Moser, C., Johansen, H. K., Song, Z., Hougen, H. P., Rygaard, J., & Høiby, N. (1997). Chronic *Pseudomonas aeroginosa* lung infection is more severe in Th2 responding BALB/c mice compared to Th1 responding C3H/HeN mice. *APMIS: Acta Pathologica, Microbiologica, et Immunologica Scandinavica*, *105*(11), 838–842.
115. Muhammad, M. H., Idris, A. L., Fan, X., Guo, Y., Yu, Y., Jin, X., Qiu, J., Guan, X., & Huang, T. (2020). Beyond Risk: Bacterial Biofilms and Their Regulating Approaches. *Frontiers in Microbiology*, *11*. https://www.frontiersin.org/article/10.3389/fmicb.2020.00928
116. Mulcahy, H., Charron-Mazenod, L., & Lewenza, S. (2008). Extracellular DNA chelates cations and induces antibiotic resistance in *Pseudomonas aeroginosa* biofilms. *PLoS Pathogens*, *4*(11), e1000213. https://doi.org/10.1371/journal.ppat.1000213
117. Müller, L., Brighton, L. E., Carson, J. L., Fischer, W. A., & Jaspers, I. (2013). Culturing of Human Nasal Epithelial Cells at the Air Liquid Interface. *Journal of Visualized Experiments : JoVE*, *80*, 50646. https://doi.org/10.3791/50646
118. Nickzad, A., & Déziel, E. (2014). The involvement of rhamnolipids in microbial cell adhesion and biofilm development – an approach for control? *Letters in Applied Microbiology*, *58*(5), 447–453. https://doi.org/10.1111/lam.12211

119. Oglesby-Sherrouse, A. G., Djapgne, L., Nguyen, A. T., Vasil, A. I., & Vasil, M. L. (2014). The complex interplay of iron, biofilm formation, and mucoidy affecting antimicrobial resistance of *Pseudomonas aeroginosa*. *Pathogens and Disease*, *70*(3), 307–320. https://doi.org/10.1111/2049-632X.12132

120. Okkotsu, Y., Little, A. S., & Schurr, M. J. (2014). The *Pseudomonas aeroginosa* AlgZR two-component system coordinates multiple phenotypes. *Frontiers in Cellular and Infection Microbiology*, *4*, 82. https://doi.org/10.3389/fcimb.2014.00082

121. Okuda, J., Hanabusa, A., & Gotoh, N. (2014). ExoS of *Pseudomonas aeroginosa* binds to a human KIF7 to induce cytotoxicity in cultured human bronchial epithelial cells. *Journal of Infection and Chemotherapy: Official Journal of the Japan Society of Chemotherapy*, *20*(2), 121–127. https://doi.org/10.1016/j.jiac.2013.09.001

122. Olivares, E., Badel-Berchoux, S., Provot, C., Prévost, G., Bernardi, T., & Jehl, F. (2020). Clinical Impact of Antibiotics for the Treatment of *Pseudomonas aeroginosa* Biofilm Infections. *Frontiers in Microbiology*, *10*. https://www.frontiersin.org/article/10.3389/fmicb.2019.02894

123. Ordovas-Montanes, J., Dwyer, D. F., Nyquist, S. K., Buchheit, K. M., Vukovic, M., Deb, C., Wadsworth, M. H., Hughes, T. K., Kazer, S. W., Yoshimoto, E., Cahill, K. N., Bhattacharyya, N., Katz, H. R., Berger, B., Laidlaw, T. M., Boyce, J. A., Barrett, N. A., & Shalek, A. K. (2018). Allergic inflammatory memory in human respiratory epithelial progenitor cells. *Nature*, *560*(7720), 649–654. https://doi.org/10.1038/s41586-018-0449-8

124. Orgad, O., Oren, Y., Walker, S. L., & Herzberg, M. (2011). The role of alginate in *Pseudomonas aeroginosa* EPS adherence, viscoelastic properties and cell

attachment. *Biofouling*, *27*(7), 787–798. https://doi.org/10.1080/08927014.2011.603145

125. Ørning, P., Hoem, K. S., Coron, A. E., Skjåk-Bræk, G., Mollnes, T. E., Brekke, O.-L., Espevik, T., & Rokstad, A. M. (2016). Alginate microsphere compositions dictate different mechanisms of complement activation with consequences for cytokine release and leukocyte activation. *Journal of Controlled Release: Official Journal of the Controlled Release Society*, *229*, 58–69. https://doi.org/10.1016/j.jconrel.2016.03.021
126. O'Toole, G. A. (2011). Microtiter dish biofilm formation assay. *Journal of Visualized Experiments: JoVE*, *47*. https://doi.org/10.3791/2437
127. Pachori, P., Gothalwal, R., & Gandhi, P. (2019). Emergence of antibiotic resistance *Pseudomonas aeroginosa* in intensive care unit; a critical review. *Genes & Diseases*, *6*(2), 109–119. https://doi.org/10.1016/j.gendis.2019.04.001
128. Pang, Z., Raudonis, R., Glick, B. R., Lin, T.-J., & Cheng, Z. (2019). Antibiotic resistance in *Pseudomonas aeroginosa*: Mechanisms and alternative therapeutic strategies. *Biotechnology Advances*, *37*(1), 177–192. https://doi.org/10.1016/j.biotechadv.2018.11.013
129. Paterson, I. K., Hoyle, A., Ochoa, G., Baker-Austin, C., & Taylor, N. G. H. (2016). Optimising Antibiotic Usage to Treat Bacterial Infections. *Scientific Reports*, *6*(1), 37853. https://doi.org/10.1038/srep37853
130. Penesyan, A., Paulsen, I. T., Kjelleberg, S., & Gillings, M. R. (2021). Three faces of biofilms: A microbial lifestyle, a nascent multicellular organism, and an incubator for diversity. *Npj Biofilms and Microbiomes*, *7*(1), 1–9. https://doi.org/10.1038/s41522-021-00251-2
131. Pennington, M. R., & Walle, G. R. V. de. (2017). Electric Cell-Substrate Impedance Sensing To Monitor Viral Growth and Study Cellular Responses to

Infection with Alphaherpesviruses in Real Time. *MSphere*, *2*(2). https://doi.org/10.1128/mSphere.00039-17

132. Pericolini, E., Colombari, B., Ferretti, G., Iseppi, R., Ardizzoni, A., Girardis, M., Sala, A., Peppoloni, S., & Blasi, E. (2018). Real-time monitoring of *Pseudomonas aeroginosa* biofilm formation on endotracheal tubes in vitro. *BMC Microbiology*, *18*. https://doi.org/10.1186/s12866-018-1224-6
133. Pestrak, M. J., Chaney, S. B., Eggleston, H. C., Dellos-Nolan, S., Dixit, S., Mathew-Steiner, S. S., Roy, S., Parsek, M. R., Sen, C. K., & Wozniak, D. J. (2018). *Pseudomonas aeroginosa* rugose small-colony variants evade host clearance, are hyper-inflammatory, and persist in multiple host environments. *PLoS Pathogens*, *14*(2), e1006842. https://doi.org/10.1371/journal.ppat.1006842
134. Priyaja, P., Jayesh, P., Philip, R., & Bright Singh, I. S. (2016). Pyocyanin induced in vitro oxidative damage and its toxicity level in human, fish and insect cell lines for its selective biological applications. *Cytotechnology*, *68*(1), 143–155. https://doi.org/10.1007/s10616-014-9765-5
135. Purushothaman, S., Cama, J., & Keyser, U. (2016). *Dependence of norfloxacin diffusion across bilayers on lipid composition.* https://doi.org/10/253340
136. Rada, B. (2017). Interactions between Neutrophils and *Pseudomonas aeroginosa* in Cystic Fibrosis. *Pathogens*, *6*(1). https://doi.org/10.3390/pathogens6010010
137. Rada, B., Gardina, P., Myers, T. G., & Leto, T. L. (2011). Reactive oxygen species mediate inflammatory cytokine release and EGFR-dependent mucin secretion in airway epithelial cells exposed to *Pseudomonas* pyocyanin. *Mucosal Immunology*, *4*(2), 158–171. https://doi.org/10.1038/mi.2010.62
138. Ramezanian, S., Ta, H. X., Muhunthan, B., & Abu-Lail, N. (2018). Role of ionic strength in the retention and initial attachment of *Pseudomonas* putida to quartz sand. *Biointerphases*, *13*(4), 041005. https://doi.org/10.1116/1.5027735

139. Rasamiravaka, T., Labtani, Q., Duez, P., & El Jaziri, M. (2015). The Formation of Biofilms by *Pseudomonas aeroginosa*: A Review of the Natural and Synthetic Compounds Interfering with Control Mechanisms. *BioMed Research International*, *2015*, e759348. https://doi.org/10.1155/2015/759348

140. Rasamiravaka, T., Vandeputte, O. M., & Jaziri, M. E. (2016). Procedure for Rhamnolipids Quantification Using Methylene-blue. *Bio-Protocol*, *6*(7), e1783–e1783. https://bio-protocol.org/e1783

141. Regina, V. R., Lokanathan, A. R., Modrzyński, J. J., Sutherland, D. S., & Meyer, R. L. (2014). Surface Physicochemistry and Ionic Strength Affects eDNA's Role in Bacterial Adhesion to Abiotic Surfaces. *PLoS ONE*, *9*(8), e105033. https://doi.org/10.1371/journal.pone.0105033

142. Reichhardt, C., & Parsek, M. R. (2019). Confocal Laser Scanning Microscopy for Analysis of *Pseudomonas aeroginosa* Biofilm Architecture and Matrix Localization. *Frontiers in Microbiology*, *10*, 677. https://doi.org/10.3389/fmicb.2019.00677

143. Reis, R. S., Pereira, A. G., Neves, B. C., & Freire, D. M. G. (2011). Gene regulation of rhamnolipid production in *Pseudomonas aeroginosa* – A review. *Bioresource Technology*, *102*(11), 6377–6384. https://doi.org/10.1016/j.biortech.2011.03.074

144. Rikalovic, M. G., Avramovic, N. S., & Karadzic, I. M. (2017). Structure-Function Relationships of Rhamnolipid and Exopolysacharide Biosurfactants of *Pseudomonas aeroginosa* as Therapeutic Targets in Cystic Fibrosis Lung Infections. In *Progress in Understanding Cystic Fibrosis*. IntechOpen. https://doi.org/10.5772/66687

145. Rybtke, M., Jensen, P. Ø., Nielsen, C. H., & Tolker-Nielsen, T. (2020). The Extracellular Polysaccharide Matrix of *Pseudomonas aeroginosa* Biofilms Is a

Determinant of Polymorphonuclear Leukocyte Responses. *Infection and Immunity*, *89*(1), e00631-20. https://doi.org/10.1128/IAI.00631-20

146. Schieber, M., & Chandel, N. S. (2014). ROS Function in Redox Signaling and Oxidative Stress. *Current Biology : CB*, *24*(10), R453–R462. https://doi.org/10.1016/j.cub.2014.03.034
147. Sharma, D., Misba, L., & Khan, A. U. (2019). Antibiotics versus biofilm: An emerging battleground in microbial communities. *Antimicrobial Resistance & Infection Control*, *8*(1), 76. https://doi.org/10.1186/s13756-019-0533-3
148. Sharma, K., & Pagedar Singh, A. (2018). Antibiofilm Effect of DNase against Single and Mixed Species Biofilm. *Foods (Basel, Switzerland)*, *7*(3), E42. https://doi.org/10.3390/foods7030042
149. She, P., Wang, Y., Liu, Y., Tan, F., Chen, L., Luo, Z., & Wu, Y. (2019). Effects of exogenous glucose on *Pseudomonas aeroginosa* biofilm formation and antibiotic resistance. *MicrobiologyOpen*, *8*(12), e933. https://doi.org/10.1002/mbo3.933
150. Singh, S., Datta, S., Narayanan, K. B., & Rajnish, K. N. (2021). Bacterial exo-polysaccharides in biofilms: Role in antimicrobial resistance and treatments. *Journal of Genetic Engineering and Biotechnology*, *19*(1), 140. https://doi.org/10.1186/s43141-021-00242-y
151. Soto, S. M. (2013). Role of efflux pumps in the antibiotic resistance of bacteria embedded in a biofilm. *Virulence*, *4*(3), 223–229. https://doi.org/10.4161/viru.23724
152. Stalder, T., & Top, E. (2016). Plasmid transfer in biofilms: A perspective on limitations and opportunities. *NPJ Biofilms and Microbiomes*, *2*, 16022. https://doi.org/10.1038/npjbiofilms.2016.22
153. Strässle, M., Laloli, L., Gultom, M., V'kovski, P., Stoffel, M. H., Crespo Pomar, S., Chanfon Bätzner, A., Ebert, N., Labroussaa, F., Dijkman, R., Jores, J., & Thiel,

V. (2021). Establishment of caprine airway epithelial cells grown in an air-liquid interface system to study caprine respiratory viruses and bacteria. *Veterinary Microbiology*, *257*, 109067. https://doi.org/10.1016/j.vetmic.2021.109067

154. Szulcek, R., Bogaard, H. J., & van Nieuw Amerongen, G. P. (2014). Electric Cell-substrate Impedance Sensing for the Quantification of Endothelial Proliferation, Barrier Function, and Motility. *Journal of Visualized Experiments : JoVE*, *85*. https://doi.org/10.3791/51300
155. Tan, M. W., Mahajan-Miklos, S., & Ausubel, F. M. (1999). Killing of Caenorhabditis elegans by *Pseudomonas aeroginosa* used to model mammalian bacterial pathogenesis. *Proceedings of the National Academy of Sciences of the United States of America*, *96*(2), 715–720. https://doi.org/10.1073/pnas.96.2.715
156. Tezel, B. U., Akçelik, N., Yüksel, F. N., Karatuğ, N. T., & Akçelik, M. (2016). Effects of sub-MIC antibiotic concentrations on biofilm production of Salmonella Infantis. *Biotechnology & Biotechnological Equipment*, *30*(6), 1184–1191. https://doi.org/10.1080/13102818.2016.1224981
157. Thakur, P., Saini, N. K., Thakur, V. K., Gupta, V. K., Saini, R. V., & Saini, A. K. (2021). Rhamnolipid the Glycolipid Biosurfactant: Emerging trends and promising strategies in the field of biotechnology and biomedicine. *Microbial Cell Factories*, *20*(1), 1. https://doi.org/10.1186/s12934-020-01497-9
158. Thurlow, L. R., Hanke, M. L., Fritz, T., Angle, A., Aldrich, A., Williams, S. H., Engebretsen, I. L., Bayles, K. W., Horswill, A. R., & Kielian, T. (2011). Staphylococcus aureus biofilms prevent macrophage phagocytosis and attenuate inflammation in vivo. *Journal of Immunology (Baltimore, Md. : 1950)*, *186*(11), 6585–6596. https://doi.org/10.4049/jimmunol.1002794
159. Tsay, T.-B., Jiang, Y.-Z., Hsu, C.-M., & Chen, L.-W. (2016). *Pseudomonas aeroginosa* colonization enhances ventilator-associated pneumonia-induced lung

injury. *Respiratory Research*, *17*(1), 101. https://doi.org/10.1186/s12931-016-0417-5

160. Tseng, B. S., Zhang, W., Harrison, J. J., Quach, T. P., Song, J. L., Penterman, J., Singh, P. K., Chopp, D. L., Packman, A. I., & Parsek, M. R. (2013). The extracellular matrix protects *Pseudomonas aeroginosa* biofilms by limiting the penetration of tobramycin: Limited tobramycin penetration protects biofilms. *Environmental Microbiology*, n/a-n/a. https://doi.org/10.1111/1462-2920.12155
161. Upadhyay, S., & Palmberg, L. (2018). Air-Liquid Interface: Relevant In Vitro Models for Investigating Air Pollutant-Induced Pulmonary Toxicity. *Toxicological Sciences*, *164*(1), 21–30. https://doi.org/10.1093/toxsci/kfy053
162. Uruén, C., Chopo-Escuin, G., Tommassen, J., Mainar-Jaime, R. C., & Arenas, J. (2021). Biofilms as Promoters of Bacterial Antibiotic Resistance and Tolerance. *Antibiotics*, *10*(1), 3. https://doi.org/10.3390/antibiotics10010003
163. Valentini, M., & Filloux, A. (2016). Biofilms and Cyclic di-GMP (c-di-GMP) Signaling: Lessons from *Pseudomonas aeroginosa* and Other Bacteria. *The Journal of Biological Chemistry*, *291*(24), 12547–12555. https://doi.org/10.1074/jbc.R115.711507
164. VAN GENNIP, M., CHRISTENSEN, L. D., ALHEDE, M., PHIPPS, R., JENSEN, P. Ø., CHRISTOPHERSEN, L., PAMP, S. J., MOSER, C., MIKKELSEN, P. J., KOH, A. Y., TOLKER-NIELSEN, T., PIER, G. B., HØIBY, N., GIVSKOV, M., & BJARNSHOLT, T. (2009). Inactivation of the rhlA gene in *Pseudomonas aeroginosa* prevents rhamnolipid production, disabling the protection against polymorphonuclear leukocytes. *APMIS : Acta Pathologica, Microbiologica, et Immunologica Scandinavica*, *117*(7), 537–546. https://doi.org/10.1111/j.1600-0463.2009.02466.x

165. Wang, X., Eagen, W. J., & Lee, J. C. (2020). Orchestration of human macrophage NLRP3 inflammasome activation by *Staphylococcus aureus* extracellular vesicles. *Proceedings of the National Academy of Sciences*, *117*(6), 3174–3184. https://doi.org/10.1073/pnas.1915829117

166. Welch, M. D. (2015). Why should cell biologists study microbial pathogens? *Molecular Biology of the Cell*, *26*(24), 4295–4301. https://doi.org/10.1091/mbc.E15-03-0144

167. Wight, T. N., & Potter-Perigo, S. (2011). The extracellular matrix: An active or passive player in fibrosis? *American Journal of Physiology - Gastrointestinal and Liver Physiology*, *301*(6), G950–G955. https://doi.org/10.1152/ajpgi.00132.2011

168. Wilton, M., Charron-Mazenod, L., Moore, R., & Lewenza, S. (2015). Extracellular DNA Acidifies Biofilms and Induces Aminoglycoside Resistance in *Pseudomonas aeroginosa*. *Antimicrobial Agents and Chemotherapy*, *60*(1), 544–553. https://doi.org/10.1128/AAC.01650-15

169. Wilton, M., Charron-Mazenod, L., Moore, R., & Lewenza, S. (2016). Extracellular DNA Acidifies Biofilms and Induces Aminoglycoside Resistance in *Pseudomonas aeroginosa*. *Antimicrobial Agents and Chemotherapy*, *60*(1), 544–553. https://doi.org/10.1128/AAC.01650-15

170. Wood, T. K., Knabel, S. J., & Kwan, B. W. (2013). Bacterial Persister Cell Formation and Dormancy. *Applied and Environmental Microbiology*. https://journals.asm.org/doi/abs/10.1128/AEM.02636-13

171. Woodworth, B. A., Tamashiro, E., Bhargave, G., Cohen, N. A., & Palmer, J. N. (2008). An in vitro model of *Pseudomonas aeroginosa* biofilms on viable airway epithelial cell monolayers. *American Journal of Rhinology*, *22*(3), 235–238. https://doi.org/10.2500/ajr.2008.22.3178

172. Wright, E. A., Fothergill, J. L., Paterson, S., Brockhurst, M. A., & Winstanley, C. (2013). Sub-inhibitory concentrations of some antibiotics can drive diversification of *Pseudomonas aeroginosa* populations in artificial sputum medium. *BMC Microbiology*, *13*(1), 170. https://doi.org/10.1186/1471-2180-13-170

173. Wu, D., Wu, C., Zhang, S., & Zhong, Y. (2019). Risk Factors of Ventilator-Associated Pneumonia in Critically III Patients. *Frontiers in Pharmacology*, *10*, 482. https://doi.org/10.3389/fphar.2019.00482

174. Wu, D., & Yotnda, P. (2011). Production and Detection of Reactive Oxygen Species (ROS) in Cancers. *Journal of Visualized Experiments : JoVE*, *57*, 3357. https://doi.org/10.3791/3357

175. Wu, J., Wang, Y., Liu, G., Jia, Y., Yang, J., Shi, J., Dong, J., Wei, J., & Liu, X. (2017). Characterization of air-liquid interface culture of A549 alveolar epithelial cells. *Brazilian Journal of Medical and Biological Research*, *51*(2), e6950. https://doi.org/10.1590/1414-431X20176950

176. Xi, C., & Wu, J. (2010). DATP/ATP, a Multifunctional Nucleotide, Stimulates Bacterial Cell Lysis, Extracellular DNA Release and Biofilm Development. *PLOS ONE*, *5*(10), e13355. https://doi.org/10.1371/journal.pone.0013355

177. Yamada, K. J., & Kielian, T. (2019). Biofilm-Leukocyte Cross-Talk: Impact on Immune Polarization and Immunometabolism. *Journal of Innate Immunity*, *11*(3), 280–288. https://doi.org/10.1159/000492680

178. Yeor-Davidi, E., Zverzhinetsky, M., Krivitsky, V., & Patolsky, F. (2020). Real-time monitoring of bacterial biofilms metabolic activity by a redox-reactive nanosensors array. *Journal of Nanobiotechnology*, *18*(1), 81. https://doi.org/10.1186/s12951-020-00637-y

179. Yin, W., Wang, Y., Liu, L., & He, J. (2019). Biofilms: The Microbial “Protective Clothing” in Extreme Environments. *International Journal of Molecular Sciences*, *20*(14), 3423. https://doi.org/10.3390/ijms20143423

180. Youk, J., Kim, T., Evans, K. V., Jeong, Y.-I., Hur, Y., Hong, S. P., Kim, J. H., Yi, K., Kim, S. Y., Na, K. J., Bleazard, T., Kim, H. M., Fellows, M., Mahbubani, K. T., Saeb-Parsy, K., Kim, S. Y., Kim, Y. T., Koh, G. Y., Choi, B.-S., … Lee, J.-H. (2020). Three-Dimensional Human Alveolar Stem Cell Culture Models Reveal Infection Response to SARS-CoV-2. *Cell Stem Cell*, *27*(6), 905-919.e10. https://doi.org/10.1016/j.stem.2020.10.004

181. Yousefpour, Z., Davarzani, F., & Owlia, P. (2021). Evaluating of the Effects of Sub-MIC Concentrations of Gentamicin on Biofilm Formation in Clinical Isolates of *Pseudomonas aeroginosa*. *Iranian Journal of Pathology*, *16*(4), 403–410. https://doi.org/10.30699/IJP.20201.524220.2584

182. Zegans, M. E., Wozniak, D., Griffin, E., Toutain-Kidd, C. M., Hammond, J. H., Garfoot, A., & Lam, J. S. (2012). *Pseudomonas aeroginosa* Exopolysaccharide Psl Promotes Resistance to the Biofilm Inhibitor Polysorbate 80. *Antimicrobial Agents and Chemotherapy*, *56*(8), 4112–4122. https://doi.org/10.1128/AAC.00373-12

183. Zhang, K., Li, X., Yu, C., & Wang, Y. (2020). Promising Therapeutic Strategies Against Microbial Biofilm Challenges. *Frontiers in Cellular and Infection Microbiology*, *10*. https://www.frontiersin.org/article/10.3389/fcimb.2020.00359

184. Zhao, X., & Bhattacharyya, A. (2018). Human Models Are Needed for Studying Human Neurodevelopmental Disorders. *American Journal of Human Genetics*, *103*(6), 829–857. https://doi.org/10.1016/j.ajhg.2018.10.009

185. Zhao, X., Yu, Z., & Ding, T. (2020). Quorum-Sensing Regulation of Antimicrobial Resistance in Bacteria. *Microorganisms*, *8*(3), 425. https://doi.org/10.3390/microorganisms8030425

186. Žukovskaja, O., Jahn, I. J., Weber, K., Cialla-May, D., & Popp, J. (2017). Detection of *Pseudomonas aeroginosa* Metabolite Pyocyanin in Water and Saliva by Employing the SERS Technique. *Sensors (Basel, Switzerland)*, *17*(8), 1704. https://doi.org/10.3390/s17081704

187. Zulianello, L., Canard, C., Köhler, T., Caille, D., Lacroix, J.-S., & Meda, P. (2006). Rhamnolipids Are Virulence Factors That Promote Early Infiltration of Primary Human Airway Epithelia by *Pseudomonas aeroginosa*. *Infection and Immunity*, *74*(6), 3134–3147. https://doi.org/10.1128/IAI.01772-05

8. APPENDIX

1. Preparation of 0.1% crystal violet

   0.1g of crystal violet was solubilised in 5ml ethanol and made upto to 100ml using distilled water and filtered through Whatmann no.1 filter paper. The solution was stored at room temperature

2. Composition of Minimal medium

   Distilled water was autoclaved, and the components of the medium was added and filtered using 0.2µm filters.

3. Preparation of NGM (Nematode growth medium

   NaCl - 0.3g
   Agar - 2g
   Peptone - 0.25g
   Distilled water – 100ml

   Components were autoclaved and cooled to 55ºC (approx.) and added with the following components

   1M CaCl2 - 0.1ml

   5mg/ml Cholesterol - 0.1ml

   1M MgSO4 - 0.1ml

   1M phosphate buffer (pH 6.0) - 2.5ml

   The components were mixed and poured into sterile petridishes allowed to set and stored at 4ºC until use

4. Preparation of Phosphate buffered saline (10X)

   NaCl - 80g

   KCl - 2g

   Na_2HPO_4 – 14.4g

   KH_2PO_4 – 2.4g

Dissolved in minimum volume of distilled water, adjusted to pH 7.4 and made up to 1Litre using distilled water filter sterilised and stored at 4ºC. 10X was diluted to 1X before use.

5. Bradford reagent (5X):

   Coomassie Brilliant blue R 250 – 50ml
   Methanol - 47ml
   Phosphoric acid (85%) - 100ml

6. Hoechst 33342 staining

   20mg/ ml stock was prepared in distilled water and stored at -20ºC. for use the stock was diluted 1:100 with PBS

7. Primers and Sequences

Gene	Sequence
GAPDH	ATTCCATGGCACCGTCAAGGCT TCAGGTCCACCACTGACACGT
Caspase-3	GGGCCTGTTGAACTGAAAAA CCGTCCTTTGAATTTCTCCA
iNOS	GAGCTTCTACCTCAAGCTATC CCTGATGTTGCCATTGTTGGT
Caspase 1	GAACAAGGAAGAGATGGAGAA TCGGAATAACGGAGTCAATC
IL1β	GACCAAGTTCTCTTCATT ATAGTTACAGCCATACCT
B actin	CTCCTTAATGTCACGCACGATTTC GTGGGGCGCCCCAGGCACCA

IL8	GCTTTCTGATGGAAGAGAGC GGCACAGTGGAACAAGGACT
IL6	CAGCCACTCACCTCTTCAGAAC TGCAGGAACTGGATCAGGAC
TNFα	CAGAGGGAAGAGTTCCCCAG CCTTGGTCTGGTAGGAGACG

9.Annexure

Publications

1. **Keerthi.S**, Pradeep Kumar SS, Dr. Kavita Raja, A. Maya Nandkumar, Role Of Antibiotics In Biofilm Formation By *Pseudomonas* Isolates, Journal Of Environmental Research And Development, Vol.10 (2), 2015, 270 -276
2. Keerthi, S., Vishnu Raj, M., & Maya Nandkumar, A. (2022). Role of Inflammasome-Mediated Pyroptosis as a Mechanism of Pathogenicity in *Pseudomonas* Biofilms. Archives of Microbiology & Immunology, 6(1), 20-38.
3. Keerthi, S., & Nandkumar, A. M. (2022). eDNA Release, a Contributor to Antibiotic Resistance in Medical Device-related Infections: *Pseudomonas* Biofilms, A Case Study. Trends in Biomaterials & Artificial Organs, 36(2), 77-83. https://www.biomaterials.org.in/tibao/index.php/tibao/article/view/612
4. Keerthi, S., Nandkumar, A.M. Electrical cell-substrate impedance sensing (ECIS) as a tool to study microbial-cell interactions. In vitro models (2022). https://doi.org/10.1007/s44164-022-00029-6

Conference presentations

1. **Keerthi.S**, Pradeep Kumar SS, Dr. Kavita Raja, Dr. Maya Nandkumar, Role of Antibiotics in Biofilm Formation by *Pseudomonas* Isolates, In the Proceeding of International Congress on Environmental Research, ICER 2014
2. **K. S**, P. Kumar, K. Raja, M. Nandkumar Antibiotic Induced Biofilm Formation and Gene Expression in Clinical Isolates of *Pseudomonas*; In the Proceedings of ASM Conference *Pseudomonas* 2015
3. **S Keerthi**, Kumar SS Pradeep, Nandkumar A Maya, eDNA – A DIAGNOSTIC TOOL FOR BIOFILM INFECTIONS? In The Proceeding of The International Conference on Biomaterials, Biodiagnostics, Tissue Engineering, Drug Delivery and Regenerative Medicine 2016
4. **Keerthi.S**, Pradeep Kumar SS, Dr. Kavita Raja, Dr. Maya Nandkumar, Genatmicin Induced Biofilm Formation Is Mediated Through the Quorum Sensing System, In the Proceeding of The International Conference on Crystal

Ball Vision On Science And Upliftment By IJAA In Collaboration With NIO, JSPS AND SERC At NIO Goa From 7-8th August 2017.

5. **S Keerthi**, Kumar SS Pradeep, Nandkumar A Maya, Monocyte Response to Planktonic and Biofilm Growing *Pseudomonas* Presented at The International Conference on Biomaterials, Bioengineering and Biotheranostics at Vellore Institute of Technology, Vellore from 26-28th July 2018
6. **Keerthi S** And Maya Nandkumar A ANTIBIOTIC RESISTANCE – ARE WE FATED TO BE VICTIMS OF BACTERIAL INFECTIONS??? Presented At The International Conference International Conference On Advancement In Science And Technology (ICAST-2018) | 3-4 September, 2018
7. **Keerthi.S** and Maya Nandkumar, Monocyte Immunomodulation by *Pseudomonas* biofilms- presented at the 17th International Biennial *Pseudomonas* Conference – *Pseudomonas* 2019 27-29th July 2019 at Kuala Lumpur Malaysia